2016

Role of Aqueous Phase Chemistry, Interfacial Film Properties, and Surface Coverage in Stabilizing Water-In-Bitumen Emulsions

Rocha Arrieta, Jair Andres

UNIVERSITY OF CALGARY

Role of Aqueous Phase Chemistry, Interfacial Film Properties, and Surface Coverage in Stabilizing Water-In-Bitumen Emulsions

by

Jair Andres Rocha Arrieta

A THESIS

SUBMITTED TO THE FACULTY OF GRADUATE STUDIES

IN PARTIAL FULFILMENT OF THE REQUIREMENTS FOR THE

DEGREE OF MASTERS OF SCIENCE

GRADUATE PROGRAM IN CHEMICAL ENGINEERING

CALGARY, ALBERTA

August, 2016

Abstract

In this thesis, several factors that influence the stability of asphaltene and bitumen stabilized water-in-oil emulsions are investigated including salt type, salt concentration, pH, interfacial film properties, surface coverage, drop size, and emulsion packing. Model water-in-oil emulsions were prepared from aqueous phases consisting of reverse osmosis water and salts (NaCl, $CaCl_2$, Na_2SO_4, KCl and Na_2CO_3). The organic phases consisted of either asphaltenes or bitumen dissolved in solutions of heptane and toluene. Salt contents as low as 0.02 wt% (or 0.03M ionic strength) were found to significantly increase the stability of the emulsions regardless of the type of salt present in the aqueous phase. The increase in stability correlated with an increase in the mass and apparent molecular weight of asphaltenes adsorbed at the interface. A mass surface coverage of 5 mg/m² and an apparent molecular weight of 7000 g/mol appear to be the threshold required for stable emulsions.

Acknowledgements

I would like to express my sincere and profound sense of gratitude to my supervisor, Dr. H.W. Yarranton for giving me the opportunity and privilege to be part of his research group. His unconditional guidance and patient as well as the long and productive discussions through my master's degree program is and it will always be deeply appreciated. Also, his encouragement and uplifting words in challenging times was essential to my personal and professional growth. I am highly obliged to him and I cannot thank enough.

I would also like to extend my thankfulness to Elaine Baydak for all her guidance and teaching in the laboratory, and also acknowledge her always good mood and positive attitude to review my writings and provide significant feedback. The important contribution and collaboration of all the members of the Asphaltene and Emulsion Research group, especially Florian and fellow graduate students, was also very important to the completion of this research work.

I am grateful to Suncor for it is sponsorship and for providing the bitumen samples for the experimental work. My special regards also goes to Dr. Danuta Sztukowski for providing valuable suggestions and important feedback that ended in the completion of this thesis.

I am thankful to the Department of Chemical and Petroleum Engineering, at the University of Calgary, for the great facilities they offer and the great staff who works with a friendly and supportive attitude.

Last but not least I want to express my deepest gratitude to my loving mother and father (Jaime and Yermis) for their unwavering and unconditional love and prayers.

Dedication

To God

"Riches and honor come from you, and you rule over all. In your hand are power and might; and it is in your hand to make great and to give strength to all". 1 Chronicles 29:12

Table of Contents

List of Tables

List of Figures and Illustrations

List of Symbols, Abbreviations and Nomenclature

English Letters

G	Gibbs free energy
A	area
T	temperature (K)
P	pressure
R	universal gas constant, 8.314 J/mol·K
C_A^{eq}	asphaltene equilibrium concentration (g/L)
K_s	Langmuir adsorption constant
C_A^0	initial asphaltene concentration (g/L)
d_{32}	Sauter mean diameter (m)
Z	charge on an ion
m	mass of asphaltenes in emulsion (Kg)
V_w	total volume of water phase (m^3)
N_A	Avogadro number
C_i	molar concentration (mol/L)
I	ionic strength
x^{org}	asphaltene mole fraction
x^{salt}	mole fraction of the salt in the aqueous phase

Greek Letters

γ	interfacial tension (mN/m)
$d\gamma$	differential change in interfacial tension (mN/m)
θ	contact angle between hydrocarbon and water
ρ	density (Kg/m^3)
Φ	volume fraction of water in settle emulsion
Γ	surface excess concentration (mg/m^2)
μ	viscosity of oil (Cp)
ε	film elasticity
τ	relaxation time (sec)

Subscripts

w	water
h	hydrocarbons
i	i^{th} component in the solution
$salt$	brine systems

s	surfactants
e	emulsions
A	area

Superscripts

o	pure solvent
eq	equilibrium
org	organic phase
aq	aqueous phase

Abbreviations

IFT	interfacial tension
VOP	vapor pressure osmometer
TI	toluene insoluble
DSA	drop shape analyser
RO	reverse osmosis water
SARA	saturates aromatics resins and asphaltenes
TAN	total acid number
API	American petroleum institute
SANS	small angle neutron scattering
SAXS	small angle X-ray scattering
TDS	total dissolved solids
OS	oil sand
CSS	cyclic steam stimulation
SAGD	steam assisted gravity drainage

CHAPTER ONE: INTRODUCTION

Virtually all petroleum production involves the co-production of water that exists naturally in the formation from which the oil is produced. During *in situ* processes, water-in-oil emulsions (water droplets dispersed in the bitumen) are formed during production and must be treated to meet pipeline specifications. In the naphthenic oil sands froth treatment process, approximately 3 vol % of the water remains in the product bitumen as small droplets (between 1 and 2 μm; Taylor *et al.,* 2002). Process water typically has a sodium ion concentration up to 1450 ppm and total salt concentrations of 3500 ppm (Kiran *et al.,* 2011; Jiang *et al.,* 2011) and this high chloride content can lead to downstream corrosion problems in pipes and equipment and hinder the water-oil separation. Hence, there is a strong incentive to understand what controls the stability of these emulsions in order to design more effective treatments to break them.

However, it is challenging to predict emulsion stability. In fact, this thesis was prompted by an observation from an oilfield operator (Suncor) that emulsions formed during the steam assisted gravity drainage (SAGD) and cyclic steam stimulation (CSS) process were easier to break and treat than oil sand (OS) emulsions, even though all three emulsions were formed from similar Western Canadian bitumens. As will be discussed in Chapter 2, there are many possible explanations for the differences in stability including differences in interfacial tension, film properties (compressibility and crumpling ratio – an indicator of irreversible adsorption), droplet sizes, emulsion packing (distance between the settled droplets), and the amount and type of solids. Interfacial tension, film properties, drop size, and packing, in turn, depend upon the type and amount of surface-active components and composition of the aqueous phase (salinity and pH). Therefore, this thesis focuses on the surface active components of the bitumen and the aqueous phase chemistry.

Most water-in-bitumen emulsions are believed to be stabilized by surface active species within the asphaltenes. Asphaltenes are the components in the bitumen that are soluble in aromatic solvents but insoluble in paraffinic solvents. They are the highest molecular

weight, mostly aromatic, and most polar components in the oil, and tend to be surface active. The asphaltenes that adsorb at a water-oil interface are enriched in oxygen and sulfur groups relative to the bulk asphaltenes (Jarvis *et al.,* 2015; Xu, 1999; Zhang *et al.*, 2003) and appear to act as weak ionic surfactants (Kumar, 2013;Moran 2007). Many researchers have demonstrated that these asphaltenes form rigid interfacial films that resist coalescence and create more stable emulsions (Gafonova and Yarranton 2001; Elsharkawy *et al.,* 2008; Ortiz *et al.,* 2010; Sztukowski, 2005; Wu, 2013; McLean and Kilpatrick 1997)). The stability may also be altered by other naturally occurring surface active components such as naphthenic acids or by biwettable fine solids. Biwettable solids contain some surfaces preferably wetted by water and some by oil (or surfaces coated with organic components); this mixture of wettabilities allows them to stabilize both oil-in-water and water-in-oil emulsions (Zahabi *et al.,* 2010; Sztukowski, 2005). When other natural surfactants are adsorbed along with the asphaltenes, emulsion stability may increase, decrease, or stay the same (Czarnecki and Moran, 2005; Varadaraj and Brons, 2007).

Asphaltenes from Western Canadian bitumens have undergone similar geochemical histories and are expected to have similar properties. However, the aqueous phase chemistry can differ significantly. The aqueous phase of SAGD and CSS emulsions consists of formation water diluted with condensed steam. Formation water contains a variety of electrolytes, and the composition ranges widely depending upon the source formation. In oil sands extraction processes, all of the formation water is processed along with the bitumen and formation solids. Much of the formation water is recycled, leading to an accumulation of electrolytes in the process water, which is controlled with makeup water and purge streams (Masliyah *et al.,* 2004).

The effect of the aqueous phase chemistry on asphaltenes and interfacial film properties is not yet well understood. It has been reported that, for most crude oils, the interfacial tension decreases with an increase in the salt content (Kumar, 2013; Lashkarbolooki *et al.,* 2014). Lower interfacial tension decreases the driving force for coalescence and contribute to greater emulsion stability (Serrano *et al.,* 2004). Salts can also increase the rigidity of the

interfacial film increasing stability to the emulsion (Alves *et al.*, 2014). However, Marquez *et al.* (2010) observed the formation of weaker asphaltene films when salts are present.

It has been documented by some authors that salts can reduce the drop size and created more stable emulsions (Aman *et al.*, 2015; Marquez *et al.*, 2010). However, other authors have reported the opposite effect, higher droplets and less stable emulsions, with an increase in salt content (Moradi *et al.*, 2013).

The role of pH must also be considered when dealing with electrolytic solutions and asphaltenes. Asphaltenes are amphoteric materials. The acid and base polar groups found in the asphaltenes can be ionized at low pH and high pH, increasing their hydrophilic behavior so that they tend to accumulate more easily at the water-oil interface, reduce the interfacial tension and increase emulsion stability (Elsharkawy *et al.*, 2008; Kokal, 2002; Moran, 2007; Arla *et al.*, 2007).

1.1 Objectives

The reported effects of salts on emulsion stability are incomplete and sometimes contradictory and yet this understanding is necessary to mitigate or treat problem emulsions. Therefore, the overall objective of this thesis was to investigate the role of aqueous phase chemistry (salinity and pH), interfacial film properties and surface coverage of asphaltenes in stabilizing water-in-bitumen emulsions. In particular, model systems were examined where the aqueous phase consists of reverse osmosis water (with various pH and salts), and the organic phases consist of either asphaltenes or bitumen dissolved in solutions of heptane and toluene. The bitumen (and their asphaltenes) are from an oil sands mining process (OS), a cyclic steam process (CSS), and a steam assisted gravity drainage process (SAGD).

The specific objectives were as follows:

1) Determine the effect of salt and pH on emulsion stability and properties of the model systems by measuring:

a. emulsion stability
b. drop size distribution and water volume fraction in the settled emulsions; calculate the interfacial area from the drop size distribution
c. interfacial tension; determine molar surface coverage by fitting the data with the Gibbs isotherm.
d. mass on the interface; determine the mass surface coverage using the calculated interfacial area; determine the apparent molar mass of the interfacial material from the mass and molar surface coverage
e. surface pressure isotherms; determine film compressibility and crumpling ratios.

2) Determine what critical factor(s) make the OS emulsions more stable than SAGD emulsions. Attempt to correlate the OS, SAGD, and CSS oil-in-brine emulsion stability tests with the properties measured in Objective 1.

The methodology followed to achieve the objectives is as follows. Model organic phases were prepared from 10 g/L of asphaltenes in a solution of 25 vol% heptane and 75 vol% toluene. The asphaltenes were extracted from the OS, CSS, and SAGD bitumen samples. A second set of model organic phases were prepared from solutions of 10, 20, and 30 wt% OS, CSS, or SAGD bitumen in the same solvent. Aqueous phases were prepared from reverse osmosis water with the specified additives (NaCl, $CaCl_2$, Na_2SO_4, KCl, and Na_2CO_3, NaOH, and HCl). Salt concentrations up to 15 wt% and pHs from 2 to 12 were evaluated.

Model emulsions were prepared by homogenizing the aqueous phase into the organic phase with a *CAT-520D* homogenizer equipped with a 17 mm rotor for five minutes at 18000 rpm. Water contents up to 40 vol% were evaluated. Emulsion stability was assessed in terms of the free water resolved over time after cycles of heating (60ºC) and centrifuging the emulsion. The water volume fraction in the settled emulsion was determined from the volume of the settled emulsion and the known initial volume for water. The mass of

asphaltenes on the interface was determined gravimetrically from the asphaltene content of the organic phase before and after emulsification.

Interfacial tension and surface pressure isotherms were measured with an IT Concept drop shape analyzer. Briefly, a droplet of the organic phase was generated at the end of a capillary placed in the aqueous phase. The image of the droplet was captured and the interfacial tension calculated from its shape. Interfacial tension was measured for 30 minutes to establish equilibrium values. Surface pressure isotherms and crumpling ratios were measured by withdrawing fluid from the droplet and measuring interfacial tension as a function of surface area. The crumpling ratio, as detailed in Section 2.3.2, is a measure of the relative rigidity of the interfacial films under the compressive forces. All the data was collected at 21ºC.

1.2 Thesis Structure

This thesis is presented in five chapters. Chapter 2 provides a background of the fundamentals of water-in-oil emulsions. The first section discusses emulsion stabilization and breaking. Then heavy crude oil chemistry is described with a particular focus on the asphaltenes and organic acids acting as natural surfactants. Finally, aqueous phase chemistry and particularly the role of salts and pH on interfacial asphaltene films properties and emulsion stability is reviewed.

Chapter 3 describes the experimental procedures to prepare emulsions, the materials, and instrumentation used in this thesis as follows:

- Chemicals and characteristics of the bitumen samples (solids and water content, asphaltene yield).
- The experimental procedure to assess emulsion stability, droplet size distribution, volume fraction of water in settle emulsions and mass surface coverage on interface.

- Principles of the drop shape analyzer and experimental techniques to evaluate interfacial tension, surface pressure isotherms, crumpling ratios and molar surface coverage.

Chapter 4 discusses the main results obtained in this research. The effect of salt concentration/ionic-strength and pH on emulsion stability, surface coverage, drop distribution and emulsion packing is presented and analysed. The effect of salts on interfacial tension, surface pressure isotherms and crumpling ratios is also discussed. Finally, the differences in the behavior and properties of the OS, SAGD, and CSS oil-in-brine emulsions are used to correlate the critical factors in the stabilization of these emulsions.

Chapter 5 summarizes the main outcomes of this thesis and presents recommendations for future research.

CHAPTER TWO: LITERATURE REVIEW

This chapter starts with a review of the fundamentals of emulsions and heavy oil chemistry. The heavy oil review focusses on asphaltenes and naphthenic acids since they are the most commonly encountered surface-active materials in crude oils. The properties of asphaltene films and the effect of co-adsorption of naphthenic acids and fine solids are discussed. Finally, the effects of aqueous phase chemistry on interfacial film properties and emulsion stability is reviewed. The focus is on water-in-oil emulsions since they are usually the most problematic emulsions encountered in oil sands mining and heavy oil *in situ* operations.

2.1 Fundamentals of Emulsions

An emulsion is defined as a mixture of two immiscible liquids in which one liquid is dispersed as droplets in the other. The droplet phase, or dispersed phase, is also referred to as the internal phase, whereas the continuous phase is the external phase. When water is dispersed in oil, a water-in-oil (W/O), or regular, emulsion is formed. When oil is the dispersed phase, an oil-in-water (O/W), or reverse, emulsion is formed Figure 2.1. Multiple emulsions (O/W/O or W/O/W) have also been observed (Binks, 1998; Langevin *et al.*, 2004). Whether an emulsion is O/W or W/O depends on a number of variables such as the water-oil ratio, type and concentration of surfactant, temperature, and electrolyte concentration (Binks, 1998). Both emulsions are common in the oil industry and their treatment present different challenges. This thesis focussed on water-in-oil emulsions.

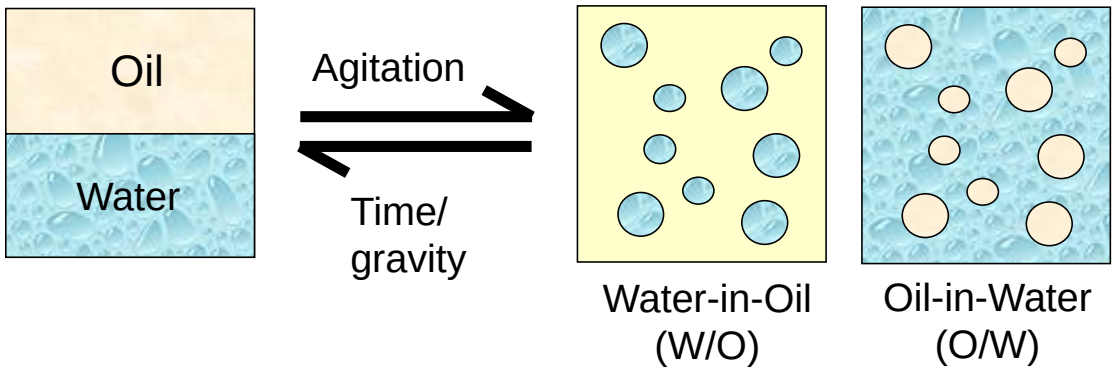

Figure 2.1 Formation of water-in-oil and oil-in-water emulsions.

Binks, (1998) defined emulsion stability as the condition where there is no significant change in the number, size distribution, and spatial arrangement of the droplets within the experimental time scale. However, the time scale could vary from seconds to years, implying also that stability is a relative concept. As will be discussed later, emulsions are thermodynamically unstable and the emulsified droplets tend to coalesce and the phases to separate unless an emulsifying agent is present, as detailed in (Section 2.1.2).

2.1.1 Emulsion Breakdown Mechanisms

Emulsion destabilization is a kinetic process which involve a series of steps that may occur simultaneously or separately depending on the conditions. The four main processes by which an emulsion can become unstable are: creaming or sedimentation, flocculation, coalescence, and Ostwald ripening.

Creaming and Sedimentation

Creaming is defined as the upward movement of oil droplets under gravitational forces or centrifugation to form a uniform phase layer at the top of the sample, Figure 2.2a. The downward movement is known as sedimentation, Figure 2.2b (Binks, 1998; Barnes, 2005). The creaming and settling rates depend on the density difference between the continuous and dispersed phases. Even though creaming and sedimentation do not directly cause phase separation, they bring droplets closer together.

(a) Creaming (b) Sedimentation

Figure 2.2 Illustration of creaming (a) and sedimentation (b) processes.

Flocculation/Aggregation

Flocculation occurs when emulsion droplets aggregate, but there is no rupture of the droplet films and the particles remain separated by a thin layer of continuous phase. Flocculation may be weak (reversible) or strong (irreversible) depending on the strength of the force between droplets. The rate of flocculation depends on the interaction energy between droplets, which is a function of the van der Waals attraction (depends on the droplet diameter and the Hamaker constant), electrostatic repulsion (depends mainly of the ionic strength of the continuous phase, droplet diameter and surface potential of the droplet), and steric repulsion (Natarajan *et al.*, 2011; Binks, 1998). Flocculation usually enhances creaming and sedimentation because larger flocs rise or settle more rapidly than individual droplets.

Coalescence

Coalescence is defined as the process in which two or more droplets merge together to form a single larger droplet and is an irreversible process (Binks, 1998). For coalescence to occur, two droplets must first approach each other as result of attractive forces, fluid motion, creaming, and/or flocculation, see Figure 2.3a. As they approach closely, their surfaces deform to create a planar region between the two droplets (Figure 2.3b). At the same time, the liquid between the two droplets begins to drain out allowing the droplets approach more closely. During drainage, the surface material spreads and gaps with less interfacial material are formed on the surface (Figure 2.3c). Bridges between droplets can form from the gaps and then fusion of the two droplets occurs (Figure 2.3d). Coalescence also leads to a reduction in the total surface area because a single droplet with the same volume as two smaller droplets has less overall surface area. Note, coalescence is more favorable for larger droplets because there is more potential contact area between the approaching droplets.

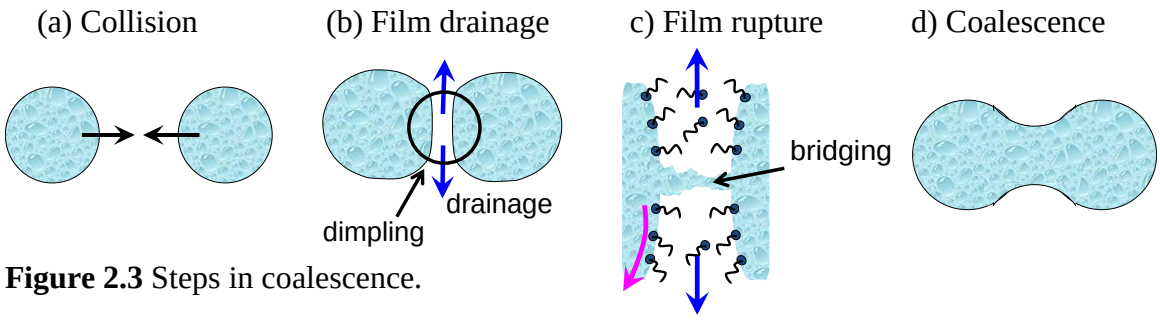

Figure 2.3 Steps in coalescence.

Ostwald Ripening

Ostwald ripening is the mass transfer of the dispersed phase molecules from small to large droplets. The concentration of the dispersed phase molecules in the continuous phase just outside a droplet depends on the curvature of the droplet (Taylor, 1995); it is greater above the surface of smaller droplets than larger droplets. Hence, there is a concentration gradient between droplets of different size to drives mass transfer. The larger droplets grow while the smaller droplets shrink and eventually disappear unless there is an irreversible film at the surface. Theoretically, the process of Oswald ripening should be completed by merging all the droplets into one, but this does not occur in a practical time scale because molecular diffusion decreases as the average droplet size increases (Binks, 1998). Ostwald ripening is a slow process and is not usually relevant for oilfield emulsion treatment.

2.1.2 Emulsifying Agents

As noted previously, emulsions will tend to coalesce unless there is material at the interface that prevents coalescence. Molecules that adsorb at the water-oil interface and stabilize emulsions are known as emulsifying agents and include surfactants and solid particles. Surfactants are the most common emulsion stabilizers. Generally, they are composed of a polar hydrophilic (water-loving) “head” and non-polar hydrophobic (water-hating) “tail” that consist of several carbon atoms. They are also known as amphiphilic compounds (Hiemenz *et al.*, 1996).

Surfactant Classification

Surfactants are generally classified on the basis of the charge on the hydrophilic group, as follows:

- Anionic: dissociate in water and the hydrophilic head group carries a negative charge; for example, carboxyl ($RCOO^- M^+$), sulfonate ($RSO_3^-M^+$) or sulfate ($ROSO_3^-M^+$) groups
- Cationic: dissociate in water and the hydrophilic head group carries a positive charge; for example, a quaternary ammonium halide ($R_4N^+Cl^-$)
- Amphoteric/zwitterionic): dissociate in water and, depending on the pH, the hydrophilic head group carries positive, negative or both positive and negative charges; for example, $RN^+(CH_3)CH_2CH_2SO_3^-$
- Non-ionic: the hydrophilic head group does not dissociate and has no charge, but contains highly polar groups; for example, polyoxyethylene ($-OCH_2CH_2O^-$) or polyol ($-RX\ (C_3H_5OH)_nOH^-$ groups.

Surfactants are attracted to the interface because their polar group can reside in the aqueous phase while their non-polar tail can reside in the oil phase. Surfactants tend to adsorb strongly at the interface because they reduce the free energy of the molecules at interface; that is, the energy required to bring a surfactant in contact with water on one side and organic components on the other side is significantly less than the energy required to bring water and organic molecules together. Surfactants can stabilize emulsions through a combination of reduced free energy, increased film thickness or viscosity, and/or electrostatic repulsion, as detailed in Section 2.1.3.

Solid Particles

Solid particles that stabilize emulsions are usually biwettable (amphiphilic) material and therefore they tend to adsorb at the water-oil interfaces where they create a steric barrier around the water droplets (Barnes, 2005). Oilfield solids are naturally hydrophilic but can

become totally or partially oil-wet (hydrophobic) after long-term exposure to the crude in the absence of water (Langevin *et al.*, 2004).

As a general rule, hydrophilic particles tend to stabilize oil-in-water emulsions while hydrophobic particles tend to stabilize water-in-oil emulsions (Asekomhe *et al.*, 2005). The ability of solids to stabilize emulsions is related to their size; solid particles contributing to emulsion stabilization are typically no more than 1 μm in diameter. Fine inorganic solids such as silica, clay and iron oxides present in crude oils are known for being good "stabilizers". (Gafonova and Yarranton 2001; Asekomhe *et al.*, 2005).

The wettability (hydrophilicity) of particles is quantified by their contact angle, θ, which is defined as the angle of contact between three phases (oil, water and a solid) measured through the aqueous phase. If $\theta > 90°$, the solids tend to form a W/O emulsion and if $\theta < 90°$, an O/W emulsion. For particles with contact angles close to 90°, both O/W and W/O emulsions can be stable for long periods. If the contact angle is too far from 90^{o}, the energy required to remove the particles from the interface will be small and the emulsion will not be very stable (Langevin *et al.*, 2004; Zhang *et al.*, 2005).

2.1.3 Emulsion Stability

Emulsions are inherently unstable because they have a large surface excess free energy (Kokal, 2002). An excess surface energy arises whenever oil and water molecules are brought together because the interaction energy between unlike molecules is greater than the interaction energies of like molecules in the bulk phase. The main increase in energy arises from the disruption of the hydrogen bonding network in the water. Emulsions have a large surface area between the dispersed droplets and the continuous phase and therefore have a much larger surface excess free energy than two separate bulk phases. Some consequences of this increased free energy are that: 1) energy is required to create an emulsion, for example, through turbulent mixing; 2) droplets tend to be spherical to minimize their surface area and surface free energy; 3) droplets tend to coalesce into larger droplets to minimize the surface area of the emulsion separating into bulk liquid phases.

However, emulsions can be metastable over a period of time if there is a barrier to coalescence. This barrier is created when molecules adsorb at the water-oil interface and create a charged layer (electrostatic stabilization), form a thick film (steric stabilization), and/or an irreversibly adsorbed film (mechanical stabilization) (Hiemenz *et al.*, 1996). Each mechanism is described below.

Electrostatic Stabilization

Electrostatic stabilization originates from a charged layer at the droplet interface created by dissociated ionic groups (or ions attracted to strong polar groups) from surface active components adsorbed at the interface. The charged surface attracts ions of opposite charge and repels ions of the same charge creating a "diffuse counterion layer." The imbalance between oppositely charged and identically charged ions decreases with increased distance from the interface until a balance is reached with a zero electrical potential at the boundary of this layer (Barnes, 2005). Outside the diffuse layer, the droplet appears electrically neutral. Inside the layer, it will appear to be charged. Hence, approaching droplets will eventually encounter an electrostatic repulsion.

The net force experienced by the approaching droplets is a balance of this repulsive force and any attractive forces. In general, dispersed droplets are attracted to each other due to the stronger van der Waals forces between the molecules in each droplet relative to the forces between the dispersed and continuous phase molecules. If a diffuse layer is present, a repulsive force arises as the diffuse layers from the approaching droplets begin to overlap. The sum of attractive and repulsive forces at short distances is described by DLVO theory (Landau *et al.*, 1941; Verwey *et al.*, 1948; Overbeek *et al.*, 1952), which relates the total energy potential to the distance between the surfaces of charged particles. If the repulsive force is relatively strong, the droplets will remain dispersed. If it is very weak, they can approach and coalesce. In intermediate cases, an energy barrier is created, Figure 2.4, and the droplets will flocculate, but not necessary coalesce.

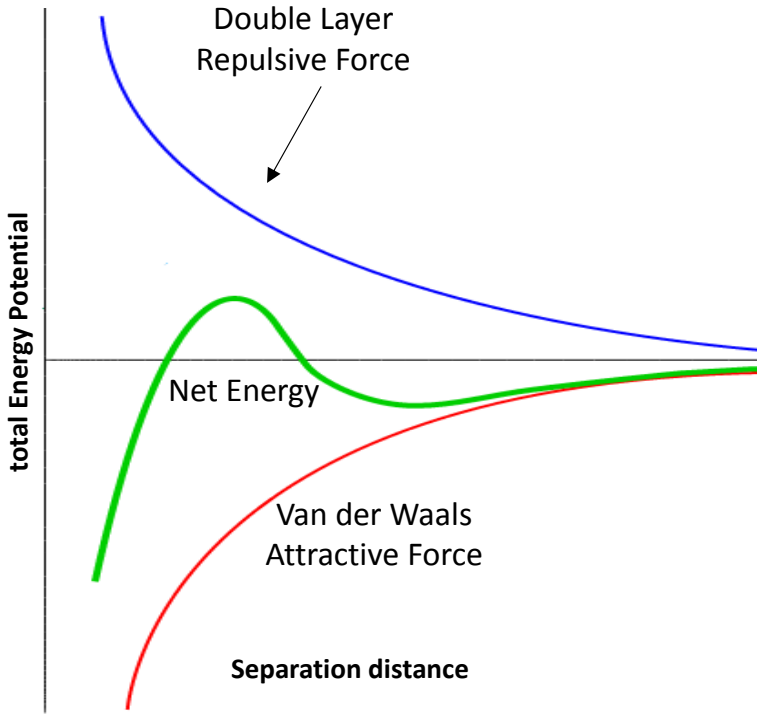

Figure 2.4 Interaction between particles, as described by DLVO theory.

Yeung *et al.* (2003) stated that crude oil droplets possessed negative surface charges caused by the dissociation of carboxylate groups, leading to double-layer repulsive forces between the droplets. According to conventional DLVO theory, the magnitude of this repulsion (based on the measured zeta potential) was sufficient to prevent coalescence of two or more oil droplets. Indeed, it was observed that when such droplets were brought together "head-on", coalescence rarely happened.

Electrostatic stabilization is only significant in oil-in-water emulsions because the counterions can diffuse readily into the continuous aqueous phase which has a high dieletric constant or electrical permittivity. Hence, a dispersed oil droplet will have a net charge even at some distance into the continuous phase from its surface due to the diffuse counter layer. In a water-in-oil emulsion, the head group and the counterions are inside the droplets, there is little or no net charge in the continuous oil phase, and therefore little or no repulsive force. Since this thesis focusses on water-in-oil emulsions, electrostatic stabilization is not further discussed.

Steric Stabilization

Steric stabilization occurs when the molecules adsorbed at the interface projects loops and tails into the continuous phase creating a physical barrier. Steric stabilization is effective primarily in water-in-oil emulsions where the hydrophilic segment holds the molecule at the droplet interface and a large lipophilic segment projects into the oil phase. The repulsive interaction of the lyophilic segments on the approaching particles prevents a close enough approach for coalescence to occur (Barnes, 2005). A steric barrier can be the result of adsorbed asphaltenes, resins, waxes, naphthenic acids or any other natural or added surfactants. Usually the steric barrier can be visualized as "long-hairy" surfactants coating the interface, as shown in the Figure 2.5. Adsorbed solids can also create a steric barrier if enough of the solid projects into the continuous phase.

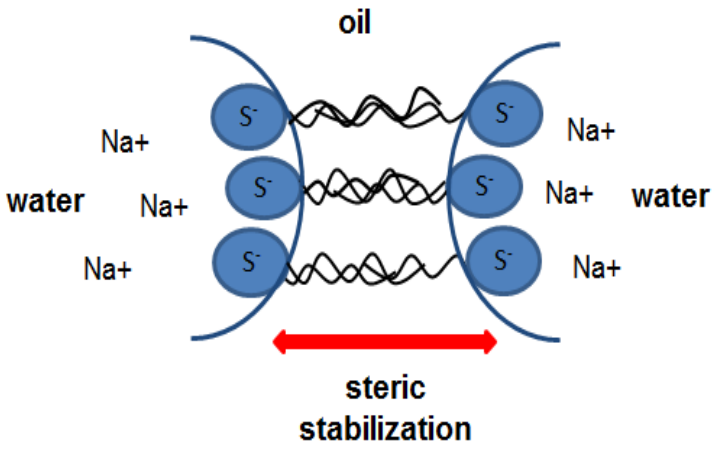

Figure 2.5 Diagram of the steric stabilization mechanism for a water-in -oil emulsion.

Mechanical Stabilization

If a surfactant adsorbs irreversibly at the interface, it will form a film that remains on the interface even when the droplet coalesces and the interfacial area is reduced. The film is therefore compressed during coalescence and eventually becomes thicker and more rigid until it resists further coalescence (Alves *et al.*, 2014; Ortiz *et al.*, 2010; Yarranton *et al.*, 2007b; Kokal, 2002; Czarnecki and Moran, 2005). Irreversible adsorption can occur when the surfactants at the interface rearrange to form a three-dimensional network on the film;

that is, a "skin-like" coating. The rigidity of the interfacial films can by quantified by measuring the film compressibility and/or interfacial rheological properties, as will be discussed in detail in Section 2.3.2

2.2 Heavy Oil Chemistry and Surface Active Components

Crude oils are a complex mixture of hundreds of thousands of organic/inorganic chemical species. They are composed primarily of hydrocarbon compounds which also include heteroatom groups that contain nitrogen, oxygen, sulfur, and metals such as vanadium, nickel, and iron. Oil composition varies according to the origin of the crude oil. Table 2.1 lists the elemental composition and properties of a typical Athabasca bitumen.

Table 2.1 Elemental Composition and Properties of Typical Athabasca Bitumen (Mullins *et al.*, 2007)

Component	Content	Property	Value
Carbon, wt%	81 - 84	API gravity	8.05
Hydrogen, wt%	10 - 11	Ramsbottom carbon, wt%	10 - 13.7
Nitrogen, wt%	0.3 - 0.6	H/C	1.46 - 1.50
Sulfur, wt%	4.6 - 5.6		
Vanadium, ppm	160 - 300		
Nickel, ppm	60 - 100		

Crude oil can be classified in several ways including by its physical properties (*e.g.*, specific gravity, viscosity), elemental composition (*e.g.*, H/C ratio, carbon distribution, heteroatom content, sulphur, nitrogen), distillation curve, nature of the residue after distillation (*e.g.*, paraffinic, naphthenic, aromatic, asphaltic), or solubility class as defined by SARA (fractionation into saturates, aromatics, resins and asphaltenes). SARA fractions provide a crude description of the crude oil chemistry. Asphaltenes, are of interest for this thesis because they are known to stabilize water-in-oil emulsions (Section 2.3.1).

2.2.1 Saturates, Aromatics, and Resins

A typical Athabasca bitumen contains about 17 wt% saturates, 43 wt% aromatics, 30 wt% resins and 17 wt% asphaltenes (Peramanu *et al.*, 1999). Athabasca bitumen contains on average approximately 3 wt% light ends with normal boiling point lower than 250°C and more than 45 wt% heavy ends with normal boiling point higher than 550°C (Mullins *et al.*, 2007). Typical properties for SARA fractions from Athabasca bitumen are shown in Table 2.2.

Table 2.2 SARA properties for Athabasca bitumen (Akbarzadeh *et al.*, 2004)

Bitumen Fraction	Fraction (wt%)	Molecular Weight (g/mol)	Density (kg/m³)
Saturates	16.3	460	880
Aromatics	39.8	552	990
Resins	29.5	1040	1044
Asphaltenes	14.7	1800+	1080+

The saturate and aromatic classes are more precisely defined than resins and asphaltenes because they contain significantly fewer and simpler types of molecules. Saturates (or aliphatics) are nonpolar compounds containing no double bonds and include alkanes and cycloalkanes. Wax is considered a subclass of saturates. Saturates are sometimes referred to as "white oils" due to their pearly color (Hellman and Ulfendahl, 1967). The molar mass and density of saturates extracted from a heavy oils and bitumen from a variety of sources was found to vary from approximately 360 to 525 g/mol and 850 to 900 kg/m³, respectively (Akbarzadeh *et al.*, 2004).

Aromatics consist of compounds with one or more benzene rings. These ring systems may be linked with naphthene rings and/or aliphatic side chains (Mullins *et al.*, 2007). The molar mass and density of aromatics are slightly greater than those of the saturates: values ranging from 450 to 550 g/mol and 960 to 1003 kg/m³, respectively, have been reported (Akbarzadeh *et al.*, 2004).

Resins molecules are similar to those found in aromatics except they are larger and contain more sulfur, oxygen and nitrogen. This fraction is operationally defined; that is, they depend on the procedure used to obtain them. For example, one definition of resins is the fraction of an oil that is soluble in light alkanes, such as pentane and heptane, but insoluble in liquid propane. In a SARA fractionation, the resins are the part of the oil that is soluble in *n*-pentane but adsorbs on attapulgus clay. Resin molar mass and densities reported for heavy oils and bitumen from a variety of sources vary between 850 to 1240 g/mol and 1000 to 1060 kg/m^3, respectively (Akbarzadeh *et al.*, 2004). Naphthenic acids, a surface active component in crude oils, are considered to be part of this fraction (Mullins *et al.*, 2007). Naphthenic acids will be discussed in more detail in Section 2.4.1.

2.2.2 Asphaltenes

Asphaltenes are a solubility class and, like resins, are operationally defined. Asphaltenes are soluble in aromatic solvents such as toluene, but precipitate in excess amounts of aliphatic solvents such as *n*-pentane and *n*-heptane (*e.g.,* 40 parts of aliphatic solvent to 1 part of bitumen). Asphaltenes include the densest, highest molecular weight, and most polar components of a crude oil. They contain the largest percentage of heteroatoms (sulfur, oxygen and nitrogen) and organometallic constituents (vanadium, nickel and iron) in the crude oil.

Zhang *et al.* (2003) determined the chemical composition, hydrogen to carbon ratio and aromaticity of asphaltenes from Athabasca bitumen samples, as shown in Table 2.3. The heteroatom content, E, is the sum of the oxygen, sulfur and nitrogen atoms and was found to be highest in the low molecular weight fraction of the asphaltenes. This fraction was also the least aromatic fraction.

Table 2.3 Chemical composition (C, H, N, O, S) and total heteroatoms *E*, hydrogen to carbon ratio (H/C), and aromaticity *f*a of asphaltenes and their low and high molecular weight fractions (Zhang *et al.*, 2003)

Asphaltene	**C**	**H**	**N**	**O**	**S**	***E***	***H/C***	f_a
Low-Molecular weight	78.88	7.66	1.26	1.26	7.79	13.31	1.16	0.55
Whole	79.06	7.93	1.14	1.37	7.62	10.13	1.20	0.53
High-Molecular weight	79.24	8.15	1.16	1.43	8.12	10.74	1.23	0.51

The average molecular weight and density of asphaltenes extracted from heavy oils bitumen from a variety of sources was found to vary from approximately 1090 to 10,000 g/mol and 1132 to 1190 kg/m³, respectively (Akbarzadeh *et al.*, 2004). Peramanu *et al.* (1999) observed Athabasca bitumen with asphaltene molecular weights ranging from 100 to more than 100,000 g/mol. The wide range of molecular weights arises because asphaltenes self-associate, as will be discussed later, and most reported molar masses are of nanoaggregates rather than molecules. The average molecular weight of asphaltene monomers is on average 1000 ± 500 g/mol, depending on the oil source (Mullins *et al.*, 2007; Akbarzadeh *et al.*, 2004; McKenna *et al.*, 2013; Powers, 2014).

Asphaltene Molecular Structure

A large number of species have been detected in the asphaltenes using high resolution mass spectrometry (McKenna *et al.*, 2013). Nonetheless, the structure of most, if not all asphaltene molecules, is believed to consist of polycyclic aromatic clusters substituted with varying alkyl side chains, alkyl bridges, and heteroatomic functional groups.

Several researchers have proposed two types of hypothetical "average" asphaltene molecules structures. The first type is the continent or "like your hand" structure, where the palm represents the single fused aromatic ring system and the fingers represent alkane substituents, as illustrated in Figure 2.6. This model is based on x-ray diffraction measurements of solid asphaltenes (Dickie and Yen, 1967). This particular hypothetical

continent structure has a formula of $C_{84}H_{100}N_2S_2O_3$, an H/C ratio of 1.19, and a molecular weight of 1276 g/mol.

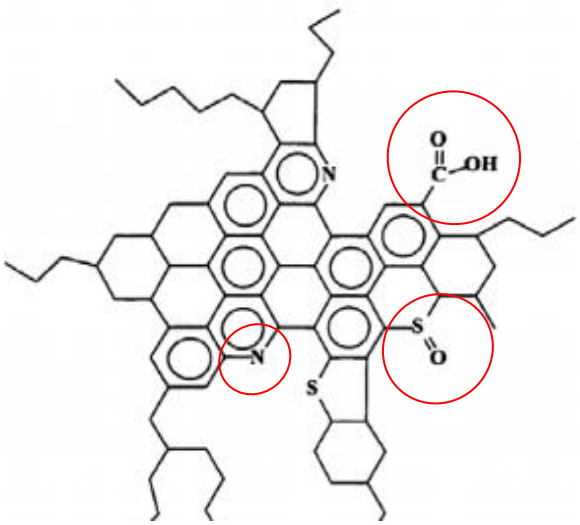

Figure 2.6 Continent structure of asphaltene molecule. Polar groups in red circles.

The second type of asphaltene molecular architecture is the "archipelago" structure, where each asphaltene molecule contains several fused aromatic ring systems linked together by alkyl chains. In other words, these asphaltenes are small aromatic islands connected by alkyl bridges, as shown in Figure 2.7. Strausz *et al. (*1992) proposed this molecular structure based on chemical and thermal degradation studies. This molecule has an elemental formula of $C_{420}H_{496}N_6S_{14}O_4V$, an H/C ratio of 1.18, and a molecular weight of 6191 g/mol. Note, the molecular weight is high for a monomer and this structure should probably be divided into several monomers. Overall, it is likely that asphaltenes are a mixture of continental and archipelago structures (McKenna *et al.,* 2013)

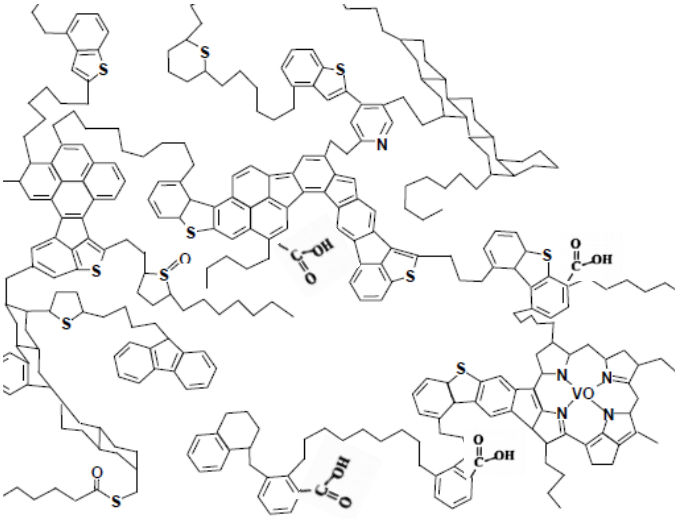

Figure 2.7 Proposed archipelago structure of asphaltene molecule (Modified From Strausz *et al.*, 1992).

A portion of the asphaltene species also contain hydrophilic moieties such as OH, COOH, and NHO functional groups. Since the hydrocarbon structure of the asphaltenes is hydrophobic, these asphaltenes include both hydrophilic and hydrophobic constituents. Hence, at least some of the asphaltenes are surface active agents which can adsorb at the water-oil interface with the hydrophilic head groups immersed in the water phase and the alkyl side chains remaining in the oil phase *(*Zhang *et al.*, 2003).

Asphaltene Aggregation

Asphaltenes are known to self-associate into nano-aggregates. The nature of this self-association and the size distribution of the aggregates is still debated. Yarranton *et al.* (2000) found molecular weights of asphaltene aggregates ranged between 4,000 to 10,000 g/mol depending on the asphaltene concentration, solvent, temperature, and source crude oil. The average nanoaggregate molecular weight in solution with toluene appears to range between 2-12 monomers per aggregate (Yarranton *et al.*, 2000; McKenna *et al.*, 2013).The association increased with concentration reaching a limiting value at asphaltene concentrations of 10 - 20 g/L. Barrera *et al.* (2013) observed average molecular weights of the asphaltenes ranging from 1,000 to 30,000 g/mol, equivalent to approximately 1−30 molecules per nanoaggregate, using vapor pressure osmometry (VPO). However, SANS

and SAXS data suggest much wider molecular weight distribution with average molecular weights in the order of 30,000 g/mol (Yarranton *et al.,* 2013). The apparent discrepancy between VPO and SAXS and SANS weight-averaged nanoaggregate molecular weights remains unresolved but it is possible that the nanoaggregates may flocculate. SAXS and SANS would detect floc dimensions, while VPO would not detect this type of aggregation (Yarranton *et al.,* 2013; Eyssautier *et al.,* 2012).

Asphaltene association has commonly been attributed to π–π bonding between aromatic sheets to create a stack-like structure. This rigid structure can be considered as a colloidal particle. Other mechanisms including acid-base interactions, hydrogen bonding, and other polar interactions have also been posed (Gray, 1994). This variety of bonding is likely to create a variety of structures including looser, more flexible aggregates. These structures may behave more like macro-molecules. Self-association may be more analogous to polymerization or oligomerization, except that the molecules are assumed to link by van der Waals attractive forces rather than covalent bonding (Agrawala and Yarranton, 2001). As will be discussed later, the behavior of asphaltene films on the interface is more consistent with flexible molecular configurations.

2.2.3 Naphthenic Acids

Naphthenic acids are classified as monobasic carboxylic acids with the general formula R-COOH, where R represents a cycloaliphatic structure (Mullins *et al.*, 2007). It is widely believed that these acids are complex mixtures of condensed ring structures where the arrangement of the COOH groups, hydrophile–lipophile balance, and the number of saturated and unsaturated rings can vary depending on the oil composition (Sjoblom *et al.*, 2003; Arla *et al.,* 2007). Naphthenic acids with similar total acid number (TAN) and average molecular weight can exhibit significantly different behaviours (Mullins *et al.,* 2007).

Naphthenic acids in crude oils are complex mixtures of approximately 1500 acids with boiling points ranging from 250 to 350 °C. An overview shows them to be C_{10}–C_{50}

compounds with 0–6 fused saturated rings and with the carboxylic acid group apparently attached to a ring with a short side chain (Arla *et al.*, 2007).

Naphthenic acids are surface active and can stabilize emulsions when they ionize at a water-oil interface. Typical naphthenate formation is given by the following reaction:

$$RCOOH + OH^- \leftrightarrow RCOO^- + H_2O$$

If a metal ion (M+) is present, then a metal-napthenate soap is formed, as follows:

$$RCOO^- + M^+ \leftrightarrow RCOO(Na)$$

For example, formation brine is naturally saturated with CO_2 and when oil production reduces the reservoir pressure enough to cause CO_2 degassing, there is an increase in the pH which allows the naphthenic acids to ionize into naphthenate anions (RCOO-). The metal ions present in the brine then bind to the naphthenates to form insoluble salts, or soaps, the most common types of which are calcium, magnesium and sodium soaps, as shown in Figure 2.8. These naphthenate soaps tend to precipitate or adsorb and accumulate at the oil- brine interface, forming a solid barrier that hinders coalescence, Figure 2.8 (Sarac and Civan, 2007). The surface activity of organic acids RCOOH is pH dependent. The lightest molecules are mostly dissolved in the water phase at neutral pH, whereas the heaviest molecules are mainly oil soluble. However, most of these molecules can be ionized and dissolved in water or adsorbed at the water-oil interface at high pH (Arla *et al.*, 2007).

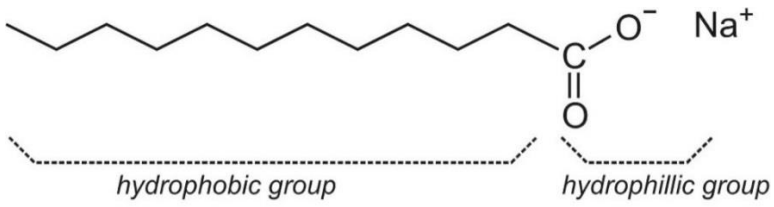

Figure 2.8 Illustration of a surface-active sodium naphthenate.

2.3 Asphaltene Stabilized Water-in-Oil Emulsions

Whenever crude oil and water are produced or processed together, the potential exists to form water-in-oil and/or oil-in-water emulsions. Oilfield emulsions can form during waterfloods or steamfloods when oil and water mix in the reservoir, at the wellbore, during transportation, in refineries and in various surface facilities. Emulsions are also formed during bitumen recovery from oil sands in a hot water extraction process. In the latter case, for example, the solvent-diluted product contains residual amount of water in the form of very small droplets which resist the coalescence and flocculation and are not easily removed under centrifugation.

Oilfield emulsions are usually a problem because they must be removed before transport and refining to meet pipeline and refinery specifications. In heavy oil and bitumen processes, the most challenging emulsions to break are water-in-oil emulsions. These emulsions have been shown to be stabilized from components within the asphaltene fraction (Czarnecki and Moran, 2005; Ortiz *et al.*, 2010; Gafonova and Yarranton, 2001; McLean and Kilpatrick, 1997; Arla *et al.*, 2007; Wu and Czarnecki, 2005). Their stability is also affected by other oil constituents such as naphthenic acids by particulates and the aqueous phase chemistry.

2.3.1 Asphaltene Constituents that Stabilize Water-in-Oil Emulsions

Asphaltenes have surface active properties that make them act as natural surfactants and therefore good emulsifiers. The interfacial activity of asphaltenes is generally related to the presence of heteroatoms that form polar functional groups. Varadaraj and Brons (2007) stated that of the heteroatoms present in the asphaltene molecule, such as nitrogen, oxygen, sulfur, vanadium and nickel, the N- and O-bearing moieties are the most likely to contribute to interfacial activity. They found that oxygen atoms are not present as COOH groups, but as ether linkages -O-. Nitrogen atoms are mostly in heteroaromatic ring structures, and about a third of the nitrogen functionalities are in basic nitrogen form and likely anchor at the interface. Yang *et al.* (2015) suggested that COOH groups were also present and that

the high polarity of sulfide in the asphaltene molecules could significantly increase their interfacial activity.

Xu *et al.* (1999) and later Yang *et al.* (2014) found that only a small fraction of the asphaltenes contributed to high emulsion stability. Yang *et al.* (2014) prepared water-in-oil emulsions stabilized by asphaltene from Athabasca bitumen. They then separated the water droplets including the interfacial material and prepared emulsions from the residual continuous phase. They found that removing just 2 wt% of the asphaltenes (the most surface active asphaltenes) caused a significant reduction in emulsion stability.

They extracted the interfacial material from emulsified water droplets to obtain the most interfacially active asphaltene (IAA) subfraction. The IAA molecules had higher molecular weight and higher heteroatom content compare with the remaining asphaltenes fractions (RA) and bulk asphaltenes (Yang *et al.,* 2015). The molecular weight of the IAA fraction averaged between 1000−1200 g/mol compared with 700−750 g/mol for the RA fraction. The oxygen content for IAA sample was 5.54% compared with 1.7% for the RA sample. The value of 1.7 wt% is within the range reported for bulk Athabasca asphaltenes (Zhang *et al.,* 2003). The IAA asphaltenes were also found to have lower aromatic content and higher cycloparaffinic and chain paraffinic contents, as was also reported by Zhang *et al.* (2003) and Groenzin and Mullins (2000).

Czarnecki, (2009) used electrospray ionization Fourier transform ion-cyclotron resonance mass spectrometry (ESI FT-ICR MS) to compare the relative abundance of selected classes containing oxygen and sulfur in the whole bitumen, asphaltenes and the interfacial material removed from the water-oil interface. They observed that most of the absorbed polar material on the interface contained "exotic" oxygen and sulfur-containing material and nonpolar low H/C ratio molecules. For instance, the interfacial material collected from the skin of water droplets emulsified in bitumen contained 3 oxygen and 2 sulfur atoms in addition to carbon and hydrogen (O_3S_2 class). The material collected from the emulsified droplet surfaces was not similar to that found in the asphaltene molecules.

Yang *et al.* (2015) proposed a representation of the IAA and RA molecular structures (Figure 2.9). In this representation most of the oxygen content found in the IAA sample is likely to associate with sulfoxide groups. The IAA molecules adsorbed at the water-oil interface with associations that may include S==O···H (water), aromatic H···O (water), aromatic π···H (water), and also acid−base interaction between pyridine moieties and water.

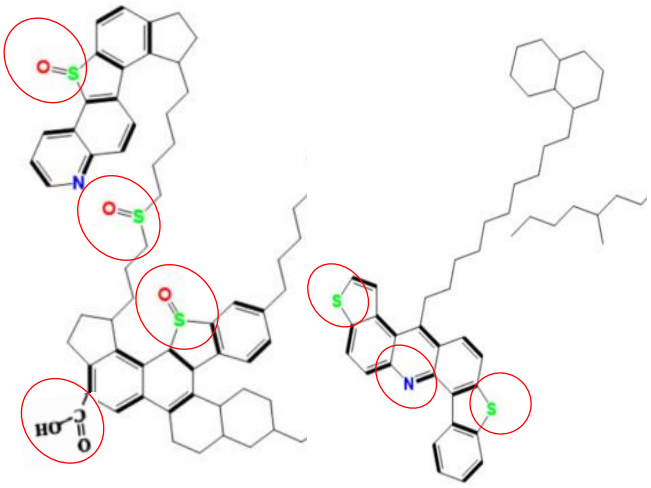

Figure 2.9 Molecular representations of the IAA (left) and RA (right) fractions. Polar groups in red circles (Modified from Yang *et al.*, 2015).

2.3.2 Properties of Asphaltene Interfacial Films

Surface active asphaltene molecules can form irreversible films at the water-oil interface which increase film rigidity, interfacial elasticity, and reduce interfacial tension, all of which increase emulsion stability (Yarranton *et al.*, 2007b; Sztukowski, 2005; Ortiz *et al.*, 2010; Alves *et al.*, 2014). As discussed previously, irreversible films can mechanically stabilize emulsions. High film elasticity can inhibit coalesce because the surfactants at the interface redistribute quickly when the droplet deforms. Lower interfacial tension decreases the driving force for coalescence and can contribute to emulsion stability (Barnes, 2005; Kumar, 2012). Asphaltene film properties (interfacial tension, compressibility, elasticity) are governed by factors such as temperature, aging time, chemistry of the solvent and the aqueous phase, asphaltene concentration and presence of

other surface active components in the crude oil such as resins and naphthenic acids (Ortiz *et al*., 2010). These film properties are reviewed below.

Interfacial Tension (IFT) and Surface Coverage

Interfacial tension is the excess free energy per surface area and is also commonly expressed as a force per length. It can be thought of as the work required to bring molecules from each bulk phase (where they are surrounded by like molecules) to the interface (where they are forced into contact with molecules of the other bulk phase).

Gibbs derived the following equation to relate the change in interfacial tension of a solution to the change in chemical activity of the components in the solution (Hiemenz *et al.*, 1996):

$$d\gamma = -RT \sum \Gamma_i \, dlna_i \tag{2.1}$$

where γ is the interfacial tension (N/m), R is the universal gas constant, T is the absolute temperature, and Γ_i and a_i are the surface excess concentration and chemical activity of component i, respectively. The summation must be taken over all species (solutes) present in the solution, but usually some terms are zero or negligibly small. For a binary system, the surface excess is defined such that the surface excess of one of the components (the solvent) is zero and the Gibbs adsorption equation can be written as:

$$d\gamma = -RT\Gamma_\beta \, d \, lna_\beta \tag{2.2}$$

where Γ_β and a_β are the surface excess concentration and activity of the solute, respectively. Note, since the surface excess concentration of a surfactant is positive, Equation 2.2 shows that the addition of surfactant decreases the interfacial tension of a solution.

The surface excess concentration of a component can be expressed as follows:

$$\Gamma_i = \theta_i \, \Gamma_{mi} \tag{2.3}$$

where θ_i and Γ_{mi} are the fractional surface coverage monolayer and surface excess concentration of component i, respesctively. The fractional surface coverage can be related to the bulk phase concentration using the Langmuir adsorption isotherm given by:

$$\theta_i = \frac{\Gamma_i}{\Gamma_{mi}} = \frac{K_{Li}C_i}{1 + K_{Li}C_i} \tag{2.4}$$

where K_{Li} and C_i are the Langmuir constant and concentration of component i, respectively. Equation 2.4 is substituted into the Gibbs adsorption isotherm, Equation 2.2, to obtain the following expression (Yarranton and Masliyah 1996).

$$d\gamma = -RT\Gamma_m \ln(1 + K_{Li}C_i) \tag{2.5}$$

The adsorption constant and monolayer surface excess concentration can be found by fitting Equation 2.5 to experimental data. The interfacial tension then becomes linearly related to the log of the activity of the surfactant. The activity is proportional to the surfactant concentration (for ideal systems and when the surfactant mole fraction is much lower than the solute mole fraction). Therefore, the interfacial tension becomes linearly related to the log of concentration. The molar surface coverage can be determined from the slope of the linear region in a plot of interfacial tension versus asphaltene mole fraction or concentration for a water/hydrocarbon system, as illustrated in Figure 2.10. Details of the calculations are discussed in Section 4.3.

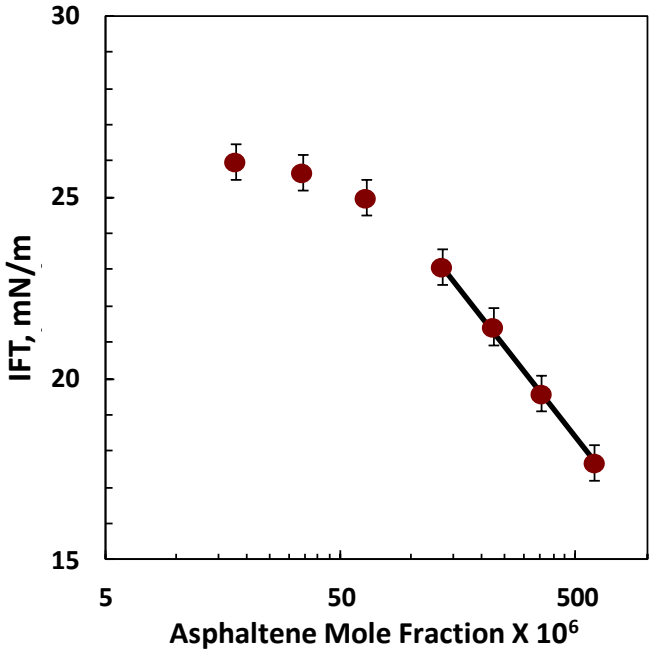

Figure 2.10 Interfacial tension versus asphaltene mole fraction in 50/50 heptol at 21 ºC. The value of surface excess can be determined from the slope of the linear region, adapted from Kumar, (2012).

Interfacial Rheological Properties

In most of the cases, when an interface with an adsorbed layer of surface active molecules is stretched, an interfacial tension gradient is generated. The tension gradients will oppose the stretching and try to restore the uniform interfacial tension state, that is, the interface will behave elastically. This is the Gibbs–Marangoni effect (Mullins *et al.*, 2007). The main effect on emulsion stability of interfacial active molecules is not the reduction of the interfacial tension they produce, but that their presence can lead to such gradients in interfacial tension able to resist tangential stresses (Mullins *et al.*, 2007). Surfactants can be drawn from the bulk phase to the interface or from interfacial regions of higher surfactant concentration (lower interfacial tension) to interfacial regions deficient in surfactant (higher interfacial tension). In practice, emulsion droplets being stretched can resist coalescence due to the elastic membrane, providing the droplet interfaces with a "self-healing" mechanism.

Interfacial rheology properties are quantified through the interfacial dilatational modulus or interfacial elasticity. This property gives a measure of resistance to the creation of interfacial tension gradients and the rate at which such gradients disappear after deformation. The interfacial elasticity, ε, is defined as the increase in interfacial tension for a unit of relative increase in surface area.

$$\varepsilon = \frac{\partial \gamma}{\partial InA} \tag{2.6}$$

A high elasticity means that a change in interfacial area significantly increases the interfacial tension and therefore the energy of the system (Sztukowski, 2005). For a small deformation of the area, the change in interfacial elasticity can be written as a sum of an elastic and a viscous contribution as follow:

$$\varepsilon = \varepsilon_d + i\omega\eta_d \tag{2.7}$$

where ε_d, η_d, and ω are the interfacial dilatational elasticity, viscosity and frequency of oscillation, respectively. The elastic modulus represents the energy stored in the system, whereas the interfacial viscosity represents the energy dissipated during relaxation.

McLean and Kilpatrick (1997) speculated that the adsorption of asphaltene colloids solvated with resinous material form films of the considerable mechanical strength at the water-oil interface. Sztukowski, (2005) measured the elasticity of the asphaltenes interfacial films in 25/75 heptol and it was shown that as the asphaltene-heptol-water interfaces age, the elastic modulus and the viscous modulus increase. Asphaltenes gradually reorganize along the interface to form a rigid irreversibly adsorbed network

Alvarez *et al.,* (2009) observed that the stability of water-in-oil emulsions plateaued at bitumen-toluene concentrations above 15 g/L (or 3g/L asphaltene) and aqueous solutions consisted of distillated water with 5g/L NaCl. The stability plateau coincided with the region of the maximum in elastic modulus, where the monolayer was highly compact and extremely rigid. Interesting, at higher bitumen or asphaltene concentrations the elastic modulus started decreasing and the asphaltene layer became less rigid (lower crumpling

ratios observed) indicating more dissipated energy when the interface was deformed, likely caused by the increasing amount of adsorbed species. The authors speculated that the adsorbed bulk aggregates were more compressible than those formed at low asphaltene concentration.

Likewise, Yarranton *et al.,* (2007a) oberved a maximum in the apparent elasticity modulus at low asphaltene concnetrations (0.1 g/L asphaltenes) in 25/75 heptol solutions. At higher concentrations, the elastic and total modulus decreased as the increasing diffusion of molecules from the bulk phase to the interface affected the moduli. Similar observations were made by Hannisdal *et al.,* (2007) who studied the viscoelastic properties of the crude oil diluted in heptol, suggesting that the decrease in viscoelastic modules at high bitumen concentrations was a combined effect of both the increased diffusion flux to the interface and the change in composition of the interfacial material. A maximum in film elasticity with the increased asphaltene concentration in solutions with high aromatic solvents has been reported by several authors (Verruto and Kilpatrick 2008; Sjoblom *et al.*,2003; Hannisdal *et al.,* 2007)

Surface Pressure Isotherms

The stability of water-in-oil emulsions stabilized by asphaltenes is related to the changes in interfacial film properties, such as surface pressure isotherms and crumpling ratios (Ortiz *et al.,* 2010; Yarranton *et al.,* 2007b). Surface pressure, π, is defined as follows:

$$\pi = \gamma_o - \gamma \tag{2.8}$$

where γ_o is the difference between the interfacial tension of the pure solvent versus the aqueous phase (no adsorbed surface layer or surface active agent) and γ is the interfacial tension when a surface active component is present. Surface pressure isotherms describe the change in surface pressure while the film is under compression and are the two-dimensional analog of pressure-volume isotherms. Surface pressure isotherms can show two-dimensional analogs of gas, liquid and solid phases. Liquid phases are less compressible than gas phases and solid phases are essentially incompressible.

An example of a surface pressure isotherm for irreversibly adsorbed asphaltenes is shown in Figure 2.11. For this experiment, an organic phase droplet is forced to compress by withdrawing fluid out of the droplet in a stepwise fashion. The initial film ratio has a high compressibility with a film ratio equal to 1. The compressibility is constant until the film is substantially reduced (Phase 1). As film compression progresses, a phase change occurs and a phase of low compressibility (Phase 2) appears. At this point small changes in the surface cause the surfactant molecules to pack more closely together on the interface, reducing the interfacial tension and increasing the surface pressure.

As the compression continues, the film reaches a maximum surface pressure and the maximum packing of molecules on the interface (minimum area occupied per molecule). If the compression continues beyond this point, the film can no longer be compressed and it crumples like a "paper bag." The film ratio at which the film crumples is known as the crumpling ratio (CR). At this point the asphaltene film becomes completely packed, very rigid, and resistant to coalescence. The existence of crumpling ratios in asphaltene films indicates that asphaltenes irreversibly adsorb at the interface. In other words, once the asphaltene are adsorbed at the water-oil interface, they do not leave the interface upon film compression.

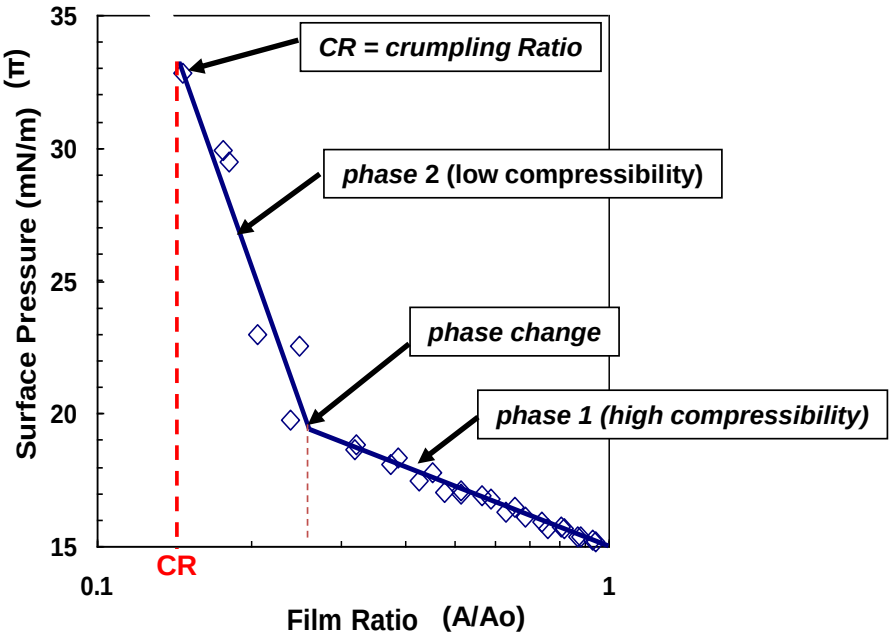

Figure 2.11 Typical behaviour of the surface pressure isotherm, π, versus film ratio. Adapted from Urrutia, (2006).

The formation of rigid interfacial films has received much of attention because they retard coalescence and hinder water-oil separation (Yarranton *et al.*, 2007b; Sztukowski, 2005; Ortiz *et al.*, 2010; Alves *et al.*, 2014). Solovyev *et al.*, (2006) observed that the surface pressure isotherms of bitumen films were nearly identical to that of the asphaltene monolayer and concluded that the bitumen film at toluene-water interfaces is composed mainly of asphaltenes.

Gao *et al.*, (2009) investigated the interfacial properties of the emulsified water droplets in heptol solutions containing bitumen or its separated components such as asphaltenes and maltenes. The crumpling tests of water droplets revealed that surface active components in asphaltenes are the major contributor to the formation of rigid films at the water-oil interface. For maltenes in heptol solutions, irreversible films (no crumpling ratios) were observed at all bitumen concentrations. Interesting, the interfacial tension of the maltenes solutions was smaller than the bitumen and pure asphaltene solutions. The authors suggested that more naturally surface-active components are adsorbed at the water drop

surface in the maltenes system than in the asphaltenes system at an equivalent concentration, and yet at the same time create less stable emulsions. The Gao *et al.*, (2009) study demonstrates that the interfacial tension alone is not sufficient to describe the stability of water-in- oil emulsions.

Zhang *et al.* (2005) fractionated asphaltenes into high molecular weight and low molecular weight portions and measured their surface pressure isotherms in solutions of heptane and toluene. They found that the compressibility of the monolayers increased from low molecular weight to whole to high molecular weight asphaltenes.

Ortiz *et al.* (2010) developed a correlation between emulsion stability (free water resolved from the emulsion) and film properties (interfacial compressibility, crumpling film ratio and interfacial tension). They found that irreversible adsorption of asphaltenes (indicating by the presence of a crumpling ratio) was a necessary factor for emulsion stability. Yarranton *et al.* (2007b) showed that asphaltene concentrations had very little effect on the surface pressure isotherms. The molecular surface coverage is similar at low and high asphaltene concentrations and so are the film properties.

Asphaltenes form films of lower compressibility in poorer solvents (lower aromaticity) (Yarranton *et al.*, 2007a; Ortiz *et al.*, 2010; Gafonova and Yarranton, 2001; McLean and Kilpatrick, 1997; Urrutia, 2006; Zhang *et al.*, (2005) . These films are more irreversibly adsorbed and difficult to displace from the interface and therefore more stable emulsions are formed (Ortiz *et al.*, 2010; Yarranton *et al.*, 2007a).

For asphaltene films, the film properties such as interfacial tension, surface pressure and viscoelastic properties seems to have very little variation with an increase in temperature to as high as 60 ^{o}C (Yarranton *et al.*, 2007b; Ortiz *et al.*, 2010; Urrutia, 2006).

2.4 Effect of Other Oil Constituents on Oilfield Water-in-Oil Emulsions

In this thesis, water-in-oil emulsions with bitumen organic phases and with organic phases consisting of asphaltenes, heptane, and toluene are considered. The focus is on asphaltene stabilized emulsions. However, when comparing results from emulsion prepared from the model organic phase with emulsions prepared from bitumen, the impact of other oil constituents must be considered. Naphthenic acids are surface active and known to affect emulsion stability. Inorganic solids can also alter emulsion stability. Both are discussed below.

2.4.1 Effect of Naphthenic Acids on Asphaltene Films and Emulsion Stability

Kiran *et al.* (2011) observed that pure asphaltenes produce more stable films than pure naphthenic acids, as was evident in the observed larger collapse pressure and low compressibility. The naphthenic acids appear to be irreversibly adsorbed and therefore do not confer mechanical stability to the emulsion. Hence, the presence of naphthenic acids may contribute to reversible film adsorption and lower emulsion stability.

It is not clear whether sodium naphthenates and asphaltenes are individually adsorbed at the oil-water interface or if they associate in the bulk and adsorb at the interface as aggregates. Either way, it is likely that naphthenic acids interact with asphaltenes leading to two possible outcomes at the interface: 1) naphthenic acid-asphaltene mixed monolayers, or; 2) naphthenic acid-asphaltene aggregates (Varadaraj and Brons 2007).

The naphthenic acid-asphaltene aggregates model posits that asphaltenes aggregate along with naphthenic acids and adsorb on the interface, as illustrated in Figure 2.12 (Varadaraj and Brons, 2007). The naphthenic groups may alter the self-association between the species adsorbed at the interface and therefore the reversibility of the adsorption.

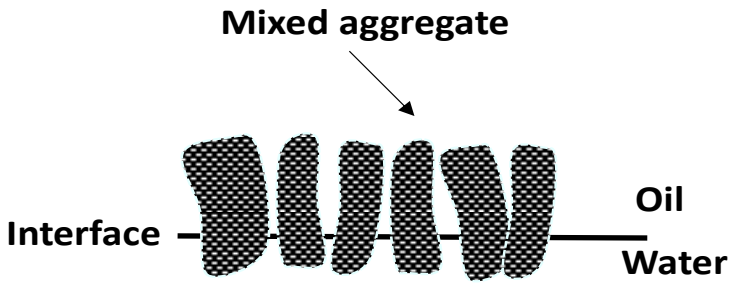

Figure 2.12 Naphthenic acid-asphaltene aggregate adsorption. adapted from (Varadaraj and Brons, 2007).

The naphthenic acid-asphaltene mixed monolayer model posits that asphaltenes are adsorbed on the interface amongst the small surface-active species such as naphthenic acids In this case, the naphthenic acids likely remain reversibly adsorbed and may prevent lateral interactions between the asphaltenes. In either case, the film, or parts of the film, would be less strongly adsorbed at the interface. Moran and Czarnecki (2007) showed that at sufficient concentration of added sodium naphthenate, the larger molecules or aggregates are either excluded from adsorbing or are competitively displaced from the water-oil interface.

Czarnecki and Moran (2005) found that in water-in-diluted bitumen emulsions, the proportion of asphaltenes on the interface decreased at higher bitumen concentrations. They measured the H/C ratio of the material adsorbed at the interface for different concentrations of bitumen in 50-50 heptol and observed that the H/C ratio of the adsorbed material increased as the bitumen concentration increased, as shown in Figure 2.13. Since asphaltenes have a low H/C ratio (approximately 1.15), the results suggest that they were replaced on the interface by other components at higher bitumen concentrations. Interestingly, the interface at high bitumen contents was flexible and the emulsion formed were very stable. The films, despite their flexibility, may have remained irreversibly adsorbed or another stabilization mechanism occurred.

Gafonova and Yarranton (2001) showed that at sufficiently high resin concentrations in model systems of asphaltenes, resins, toluene, and heptane, the resins appeared to replace asphaltenes at the interface. They interpreted this behavior as competitive adsorption. Interestingly, in this case, the adsorption of the smaller resin molecules reduced emulsion stability. Hence, the high stability observed for concentrated bitumen emulsions may indeed come from a different mechanism.

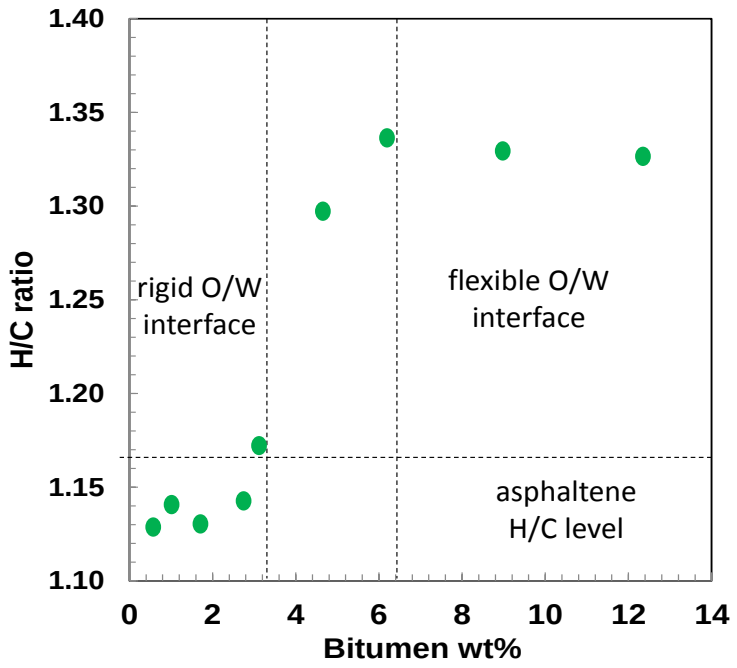

Figure 2.13 Hydrogen-to-carbon (H/C) ratio for interfacial material recovered from emulsion droplets at different bitumen concentrations in the oil phase, adapted from Czarnecki and Moran, (2005).

Czarnecki and Moran (2005) also hypothesized that asphaltene components compete with the low-molecular weight, but highly surface active material (*e.g.*, sodium naphthenates) to adsorb at the interface. The small molecules are assumed to adsorb quickly and reach the equilibrium on the interface. Asphaltene adsorption seems to be slow and irreversible. Therefore, the asphaltenes can accumulate over time and displace the other reversibly adsorbed from the interface. A schematic of asphaltene adsorption in the presence of higher surface active molecules is shown in the Figure 2.14. After a sufficiently long enough time, the interface becomes completely saturated by asphaltene material despite their lower

affinity for the interface compared with other surface active materials. If this mechanism is correct, some of the differences in bitumen films, Figure 2.13, may be time dependent.

2.4.2 Effect of Inorganic Solids on Asphaltene Films and Emulsion Stability

As noted previously, heavy oil and bitumen can contain inorganic solids including silica and clays from the reservoir and corrosion products acquired during production and processing (Zahabi *et al.*, 2010; Jiang *et al.* 2011; Masliyah *et al.* 2004). These solids can adsorb directly at the water-oil interface or on or with an existing surfactant film (Sztukowski and Yarranton, 2005). Biwettable solids can create emulsions stabilized solely by solid particles, Pickering emulsions (Yang *et al.*, 2006). However, the solids in heavy oil oilfield emulsions are believed to interact with the surface active components of the crude oil. Vander Kloet *et al.* (2001) used a micropipette technique to study the effect of asphaltenes and solids in the interfacial films properties and emulsion stability. It was found that solids exhibited a marked tendency towards the formation of interfacial skin layers and lowered the interfacial tension in heptol-asphaltene solutions, but the presence of these skin layers did not necessarily provide a barrier to droplet coalescence.

Most researchers have found that emulsions with both solid particles and asphaltenes combined tend to be more stable than those stabilized by asphaltenes alone. Sztukowski and Yarranton (2005) observed that fine particles (*i.e.,* platelet-shaped particles ranging from 50 to 500 nm) enhanced emulsion stability as long as enough asphaltenes were present in the organic phase to occupy the majority of the interface. Sztukowski and Yarranton (2005) also found that at low solids concentrations, coarse solids replaced asphaltenes on the interface acted as bridges between individual water droplets, increasing then the mean diameter of water droplets, and improving the water-oil separation. Conversely, relatively high concentrations of coarse solids strongly stabilized emulsions by preventing close contact between water droplets and formed multilayers on the interface. Solids may also increase the overall emulsion viscosity and reduce the chances of segregation of water and oil (Yan, 2001).

2.5 Effect of Salinity and pH on Oilfield Water-in-Oil Emulsions

Virtually all petroleum production involves the co-production of water that exists naturally in the formation from which the oil is produced. Formation water contains a variety of electrolytes and the composition ranges widely depending on the source formation. The high chloride content and/or pH of the water emulsified in oil can lead to operational problem such as downstream corrosion and formation of stable emulsions (Asekomhe *et al.*, 2005). Salinity and pH are also known to affect interfacial properties and emulsion stability (Liu *et al.*, 2006; Langevin *et al.*, 2004).

2.5.1 Formation Brine Chemistry

Reservoir water contains salts and dissolved solids including sodium chloride, calcium chloride, magnesium chloride, potassium chloride, sodium sulfate, and sodium bicarbonate (Dandekar, 2006; Kiran *et al.*, 2011). The brine composition varies considerably from field to field. In general, sodium chloride is found in greater concentration than the other salts and can vary from 50 to 250,000 ppm depending on the oil field.

Table 2.4 shows the ranges of sodium and chloride ions and the total dissolved solids for a number of major oil producing regions, as reported by Collins (1992). Dissolved salt concentration is usually expressed in milligrams of each solid per liter or parts per million on a mass basis (ppm). The majority of the reservoirs were found to have total dissolved solids (TDS) content from 0 to 250,000 ppm (0 to 25 wt %).

Table 2.4 Oil field water compositions for some major oil producing regions

Field	Na^+ (ppm)	Cl^- (ppm)	TDS (ppm)
Appalachian	50 - 98,300	70 – 216,300	475 - 344,110
California	40 - 15,015	10 - 27,100	80 - 47,995
Gulf Coast	30 - 61,000	20 – 105,000	353 - 171,300
Mid-continent(Texas)	210 - 122,500	460 – 212,000	1,710 - 356,600
Rocky Mountain	5 - 20,000	3 - 27,900	98 - 57,340

Canadian	660 - 104,600	200 – 173,500	1,205 - 290,070
Venezuelan	1,260 - 12,360	90 - 19,800	4,424 - 36,500

In oil sand extraction processes, much of the formation water is recycled leading to an accumulation of electrolytes in the process water which is controlled with make-up water and purge streams (Masliyah *et al*., 2004). Sodium ion concentrations up to 1,450 ppm and total salt concentrations of 3,000 ppm have been reported in oil sands industrial process water (Kiran *et al.*, 2011; Jiang *et al.*, 2011). In SAGD operations, the salt concentration of the produced water can range between 400 and 5000 ppm depending on the reservoir source (Dilip *et al.*, 2012; Whittaker *et al.*, 2014; Thimm, 2005). Thimm, (2005) reported chloride concentrations of SAGD produced water up to 2830 ppm for the McMurray formation.

2.5.2 Effect of Salinity on Interfacial Film Properties and Emulsion Stability

Film Properties

When inorganic salts are present in the aqueous phase, in the absence of natural surfactants, the salt ions are surrounded by a cage-like hydrogen-bonded structure, as illustrated in Figure 2.14. At the interface, water molecules are in contact with another phase and the hydrogen bonding is disrupted creating a higher energy environment for the ions. Hence, salt ions are depleted near the interface leading to a negative surface excess concentration. As dictated by the Gibbs adsorption isotherm Equation 2.2, interfacial tension increases at negative surface excess concentration (Kumar, 2012; Lashkarbolooki *et al.*, 2014). Hence, salt addition, in the absence of other surface active components, increases interfacial tension.

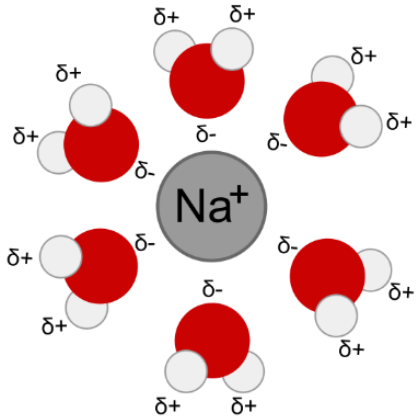

Figure 2.14 Schematic diagram showing hydrogen bonding in water and the formation of a cage-like structure surrounding an inorganic ion such as Na^+, adapted from Kumar, (2012).

In general, when surfactants are present, salt addition can cause anything from a slight increase to a significant decrease in IFT (Serrano-Saldaña *et al.*, 2004; Kumar, 2012; Lashkarbolooki *et al.*, 2014). For non-ionic surfactants there is not a significant interaction between the surfactant and salts. The interfacial tension between hydrocarbon/brines with a non-ionic surfactant was found to increase with increasing salt concentration at any given concentration of surfactant (Paul , 1997; Kumar, 2012).

For ionic surfactants such as asphaltenes and naphthenic acids, salt addition alters the activity of the surfactants so that the surface excess concentration on the interface increases and the interfacial tension decreases (Kumar, 2012; Kent and Saunders, 2001; Ghannam *et al.*, 2007; Márquez *et al.*, 2010). The salt ions likely help to neutralize the charge between the polar groups on the surfactant so that a closer packing on the interface is attained. The salt effect on IFT appears to be eliminated at sufficiently high surfactant concentration (Kumar, 2012). The IFT of a crude oil and its response to salt content cannot be predicted *a priori* because small quantities of surfactant and salts have a significant effect on the IFT and the amount and nature of this surface active material is not easily measured (Kumar, 2012).

In addition to the changes on IFT, salts can also alter the properties of the interfacial film. For instance, Alves *et al.* (2014) observed an increase on the interfacial viscoelastic properties and/or rigidity of the interfacial films when salts were added into a crude oil and brine system; 45wt% NaCl-brine and 55 wt% oil. Film rigidity and emulsion stability also increased more with aging time for brines compared to pure water. They attributed these results to a faster or rearrangement of asphaltenes at the interface when salts were present; that is, the adsorbed asphaltene molecules reorganize into a different molecular configuration at the interface (with lower free energy) over time (Moradi *et al.*, 2011). In contrast, Márquez *et al.* (2010) showed that the addition of calcium chloride in the aqueous phase of emulsions prepared with refined oil and polyglycerol-polyricinoleate as emulsifier, significantly reduced the interfacial tension and drop size, indicating a higher adsorption of emulsifier at the water-oil interface, but at the same time more compressible films were observed.

Emulsion Stability

Salt addition has been found to increase emulsion stability (Alves *et al.*, 2014; Kent and Saunders, 2001; Márquez *et al.*, 2010; Ghannam *et al.*, 2007). One possible explanation is a decrease in the average drop size. Aman *et al.* (2015) investigated the change in drop size after 24 hours of settling on emulsions prepare with 70vol% of crude oil (4.7 cP, density of 0.85g/mL at 20 ^{o}C) and 30vol% NaCl-brine, and found that the average droplet size decreased by 50% at salt contents higher than 0.1 wt% NaCl in the aqueous phase. However, Moradi *et al.* (2011) showed that, at concentrations higher than 2 wt% salt in emulsions prepared with crude oil (15.8cP,density of 0.86g/mL at 22^{o}C) and brine (NaCl, $CaCl_2$, Na_2SO_4,$MgSO_4$) at an oil-water ratio of 3:1, there was a significant increase in droplet size. Kent and Saunders (2001) found that the addition of $MgSO_4$ to emulsions prepared with 50 vol% of aqueous phase and 50 vol% of organic phase (50:50 *n*-decane-kerosene) increased the average drop size and at the same time significantly increased the emulsion stability. They did note a reduction in interfacial tension with the increased $MgSO_4$ content.

Ghannam *et al.* (2007) studied the effect of salt on water-in-oil emulsions prepared with light crude oil (31.2 ^{o}API). They observed that the water content within the emulsions strongly increased (less water resolved) with the addition of 5 wt% NaCl and the high stability was maintained after 48 hours. They also noted lower IFT between the crude oil and brine. Márquez *et al.* (2010) concluded that the high stability of emulsions was a consequence of the reduction of the IFT rather than the viscoelastic properties of the film. On the other hand, Alves *et al.* (2014) attributed the high stability of crude oil/brine emulsions with increased salt content to the enhanced interfacial viscoelastic properties and/or rigidity of the interfacial films.

Moradi *et al.* (2013) concluded that the ionic strength affected the adsorption of naphthenic acids in competition with asphaltenes at the water-oil interface. They found that high salinity hindered the asphaltene adsorption and therefore more of the interface was available for the adsorption of organic acids, thus lowering the emulsion stability.

2.5.3 Effect of pH on Film Properties and Emulsion Stability

The pH of produced water strongly depends on factors such as origin of the crude oil, its TAN (*i.e.*, the amount of available RCOOH), the molecular weights of RCOOH (*i.e.*, the degree of biodegradation of the crude oil), the volume of emulsified aqueous phase, the bicarbonate concentration, and the nature and concentration of salts present in the brine. In acidic oil fields, the final pH of aqueous phases is mainly controlled by the equilibrium between CO_2 in the gas phase during oil depressurization and the carbonated species dissolved in the aqueous phase, such as HCO_3^- and CO_3^{2-} (Arla *et al.*, 2007).

Due to their amphoteric properties, asphaltenes can be charged at low pH (cationic) and high pH (anionic) increasing their hydrophilic behavior and tendency to accumulate more easily at the water-oil interface. For example, Arla *et al.* (2011) prepared water-in-oil emulsions using acid crude oil. Initial pHi and final pH_f of aqueous phases where measured before and after emulsification with the crude oil. Figure 2.15 shows a significant decrease in final pH_f compare with the initial pHi after the contact with the oil phase. This reduction

occurs because some of the hydroxyl groups react with organic acids, RCOOH, to form ionized carbonic acids, RCOO-; in other words, the most naphthenic acids present in the crude oil were converted into naphthenates, as reported by (Arla *et al.*, 2007; Mclean and Kilpatrick, 1997). Experiments performed for two different bitumen samples showed that the higher the acid content of the bitumen, the higher the ionization and the lower the final pH_f. The ionization of the asphaltenes affects the interfacial tension, film properties, and emulsion stability.

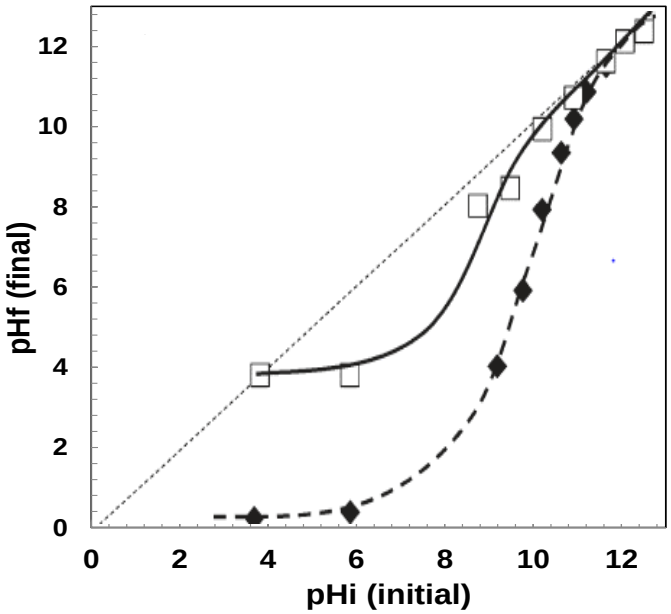

Figure 2.15 Initial *pH*i and final *pH*f of aqueous phases for two bitumen samples: bitumen 1 full-symbol (*60 wt% of total acids)*, bitumen 2 open-symbol (*9wt% of total acids*), adapted from Arla *et al.,* (2011).

Film Properties

Several authors have reported significant decrease in interfacial tension between water and crude oils at high and low pH, confirming that the acidic and basic functional groups contained in the asphaltenes can be ionized at different pH (Kokal, 2002; Langevin *et al.*, 2004; Poteau *et al.*, 2005; Arla *et al.*, 2007; Jestin *et al.*, 2007; Elsharkawy *et al.*, 2008; Aguilera *et al.*, 2010; Ortiz *et al.*, 2010). The ionized asphaltenes likely adsorb more strongly at the interface than their corresponding non-ionized form, both reducing interfacial tension and contributing to irreversible film formation.

Ortiz *et al.* (2010) studied the effect of pH on the surface pressure isotherms of asphaltene films in organic phases of 5 g/L asphaltenes dissolved in 25/75 heptol. They observed low compressibility films at pH 3.3 and more compressible films at pH 4.5 and neutral pH 7. However, Zhang *et al.* (2003) evaluated the surface pressure isotherms of bitumen diluted with toluene (5:1 toluene: bitumen) at pH values of 3.3, 5.8, and 11.2 in the aqueous phase and observed that, for a monolayer of asphaltene, the packing of polyaromatic rings and alkyl side chains dominated the interactions of the ionized hydrophilic headgroups of an asphaltene molecules. Consequently, they concluded that the shape of the surface pressure isotherm was not sensitive to pH. The reason for the different results from the two studies is not known. It is possible that Zhang *et al.* used the highest molecular fraction of the asphaltenes for their measurements (see Table 2.3). If that is the case, the packing effect of these large species may dominate more than would be observed for the whole asphaltenes used by Ortiz *et al*.

Arla *et al.* (2011) used oscillating drop tensiometry to evaluate the interfacial rheological properties in acidic crude oils at different pH. They observed the formation of a 2-dimensional gel-like adsorbed layer at the water-oil interface at neutral and alkaline pH conditions. Apparently, the acidic macromolecules, mostly asphaltenes and heavy naphthenic acids, were the main components of the interfacial gel-like structures. When gel films were formed at droplet interfaces, water-in-oil emulsions became extremely stable against coalescence even after centrifugation.

At high pH, the formation of sodium naphthenate (detailed in Section 2.2.3) can lead to the formation of a liquid crystal layer, which is primarily produced *in-situ* at the water-oil interface. Liquid crystals can dissolve in the water phase at low oil-to-water ratios, but at high oil-to-water ratios, it can also spread spontaneously at the interface and form an equilibrium phase. According to Horváth-Szabó *et al.* (2002), the presence of liquid crystals explains the difficulty in removing water from oil crudes below 2% water concentration. The presence of liquid crystals at water-oil interfaces could also explain the

high stability of rag layers encountered frequently in industrial process (Czarnecki, 2009; Sarac and Civan, 2007).

Verruto and Kilpatrick (2008) investigated the interfacial film thickness and the compositional makeup of the interfacial films stabilizing water-in-oil emulsions at different pH of aqueous phase. Results showed that for 3 wt% asphaltene in toluene solutions prepared at pH 7 and pH 10, the asphaltene mass on interface increased from 2.2 to 2.6 mg/m^2, respectively. Interestingly, the results showed that, in addition to asphaltenes and solvent, the films also contained water. At pH 7, about 8 vol% of the interfacial film structure was determined to be aqueous, at pH 10 the water composition in the film increased to 12 vol%. They speculated that the film-based water arose from the affinity of the asphaltenes at the interface to polar groups, such as, phenols, pyrroles, pyridines and carboxylic acids. This increase in film water composition may be necessary to maintain the deprotonated state of the resulting carboxylate ion, which has a high affinity for briny water.

Emulsion Stability

Several authors have reported a high increase in emulsion stability at high pH and a moderate or strong increase at very low pH (Kokal, 2002; Langevin *et al.*, 2004; Poteau *et al.*, 2005; Arla *et al.*, 2007; Jestin *et al.*, 2007; Elsharkawy *et al.*, 2008; Aguilera *et al.*, 2010; Ortiz *et al.*, 2010). For instance, Poteau *et al.* (2005) measured the stability of water-in-oil emulsions at different pH of aqueous phase. They observed a low fraction of water resolved (more stable emulsions) at extreme pH values (2 and 12), as shown in Figure 2.16. At high and low pH, asphaltenes had a strong affinity for the interface, the interfacial tension was reduced, the viscoelastic properties increased, and coalescence was hindered. Emulsion stability increased with aging time consistent with slow adsorption kinetics and interfacial film formation. Experiments using only maltenes (deasphalted bitumen) were also performed and very unstable emulsions were obtained (100% water resolved). The exception was at pH 12 where small surface active molecules that remained in the maltenes, such as carboxylates, were likely ionized and adsorbed at the interface.

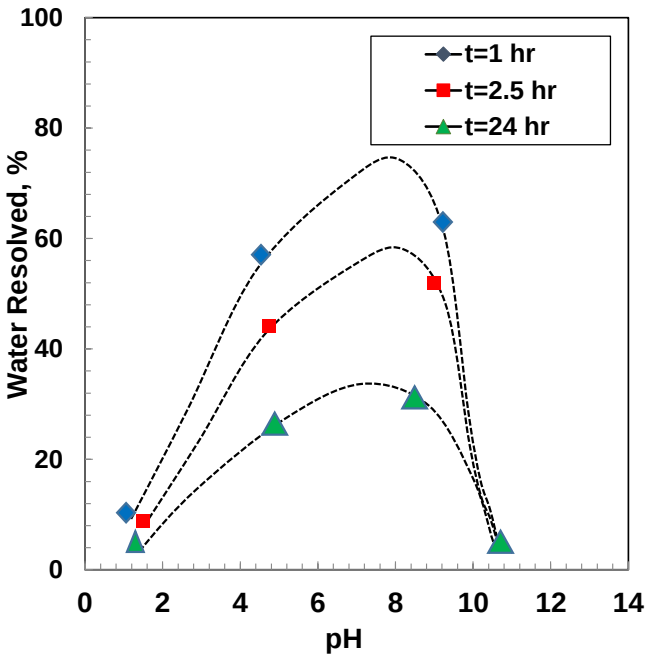

Figure 2.16 Water resolved as a function of pH of the aqueous phase after centrifugation at different aging times, adapted from Poteau *et al.*, (2005).

Li *et al.* (2006) concluded that interfacially active components formed in the reaction between asphaltene surface-active fractions and alkaline solutions had the highest mechanical strength and were able to enhance the stability of water-in-oil emulsions. However, McLean and Kilpatrick (1997) observed low emulsion stability in alkaline solutions (pH 12). They stated that the ionization of the surface-active material followed by an internal repulsion on the films destroyed the mechanical stabilization and improved coalescence. Kokal (2002) reconciled these contradictions by suggesting that for most crude oil-brine systems, an optimum pH range exists for which the interfacial film properties exhibits minimum emulsion stabilizing, or maximum emulsion breaking properties. The optimum pH for minimum emulsion stability depends on both the crude oil and brine composition.

2.6 Chapter Summary

Water-in-crude oil emulsions are often encountered in oil production, transport and processing. The stability of these emulsions is mainly attributed to the adsorption of natural emulsifiers at the water-oil interface such as asphaltenes, naphthenic acids, and biwettable fine solids. For water-in-heavy oil emulsions, asphaltenes appear to be the main contributing factor to emulsion stability. Asphaltene molecules tend to adsorb irreversibly at the interface, increasing film rigidity and reducing interfacial tension; both of these factors create more stable emulsions. The absorbed material on the interface, seems to be primarily made of the polar fraction of the asphaltene particularly components relatively rich in oxygen and sulfur.

Asphaltenes are amphoteric materials, that is, they can be charged at extreme pH values, increasing their surface activity and enhancing emulsion stability. The ionization seems to be more marked at high pH values and strongly depends on the crude oil composition and aqueous phase chemistry.

The interaction between asphaltenes and organic acids is not well understood and the literature presents conflicting opinions. Asphaltenes may aggregate with naphthenic acids and adsorb irreversibly on the interface. However, it is also possible that asphaltene compete with the low-molecular weight but highly surface active material (*e.g.*, sodium naphthenates) to adsorb at the interface. Small molecules are assumed to adsorb quickly and reach the equilibrium on the interface, while asphaltene adsorption seems to be slow and irreversible.

Salt addition decreases the interfacial tension between oil and water when an ionic surface active components, such as asphaltenes, are present. However, the effect of salt and pH on emulsion stability is not yet well understood and the reported effect of salts on emulsion stability are incomplete and sometimes contradictory. Some authors have observed an increased on emulsion stability and rigidity of the interfacial films even at very small salt contents. On the other hand, weaker films and less stable emulsions with the increased salt

content have also been reported. Similarly, some authors have observed that salt addition decreases the average water drop size with others observed an increase in drop size.

CHAPTER THREE:

EXPERIMENTAL METHODS

This chapter describes the experimental procedures used to measure the stability of water-in-oil emulsions, determine the mass surface coverage, and measure the interfacial film properties. Emulsion stability was assessed in terms of water resolved after several cycles of centrifugation and heating at 60°C. From the settled emulsions, the following information was also obtained: 1) the mass of asphaltenes on the interface; 2) the drop size distribution, and; 3) the volume fraction of water in the settled emulsions. Interfacial film properties were assessed by measuring interfacial tension and surface pressure isotherms at 21°C. The experiments were performed on two types of emulsion systems: 1) model emulsions consisting of solids-free asphaltenes diluted in heptol, and; 2) crude oil bitumen diluted in heptol.

3.1 Materials

3.1.1 Chemicals

Asphaltenes were precipitated from bitumen using technical grade *n*-heptane obtained from Anachemia. Solids were removed from the asphaltenes ACS grade toluene from BDH. *n*-Heptane (99.4% purity) and toluene (99.99% purity), both from EMD Millipore, were used to prepare the organic phase for the model and diluted bitumen emulsions, and for interfacial tension measurements. Brine phases were prepared from reverse osmosis (RO) water provided by the University of Calgary and the following salts (all ACS grade or better): sodium chloride (NaCl) and calcium chloride ($CaCl_2$) from EMD Millipore, potassium chloride (KCl) from Anachemia, sodium sulfate (Na_2SO_4,) from BDH, and sodium carbonate (Na_2CO_3) from J.T. Baker. The pH in the aqueous phase was adjusted with 1 M sodium hydroxide (NaOH) and 1 M hydrochloric acid (HCl). The pH of the solutions were measured using a VWR Symphony H10 pH meter.

3.1.2 Oil Samples

Oil sand (OS) bitumen and a steam-assisted gravity drainage (SAGD) bitumen were supplied by Suncor Energy, Inc., and a cyclic steam stimulation (CSS) bitumen was provided by Shell Canada, Ltd. The SAGD sample had been treated directly in the field to remove most of the water, and no chemicals were added. The OS bitumen had been blended with naphtha and then centrifuged to facilitate the water separation. The final product OS bitumen was collected in the field and had been sent to Maxxam Analytics, Inc. for distillation to remove residual naphtha diluent. The CSS sample was recovered from the field prior to the addition of any chemicals and had to be treated to remove most of the water. First, the CSS sample was sonicated at room temperature for at least 7 days to separate the water from the oil matrix. Finally, the sample was placed in a separatory funnel and left to settle for 5 days at 50°C. The water was then separated through the bottom of the funnel by decantation. The water contents of the bitumens were determined by Karl Fischer titration and are given in Table 3.1.

Table 3.1 Water content of bitumen samples

Sample	Water, wt%
OS Bitumen	3.4
CSS Bitumen	3.0
SAGD Bitumen	1.2

3.2 Asphaltene Extraction and Fractionation

3.2.1 Extraction of Asphaltenes from Bitumen

Asphaltenes were precipitated from bitumen with *n*-heptane and are designated as C7-asphaltenes. Toluene insoluble (TI) material (inorganic solids and associated hydrocarbons), which precipitate with asphaltenes, were removed to obtain "solids-free" C7-asphaltenes. The procedures were established previously (Sztukowski and Yarranton, 2005; Gafonova and Yarranton, 2001) and are described below. All experiments were performed using "solids-free" C7-asphaltenes. Sztukowski *et al.* (2005) showed that any

fine solids remaining in the asphaltenes after performing the above procedure had no significant effect on emulsion stability or surface pressure isotherms.

Asphaltenes were precipitated using *n*-heptane at a 40:1 (cm^3:g) *n*-heptane-to-bitumen ratio. The mixture was sonicated in an ultrasonic bath for 60 minutes at room temperature and then left to settle for a total contact time of 24 hours. After settling, the supernatant was filtered through a VWR #413 (equivalent to a Whatman #2) filter paper until about 20 vol% of the solution was left unfiltered. Additional *n*-heptane was added to the unfiltered mixture at a 4:1 (cm^3:g) ratio to the initial bitumen mass. The mixture was sonicated for 45 minutes, left to settle overnight for a contact time of approximately 18 hours, and filtered again using the same filter paper. The asphaltene-solids were left to dry in the filter paper for several days in a fume hood, and then dried overnight in a 60°C vacuum oven until the mass was constant.

To remove the TI, a solution of 10 g/L of asphaltene-solids in toluene was prepared. Usually, two grams of asphaltene were dissolved in 200 mL of toluene by sonicating the solution for 40 minutes and equilibrating the mixture for 60 minutes. The mixture was then divided into tared centrifuge tubes and centrifuged for 6 minutes at 4000 rpm, or 2952 RCF, in a Heraus Megafuge, The supernatant was decanted into a clean, tared beaker, dried for 5 days or until all the solvent was evaporated, and then dried overnight at 60°C in a vacuum oven. Most of the TI remained behind at the bottom of the tubes and were dried and weighed to calculate their mass.

The TI content of the asphaltenes is the mass of the TI divided by the mass of asphaltenes-solids. The solids-free C7-asphaltene yield is the mass of the asphaltene-solids less the mass of the TI all divided by the original mass of bitumen. The asphaltene yields and toluene-insoluble contents of the OS, SAGD and CSS asphaltenes are summarized in Table 3.2. Asphaltene yields and TI contents are repeatable to ±0.5 and ±0.2 wt %, respectively, based on a 90% confidence interval. Asphaltene molecular weights were measured with a

Jupiter model vapor pressure osmometer, and were repeatable to ±15%. The error analysis is provided in Appendix C, Sections C.1.

Table 3.2 C7-asphaltene (solids-free) yield and toluene insoluble content of asphaltene-solids for the bitumen samples used in this study

Sample	C7-Asphaltene wt% of bitumen	Toluene Insolubles wt% of asphaltene-solids
OS Bitumen	14.5	4.65
CSS Bitumen	16.2	1.70
SAGD Bitumen	18.3	0.41

3.3 Emulsion Experiments

3.3.1 Emulsion Preparation

All emulsions were prepared as 40 vol% aqueous phase and 60 vol% organic phase. For the model emulsions, the organic phase was 10 g/L solids-free C7-asphaltenes in 25/75 heptol (25 vol% *n*-heptane and 75 vol% toluene). Asphaltenes were first dissolved in toluene and sonicated for 20 minutes to ensure complete dissolution. Then, *n*-heptane was added and the mixture was sonicated for an additional five minutes to ensure homogeneity. For the water-in-bitumen emulsions, the bitumen solutions were prepared using concentrations of 10, 20 and 30 wt% of bitumen dissolved in 25/75 heptol. The mixture was sonicated between 60 and 240 minutes as required to ensure completely homogeneity. In both cases, the aqueous or brine phase consisted of the specified salt completely dissolved in RO water. The salts used in this study were NaCl, KCl, $CaCl_2$, Na_2SO_4 and Na_2CO_3. Salt solutions were prepared by serial dilution. Experiments were performed at salt concentrations ranging from 0 to 1 wt% salt (10,000 ppm).

Emulsions were prepared using a CAT 520D homogenizer at 18,000 rpm for 5 minutes. The aqueous phase was added dropwise to the organic phase while mixing. After mixing, the emulsion was settled for 1.5 hours, after which two phases were visible: a continuous organic phase (supernatant) and a concentrated or settled emulsion. The continuous phase was decanted; its volume was measured; and a sample was taken to determine the

equilibrium asphaltene concentration and the mass of asphaltene on interface. The settled emulsion was tested for emulsion stability, and the volume fraction of water in the settled emulsions and drop size distribution were measured, as outlined in Figure 3.1.

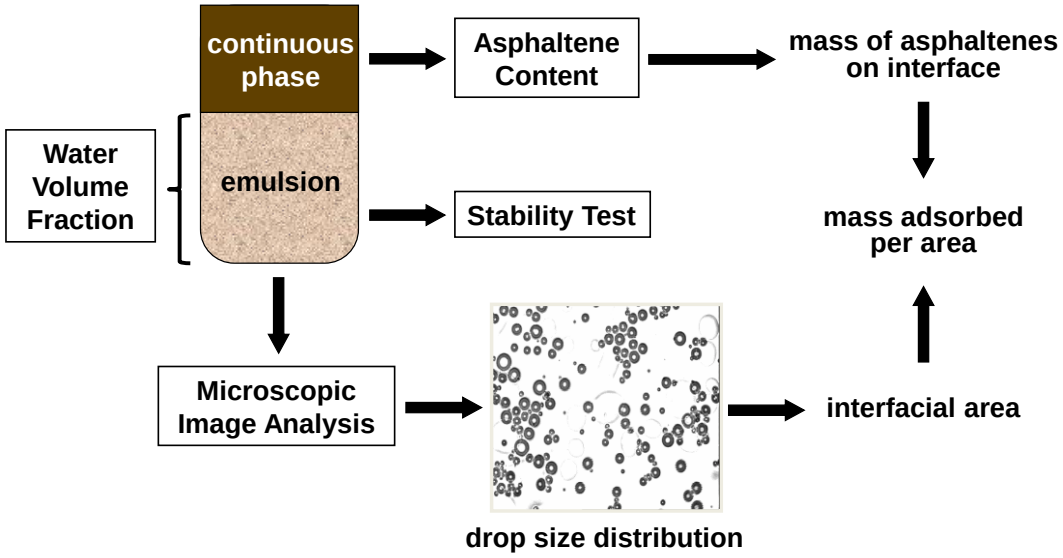

Figure 3.1 Schematic of emulsion tests.

3.3.2 Volume Fraction of Water in Settled Emulsions

The volume fraction of water or aqueous phase emulsified in the settled emulsion was calculated as the ratio between the volume of water emulsified in settled emulsion and the total volume of the settled emulsion,

$$\phi_{we} = \frac{\text{Vol. water in settled emulsion}}{\text{Vol. of settled emulsion}}, \tag{3.1}$$

where ϕ_{we} is the volume fraction of water in the settled emulsion. After 1.5 hours of settling, all the water remained emulsifed (no water settled out). Therefore, the volume of water in the settled emulsions was equal to the initial volume of water. For these experiments, emulsions were prepared with 20 mL of water and 30 mL of organic phase for a total of 50 mL of emulsion (or equivalent proportions). The volume of the settled emulsion was calculated as the initial volume of the whole mixture minus the volume of organic phase removed as supernatant.

3.3.3 Emulsion Stability

Emulsion stability was measured in terms of water resolved from the settled emulsion after repeated treatment cycles of heating and centrifugation. The settled emulsion was placed into 12 cm^3 graduated glass centrifuge tubes, capped and centrifuged for 5 minutes at 3500 rpm, or 2260 RCF. The tubes were immersed in a 60°C water bath for 2 hours and centrifuged again for five minutes. The heat-centrifuge cycles were repeated for a total of 10 hours (5 cycles). The volume of free water was recorded at the end of each cycle.

The amount of free water is reported as a percentage of the amount of initial water in the emulsion. The more resolved water, the less stable the emulsion. For concentrations exceeding 0.05 wt% of salt, the free water resolution varied by less than 1%. The reported free water percentages are an average of four measurements for the OS model emulsions and two measurements for the other emulsions. The repeatabilities were ±2.4, ± 6.4 and ±11% for the OS model emulsions, other model emulsions, and bitumen emulsions, respectively, based on a 90% confidence interval. The details of the analysis are shown in Appendix C, Section C.2.1.

Note, in all cases, the amount of free water increased monotonically over time as shown in Figure 3.2. Therefore, only the resolved water after 10 hours of treatment is presented later when the results are discussed.

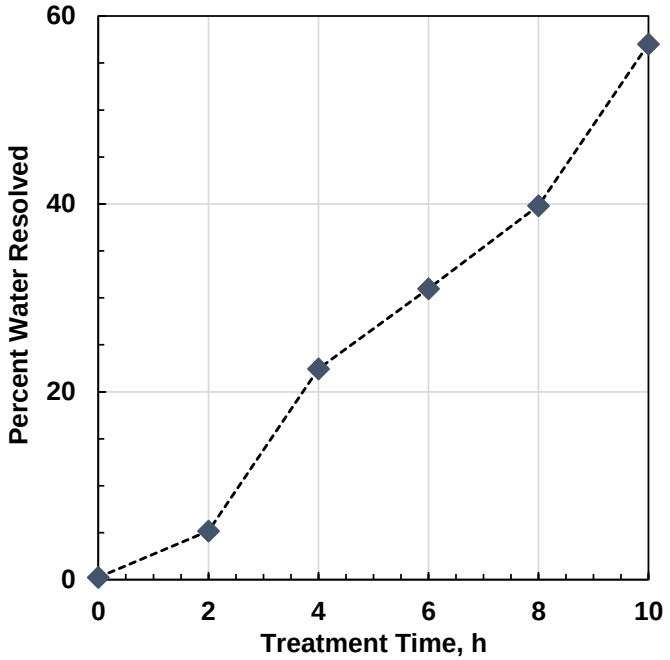

Figure 3.2 Water resolved from a settled emulsion versus time for a model system (40 vol% brine) with an organic phase of 10 g/L of C7-asphaltenes in 25/75 heptol, and an aqueous phase of 0% NaCl brine.

3.3.4 Emulsion Drop Size Distribution

After 1.5 hours of settling, a drop of settled emulsion was placed onto a hanging-drop glass slide. A drop of 25/75 heptol or continuous phase was added to the slide to ensure better separation of individual water droplets for the image analysis. Images were taken with a Carl Zeiss Axiovert S100 inverted microscope equipped with a video camera using Axiovision software. Figure 3.3 shows an example of a microphotograph of emulsified water droplets. Drop sizes of at least 500 droplets from accumulated images were measured. The Sauter mean diameter, d_{32}, was calculated as follows:

$$d_{32} = \frac{\sum_{i=1}^{N} f_i d_i^{\,3}}{\sum_{i=1}^{N} f_i d_i^{\,2}} \tag{3.2}$$

where f_i is the frequency of the i^{th} droplet. The reported free water percentages are an average of four measurements for the OS model emulsions and two measurements for the other emulsions. The repeatabilities were ±0.6 and ±0.9 μm for the OS model emulsions

and other model emulsions, respectively, based on a 90% confidence interval. Detail of the statistical analysis is presented in Appendix C, Section C.2.2.

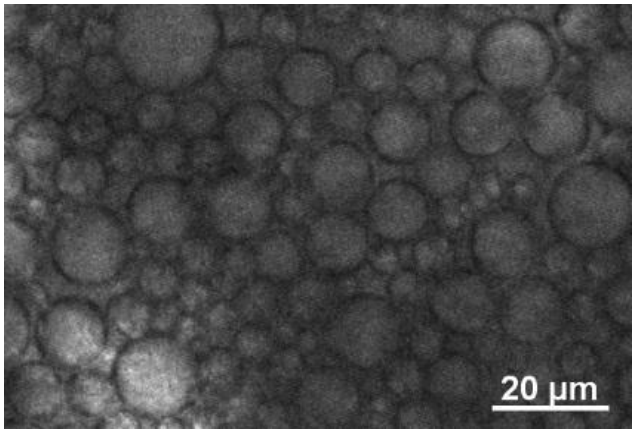

Figure 3.3 Microphotograph of emulsified water droplets from a model system (40 vol% brine) with an organic phase of 10 g/L of C7-asphaltenes in 25/75 heptol, and an aqueous phase of 0% NaCl brine.

3.3.5 Asphaltene Mass Surface Coverage

The procedure to calculate the amount of mass adsorbed on the interface was described by Gafonova and Yarranton (2001). The surface coverage of asphaltenes on the water/oil interface is given by:

$$\Gamma_A = \frac{m_{AI}}{SA} \tag{3.3}$$

where Γ_A is the surface coverage of asphaltenes, m_{AI} is the mass of asphaltene on the interface, and SA is the total surface area of the emulsified droplets. The mass of asphaltenes on the interface is equivalent to the mass lost from the continuous phase,

$$m_{AI} = m_{AT} - m_{eq}, \tag{3.4}$$

where m_{AT} is the total mass of asphaltenes and m_{eq} is the mass of asphaltenes remaining in the continuous phase after settling. Since the total volume of the continuous phase does not change, Equation 3.4 can be expressed as follows:

$$m_{AI} = m_{AT}\left(1 - \frac{C_A^{eq}}{C_A^0}\right) \tag{3.5}$$

where $C_A°$ and C_A^{eq} are the initial and equilibrium asphaltene concentration in the continuous phase, respectively.

The total surface area of the interface in the settled emulsion is related to the total volume of water as follows:

$$SA = \frac{6V_w}{d_{32}} \tag{3.6}$$

where V_w is the total volume of water and d_{32} is the Sauter mean diameter, given by:

$$d_{32} = \frac{\sum_{i=1}^{n} d_i^3}{\sum_{i=1}^{n} d_i^2} \tag{3.7}$$

Equations 3.5 and 3.7 are combined to obtain the following expression for the mass on interface:

$$\Gamma_A = \frac{m_{AT} d_{32}}{6V_w}\left(1 - \frac{C_A^{eq}}{C_A^0}\right) \tag{3.8}$$

The total mass of asphaltenes, the volume of water, and the initial asphaltene concentration are experimentally controlled variables. The Sauter mean diameter was determined from the drop size measurements as discussed previously. The equilibrium asphaltene concentration was determined experimentally as follows. The continuous phase (supernatant) was decanted after 1.5 hours of settling and its volume measured. The solvent was completely evaporated and the mass remaining was calculated. The equilibrium asphaltene concentration is simply the residual mass divided by the volume of the decanted continuous phase or supernatant. The reported mass surface coverages are an average of four measurements for the OS model emulsions and two measurements for the other emulsions. The repeatabilities were ±2.9 mg/m² for the OS and CSS emulsions and ±1.5 mg/m² for the SAGD emulsions, based on a 90%confidence interval. The errors were lower for smaller surface coverages but were better represented with absolute error rather than relative errors. Details are provided in Appendix C, Section C.2.3.

3.4 Interfacial Tension and Surface Pressure Isotherms Measurements

Interfacial tension (IFT) was measured using an IT Concept (now Teclis) Tracker drop size analyzer (DSA) and Windrop software. Drop shape analysis determines IFT from the shape of a drop at the tip of a capillary. The shape is dictated by the balance between the interfacial and gravity forces acting on the surface. The IFT acts to minimize the surface free energy of the system by reducing the surface area, drawing the drop towards a spherical shape. The gravity force acts upward on the droplet and tends to elongate the droplet (for a sessile drop when the fluid in the drop is less dense than the surrounding continuous phase). The force balance is solved using the Laplace equation and hydrostatic calculations and the required inputs are the drop radius, the density of the two phases, and the IFT. Since the density of the two phases and the shape of the droplet are known, the equations are fitted to the measured drop profile to obtain the best fit IFT value.

3.4.1 Drop Shape Analyzer Apparatus

The drop shape analyzer, Figure 3.4, consists of five main parts: 1) syringe piston actuator; 2) sample cell; 3) light source; 4) lens and charge-coupled device (CCD) camera, and; 5) instrument control with a personal computer and a manual motor control. For the IFT measurements, a syringe is loaded with the less dense fluid (hydrocarbon phase) and injected through a U-shaped needle. The syringe is placed in a motor driver piston (Item 1) and the tip of the needle is placed into an optical glass cuvette that contains the more dense aqueous fluid (Item 2). The hydrocarbon droplet is formed at the tip of the needle and illuminated by the light source (Item 3). The CCD camera captures the drop profile (Item 4) and is analyzed using the drop shape analysis software to calculate the IFT, the drop surface area, and the drop volume. The entire apparatus equipment is placed on an anti-vibrational bench to avoid disturbances during the measurements.

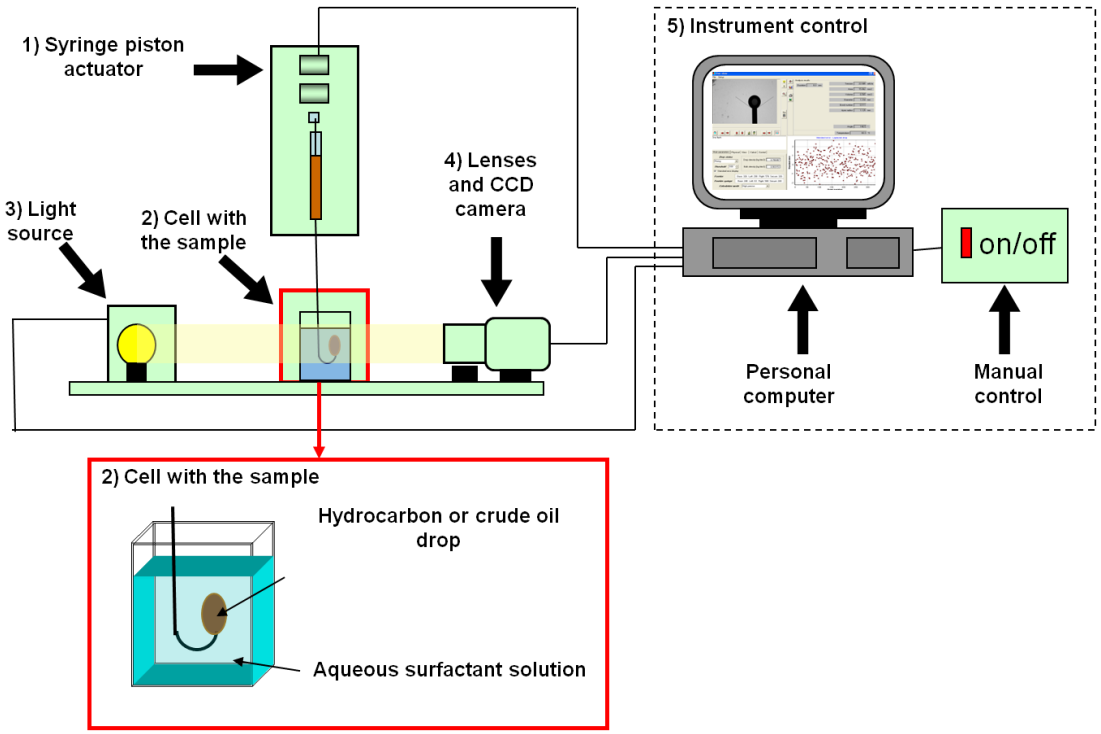

Figure 3.4 Schematic of Drop Shape Analyzer configuration.

The drop shape analyzer apparatus works on three different modes of calculation: high precise, precise, and normal. These calculation modes set the precision to which the software solves the Laplace equation and the number of iterations done per second to converge the solution; hence, setting the speed and accuracy of the measurement. High-precise and precise mode allow a very high precision and perform up to 20 and 15 iterations per second, respectively. However, these mode results in fewer measurements per second because the time required to solve the Laplace equation with more precision is longer. Normal mode allows a slightly less precise measurement and performs up to 10 iterations per second. In the present work, the high precise mode was used for measuring the interfacial tension.

3.4.2 Drop Shape Analysis Procedures

Solution Preparation

The organic phase used to measure the IFT for model systems was prepared using 10 g/L of asphaltenes diluted in 25/75 heptol and then sonicated for 20 minutes to ensure complete

dissolution. The diluted bitumen solutions were prepared in most the cases using 10 wt% of bitumen diluted in 25/75 heptol (unless otherwise specified). Bitumen solutions were sonicated for 40 minutes to ensure homogeneity. In both cases, fresh emulsions were prepared daily to avoid aging effects. Before the experiments, each of the two phases were presaturated with the other phase by adding two droplets of organic phase into the aqueous phase and *vice versa*, and contacting for 90 minutes. For the IFT and surface pressure measurements, the aqueous phases consisted of NaCl solutions. The aqueous phase was prepared using the same procedure as for the emulsion preparation (Section 3.3.1). The density of the brine and organic phases were measured using an Anton Paar DMA 4500M density meter at 20^{o}C.

Preparation of the Drop Shape Analyzer

In order to have accurate and reproducible measurements, the syringe, needle and cuvette were rigorously and repeatedly flushed with RO water, 2-propanol, toluene, and heptane. The cuvette was also soaked in 6 M nitric acid overnight periodically to ensure cleanliness. Before measuring the interfacial tension of the asphaltene-solvent and brine systems, the cleanliness of the instrument was verified by measuring the interfacial tension of pure hydrocarbons versus reverse osmosis water and comparing the measurements to literature value. Example validation measurements are shown in Table 3.3 and indicate good agreement with the literature.

Table 3.3 Interfacial tension (IFT) of hydrocarbons versus RO water at 21^{o}C

	Interfacial Tension (mN/m)	
Solvent	IFT, mN/m, DSA	IFT, mN/m, Literature
Toluene	36.2	35.8[a] 34.4[b], 35.4[c]
n-heptane	49.5	50.1[a], 49.7[b] ,50.1[c]

[a]Li and Fu, 1992; [b]Kumar, 2012; [c]Backes *et al.*, 1990

Interfacial Tension Measurement Procedure

The organic phase was loaded into a 1 mL syringe with a U-shaped needle and all air bubbles were removed. The syringe was immersed into the cuvette containing the aqueous phase and covered with a lid to avoid contamination and evaporation. The volume of the droplet was selected to be small enough to remain attached at the tip of the needle throughout the experiment, but large enough to provide an accurate value of interfacial tension. The droplets were typically 8-20 μL for the model hydrocarbon/brine systems. In the current work, 20 μL droplets were employed for most measurements.

The interfacial tension was recorded for between 60 and 120 minutes and a typical equilibrium interfacial tension versus time plot is show in Figure 3.5. The IFT initially decreases rapidly as the surface active material adsorbs at the interface. Then, there is a slower decrease in IFT as the material rearranges at the interface to minimize the free energy (Buckley and Fan, 2007). According to Hunsel (1988), the process is primarily controlled by a free-energy barrier situated at the interface and can be approximated as follows:

$$\gamma = \gamma^{\circ} + (\gamma_o - \gamma_e) e \frac{-t}{\tau} \tag{3.9}$$

where γ° is the interfacial tension at time zero, γ_e is the equilibrium interfacial tension and τ is a parameter with the same unit as time which signifies the relaxation time. This mono exponential model has been applied to find the equilibrium IFT for asphaltenes and crude oil systems (Kumar, 2012; Keleşoğlu *et al.*, 2011; Buckley and Fan, 2007). In the example shown in Figure 3.5, the IFT appears to reach equilibrium within 2000 s (33 min) and the equilibrium IFT can be taken directly from the data after 100 s. However, in some cases at asphaltene concentrations of 2 g/L, equilibrium was not reached within two hours. In these cases, Equation 3.9 was fitted to the data collected after the first ten minutes to obtain the equilibrium interfacial tension value.

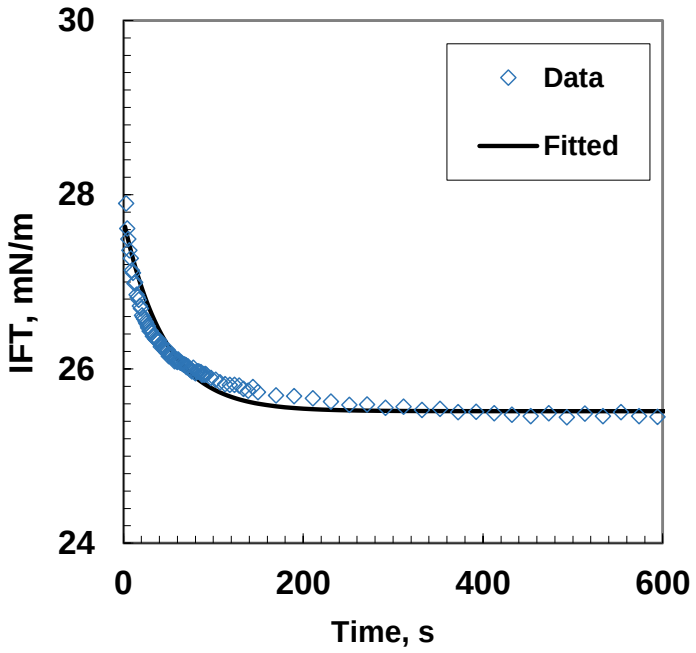

Figure 3.5 A typical plot of dynamic interfacial tension of C7-asphaltenes in 25/75 heptol, and an aqueous phase of 0% NaCl brine at 21°C. The data are fit with the exponential model.

The rapid initial decrease in interfacial tension over a short period of time is a result of asphaltenes diffusing from the bulk phase to the interface. The small changes on interfacial tension over longer periods of time might indicates that there is a replacement of some of the low molecular weight adsorbed material with asphaltene components (Czarnecki and Moran 2005) or that there is a slow structural rearrangement on the interface.

The reported interfacial tensions are an average of two measurements at each condition. The repeatabilities were ±0.75 and ±0.95 mN/m for the model and bitumen emulsions, respectively, based on a 90% confidence interval. Details are provided in Appendix C, Section C.2.4.

Surface Pressure Measurement Procedure

Recall that surface pressure, π, is defined as follows:

$$\pi = \gamma_o - \gamma \tag{3.10}$$

where γ_o is the difference between the interfacial tension of the pure solvent versus the aqueous phase (no adsorbed surface layer or surface active agent), and γ is the interfacial tension with an adsorbed layer. In this study, surface pressure isotherms (plots of surface pressure versus film ratio) were constructed where film ratio is defined as the ratio of the surface area at any given compression to the initial surface area of the droplet (SA/SA_o).

For the surface pressure isotherms, the interfacial films were aged 10, 30, 60 and 240 minutes. After aging, a stepwise compression was performed by withdrawing fluid from the droplet. At the end of each step, the surface area, drop volume and interfacial tension were recorded. After each step, the interface was allowed to stabilize for an interval of 30 seconds. The film compression steps ended when crumpling was observed or when the drop was so small that an accurate measurement was not possible. Figure 3.6 shows the sequence of compression steps, where two possible scenarios can occur: 1) the surfactants are irreversible adsorbed on the interface and the film crumples during the compression and 2) the surfactants are not irreversible adsorbed, which means, they tend to leave the interface during the compression and the film does not crumple. In most cases, the experiment ended when the film crumpled upon further compression and the crumpling ratio ($CR = A/A_o$ when the film crumpled) was recorded.

The film ratio at which the crumpling occurred is always the point at the lowest reported film ratio shown for a given isotherm. The reported crumpling ratios are an average of two measurements at each condition. The repeatability was ±0.05 for model and diluted bitumen systems, based on a 90% confidence interval. The details of the error analysis are shown in Appendix C, Sections C.2.5

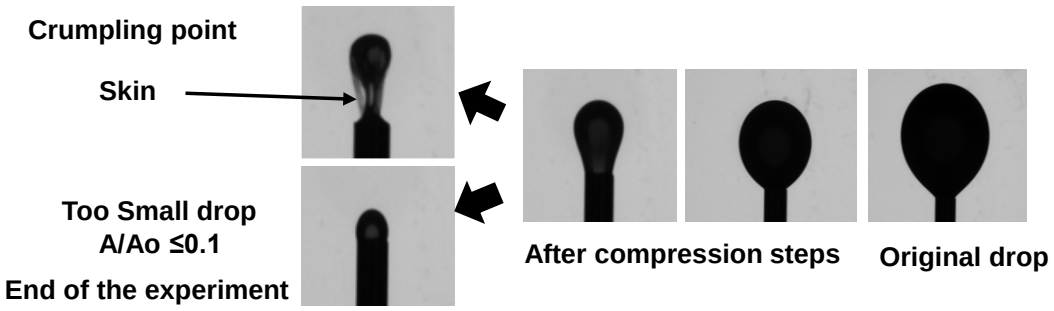

Figure 3.6 Compression steps during the surface pressure isotherms measurements for: 1) irreversible adsorption (upper left side), 2) reversible adsorption (lower left side).

CHAPTER FOUR:

RESULTS AND DISCUSSION [1]

In this chapter, the effects of salt type, salt content, and pH on emulsion stability are presented. The experiments were conducted on model systems stabilized by asphaltenes and diluted bitumen emulsions. To investigate the role of salts in emulsion stability, the effect of salt content on the interfacial properties of the emulsions are examined, including interfacial tension, surface pressure, molar and mass surface coverage. Drop size and emulsion packing are also considered. Finally, the differences in the stability and properties of the OS, SAGD, and CSS oil-in-brine emulsions are used to determine the critical factors affecting the stabilization of these emulsions

4.1 The Effect of Aqueous Phase Chemistry on Model Emulsion Stability

4.1.1 *Asphaltene Stabilized Model W/O Emulsions*

The effect of salinity and pH on water-in-oil emulsions was examined for model systems of 10 g/L OS asphaltenes dissolved in 25/75 heptol. The salt content of the aqueous phases varied from 0 to 15 wt% and the pH ranged from 2 to 12. Figure 4.1 shows the water resolved as a function of salt content for asphaltene stabilized emulsions at neutral pH (approximately 7.1). The addition of approximately 0.02 wt% of any salt sharply increased the emulsion stability, as shown by decreased resolved water. With an increase from 0.02 to 1 wt% salt, the stability increased slightly. At higher salt content, the stability was unchanged.

1. **The contents of this chapter were published in:** J. A. Rocha, E. N. Baydak, H. W. Yarranton, D. M. Sztukowski, V. Ali-Marcano, L. Gong, C. Shi, and H. Zeng, "Role of Aqueous Phase Chemistry, Interfacial Film Properties, and Surface Coverage in Stabilizing Water-in-Bitumen Emulsions," Energy & Fuels, *30*, 5240–5242.

The stability data were also plotted as a function of the ionic strength, I (M), Figure 4.2. The ionic strength is a measure of the ions concentration in aqueous solutions and can be described as follows:

$$I = \frac{1}{2}\sum_{i=1}^{N} c_i z_i^2 \tag{4.1}$$

where c_i is the molar concentration and z_i is the valence of the ion i (mol/L). Figure 4.2 shows that high emulsion stability is reached at ionic strengths above 0.03 M. These results confirm that the ionic strength significantly impacts the stability of the emulsions regardless of the type of salt present in the aqueous phase. Since the trends were similar for any type of salt, all further measurements were made with NaCl brine.

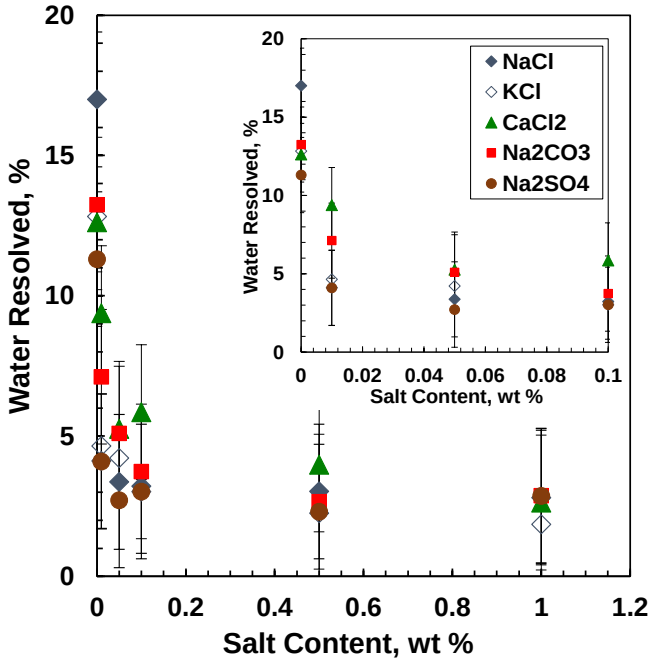

Figure 4.1 Effect of salt type and content on water resolved after 10 hours of treatment from model emulsions prepared with OS asphaltenes at 21°C. The inset shows an expanded scale from 0 to 0.1 wt% salt content. Organic phase: 10 g/L asphaltenes in 25/75 heptol; aqueous phase: RO water and salt; 40 vol% aqueous phase.

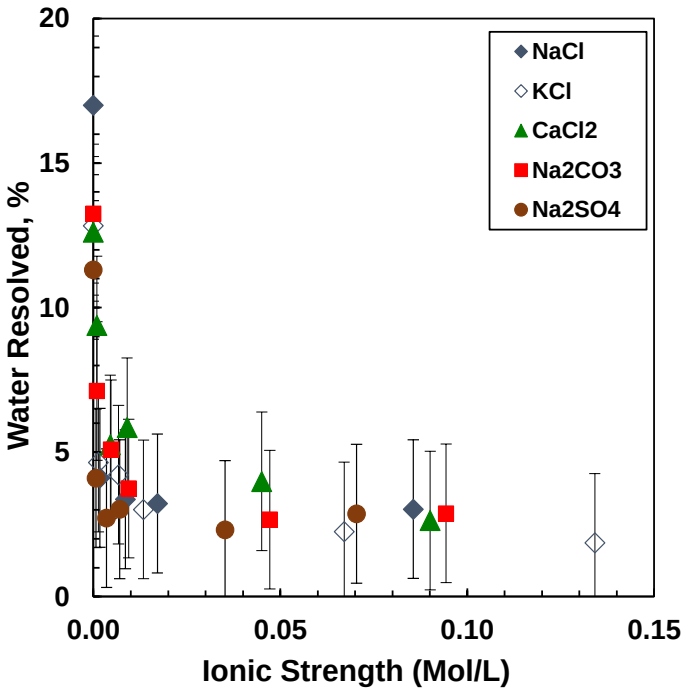

Figure 4.2 Effect of salt on water resolved from model emulsions prepared with OS asphaltenes at 21°C. Organic phase: 10 g/L asphaltenes in 25/75 heptol; aqueous phase: RO water and salt; 40 vol% aqueous phase.

Figure 4.3 compares the water resolved as a function of salt content for the emulsions prepared from OS, CSS and SAGD asphaltenes after 10 hours of stability treatment. In all cases, the emulsion stability increased dramatically (less resolved water) with a salt content of approximately 0.1 wt% and remained constant at higher salt contents. Note, the stability of the emulsions prepared from CSS and OS asphaltenes were almost identical once salt was added, but the emulsions prepared from SAGD asphaltenes were relatively less stable at all salt contents.

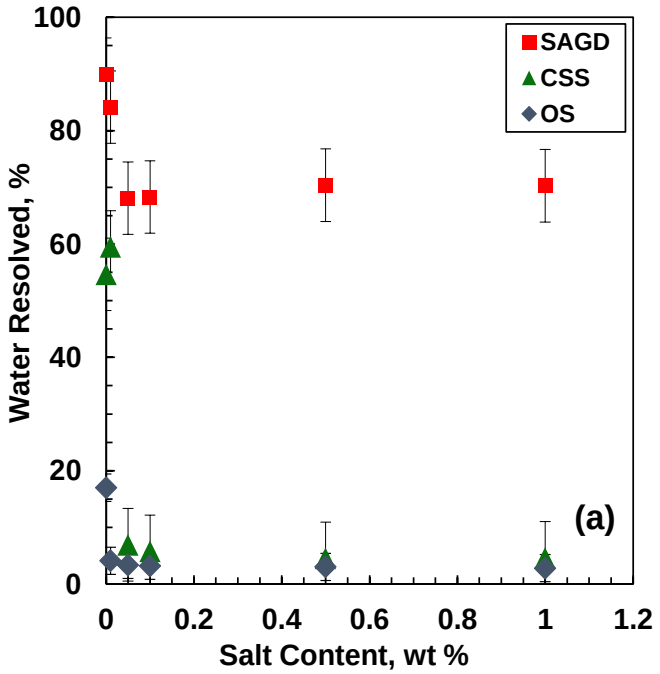

Figure 4.3 Effect of salt content on the water resolved for OS, CSS and SAGD model emulsions. Organic phase: 10 g/L of asphaltenes in 25/75 heptol; aqueous phase: RO water and NaCl; 40 vol% aqueous phase.

Figure 4.4a shows the water resolved as a function of the pH for the OS asphaltene emulsions. When no salts were present in the system, emulsion stability increased at high pH (10 and above). Note that the emulsion stability data were quite scattered at low and high pH, suggesting that the ionization of the asphaltenes at extreme pH values changes significantly with pH and therefore is sensitive to small errors in pH. The relative error was high but the absolute error was less than 5 percentage units.

When salt at any concentration above 0.1 wt% was present in the aqueous phase, the emulsion stability increased dramatically at all pH although it was greatest at low pH (<4) and high pH (>12). Figure 4.5b shows that similar trends were observed for CSS asphaltene emulsions although in this case the overall emulsion stability was lower and it decreased at low pH.

As detailed in Section 2.5, high emulsion stabilities at extreme pH have been previously reported (Kokal, 2002; Arla *et al.*, 2007; Ortiz *et al.*, 2010; Elsharkawy *et al.*, 2008; 2004; Poteau *et al.*, 2005). The protonation of sulfates and/or nitrogen bases, such as amines and amides, at the water-oil interface in acid environments increases surface activity of basic asphaltenes which alter the interfacial composition to reduce the interfacial tension and modify the film properties (Poteau *et al.*, 2005; Moran, 2007; Arla *et al.,* 2011; Gu *et al.,* 2003; Moran *et al.,* 2000). In basic environments, the dissociation anionic surfactants (*e.g.,* carboxylate or other acidic groups) has a similar effect. The reduced interfacial tension tends to create more stable emulsions (Ortiz *et al.*, 2010; Poteau *et al.*, 2005). Usually, the more strongly adsorbed asphaltenes create stronger mechanical films which further increase emulsion stability. On the other hand, McLean and Kilpatrick (1997) noted that the ionization of polar groups at extreme pH can create high surface charge densities that cause a repulsion between the molecules adsorbed on the interface which can disrupt the mechanical protection against coalescence. Hence, the response at extreme pH depends on the nature of the acid and basic groups in the oil. In most cases reported in the literature, stability increased at extreme pH. Note, NaOH addition also contributes to the concentration of dissociated sodium ions which increases the ionic strength of the aqueous phase and may also contribute to the emulsion stability.

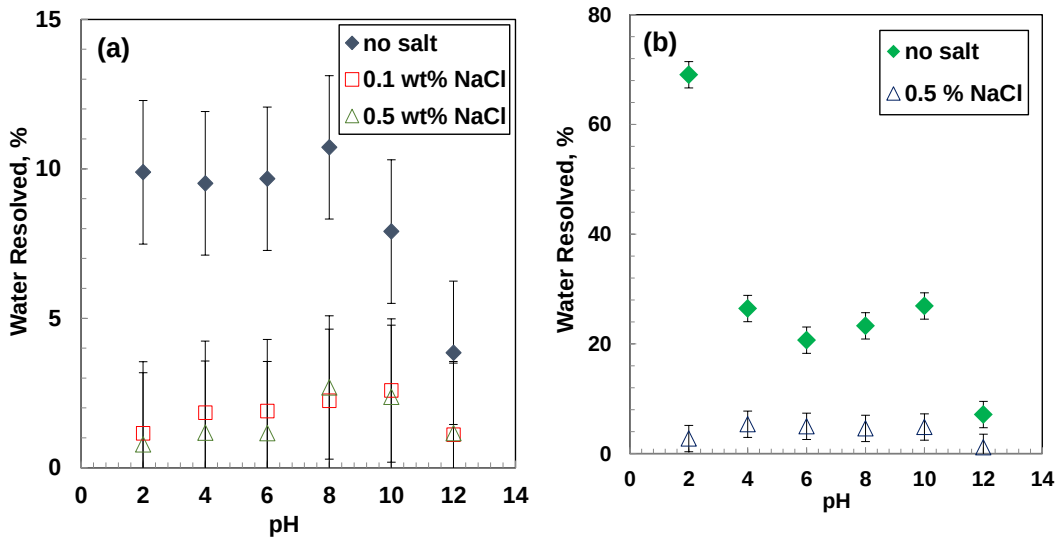

Figure 4.4 Effect of pH and salt on water resolved from model emulsions prepared at 21°C with a) OS asphaltenes; b) CSS asphaltenes. Organic phase: 10 g/L asphaltenes in 25/75 heptol; aqueous phase: RO water and NaCl; 40 vol% aqueous phase.

4.1.2 *Bitumen Stabilized Model Emulsions*

The effect of salts on emulsion stability was investigated for bitumen solutions at different concentrations; organic phases were prepared at 10, 20 and 30 wt% bitumen in a 25/75 solvent mixture. Table 4.1 shows the bitumen dilutions used for these experiments and their respective asphaltene content for the OS bitumen sample. Similar asphaltenes contents were obtained for CSS and SAGD samples, as detailed in Appendix A. The asphaltene content of the 10 wt% bitumen is nearly equivalent to the 10 g/L asphaltene concentration used for the model asphaltene stabilized emulsions. Therefore, most experiments were performed with 10 wt% bitumen.

Table 4.1 Bitumen wt% and their equivalent in asphaltene (g/L) for OS sample

Bitumen wt %	Density of Solution kg/m³	Asphaltene Concentration g/L
10	0.8344	12.2
20	0.8551	24.8
30	0.8708	37.9

Figure 4.5 shows the water resolved as a function of the salt content for solutions prepared with 10 wt% of OS bitumen after 10 hours of stability treatment. Note, the stability of the emulsions prepared from SAGD and OS bitumen solutions was very similar to those obtained with the model systems. However, the emulsions prepared with the CSS sample showed an unexpected decrease in stability at approximately 0.5 wt% salt content. Similar trends were also observed at 20 and 30 wt% bitumen, Figure 4.6b. The reason for this effect is not clear but it is possible that it arises from competitive adsorption. For instance, Czarnecki *et al.,* (2005) observed that asphaltenes may compete to absorb at the interface with low-molecular weight surface active material such as naphthenic acids. Asphaltenes are less likely to adsorb (or may adsorb much more slowly) at the interface when other surface-active components are present.

Moradi *et al.,* (2013) proposed that, in the presence of naphthenic acids, the asphaltene adsorption rate at the interface decreases as the salinity of the aqueous phase increases. At high ionic strength the naphthenic components accumulate on interface and serve as barriers for further adsorption of asphaltenes, lowering the emulsion stability. The CSS sample may contain a component(s) that, at high salinity, replaces the asphaltenes initially adsorbed at the interface.

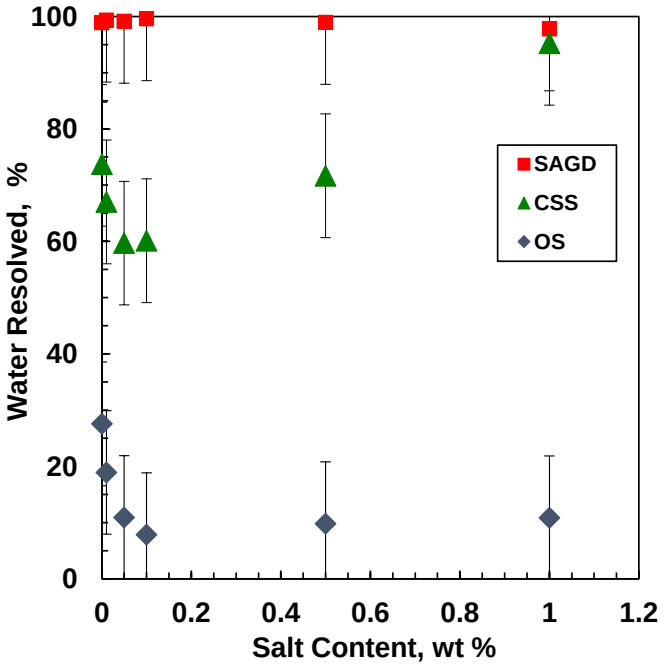

Figure 4.5 Effect of salt content on the water resolved for OS, CSS and SAGD dilute bitumen emulsions. Organic phase: 10 wt% of bitumen in 25/75 heptol; aqueous phase: RO; 40 vol% aqueous phase.

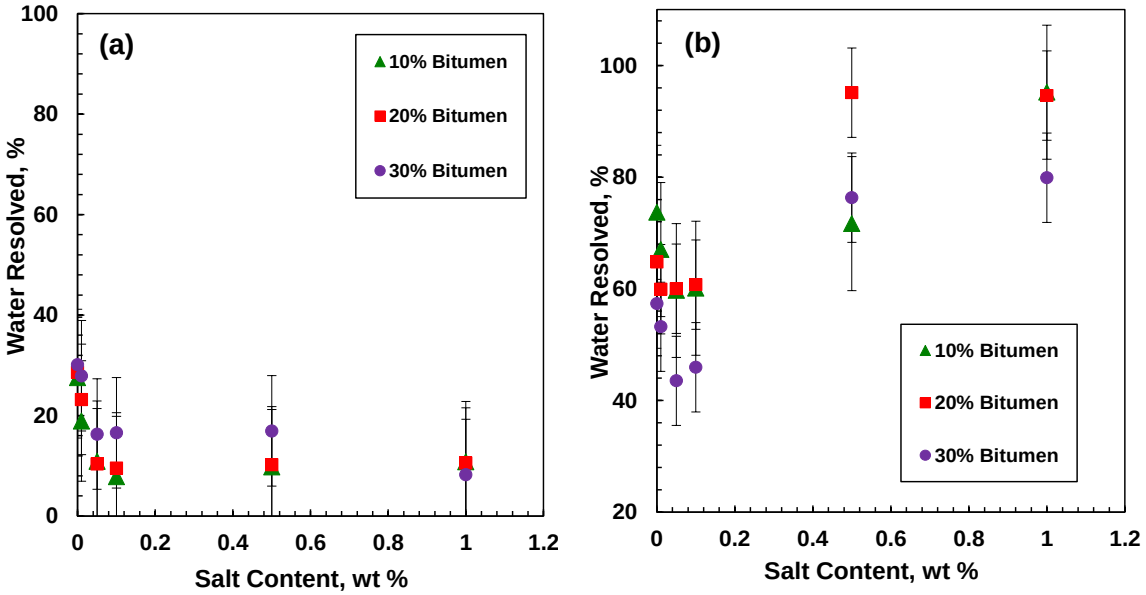

Figure 4.6 Effect of salt content on the water resolved for dilute bitumen emulsions: a) OS; b) CSS. Organic phase: 10, 20 and 30 wt% bitumen in 25/75 heptol; RO water and NaCl; 40 vol% aqueous phase. For the SAGD bitumen sample, 100 vol% of the water was resolved any bitumen concentration.

4.2 The Effect of Salt on Interfacial Film Properties

4.2.1 *Interfacial Tension (IFT)*

Typical plots of interfacial tension versus time for model and bitumen systems are shown in Figure 4.7. The IFT measurements were recorded over 1 hour or 3600 seconds. The IFT data in equilibrium was calculated using the decay model described in Section 3.4. Previous work had demonstrated that the type of salt had no effect on IFT (Kumar, 2012). Therefore, the IFT of asphaltene/brine systems was investigated with only one salt, NaCl.

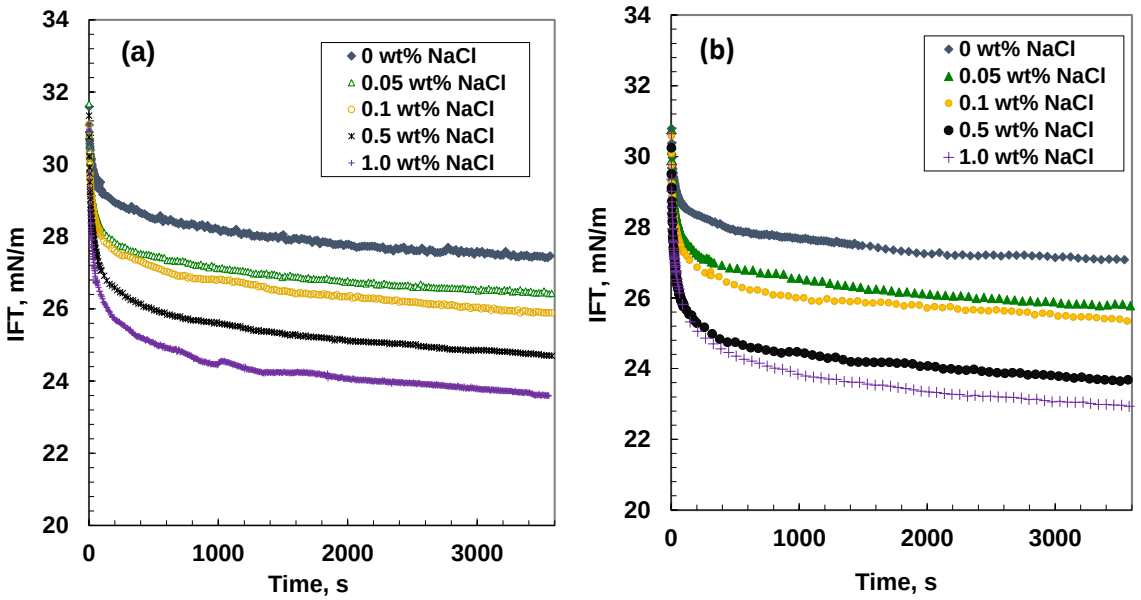

Figure 4.7 Interfacial tension versus time. (a) 10 g/L OS asphaltene in 25/75 heptol (b) 10 wt% OS bitumen in 25/75 heptol; both versus NaCl brine at 21°C**.**

Figure 4.8 shows the effect of salt content on the IFT of model systems of 10 g/L asphaltenes in 25/75 heptol and bitumen solutions of 10 wt% of bitumen diluted in the same solvent. In both cases, salt addition decreases the interfacial tension for all the different bitumen samples. Since asphaltenes behave like weak ionic surfactants, the salts can ionize and increase the solubility of the polar groups in the aqueous phase, reducing the IFT (Kumar, 2012; Lashkarbolooki *et al.*, 2014; Moran, 2007; Serrano *et al.*, 2004). The similar trends observed for the asphaltene and bitumen stabilized emulsions suggest

that the components absorbed at the interface come from the asphaltene fraction of the bitumen. Note that the IFT of the CSS bitumen/water system deviates slightly to lower IFTs compared to the trend observed for the CSS asphaltenes. This deviation supports the previously discussed idea that other components in this bitumen may replace the asphaltenes at the interface at higher salinities.

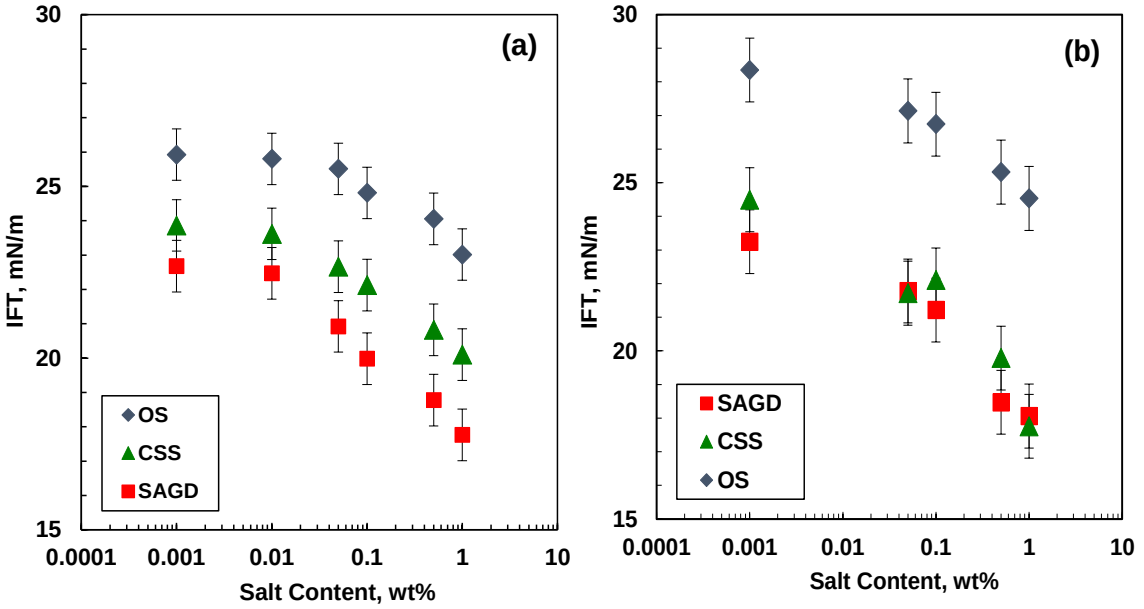

Figure 4.8 Effect of salt content on IFT (a) 10 g/L asphaltene in 25/75 heptol (b) 10 wt% bitumen in 25/75 heptol; both versus NaCl brine at 21°C.

4.2.2 *Surface Pressure Isotherms*

Salts may modify the composition of the interfacial film (via selective adsorption) or modify the interaction between the molecules at the interface *(e.g.*, by altering their configuration at the interface). Either mechanism may alter the properties of the interfacial film. Figure 4.9 shows surface pressure isotherms of 10 g/L OS asphaltene interfacial films aged for 60 minutes before compression at 21°C. The films exhibit crumpling indicating that the asphaltenes are irreversibly adsorbed. Irreversible films were observed at all salt contents and at different asphaltene contents and aging times (Appendix A.1). Note that

the crumpling ratio is the lowest film ratio shown in each surface pressure isotherm, as indicated in Figure 4.9.

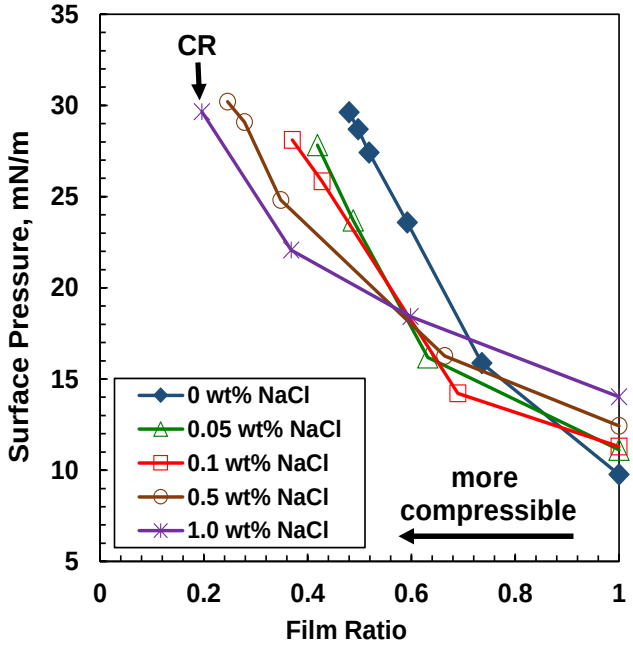

Figure 4.9 Surface pressure isotherms for 10 g/L OS asphaltene in 25/75 heptol, after 60 minutes; aqueous phase: NaCl brine at 21°C.

Figure 4.9 also shows that the addition of salt to the OS asphaltene film reduced the crumpling ratio (more compressible films). The trend is consistent with Márquez *et al.* (2010) who reported a decrease in both the viscous and elastic moduli (more compressible films) and increased emulsion stability with increased salt content, in solutions prepared with $CaCl_2$ brine and refine oil. On the other hand, Alves *et al.* (2014) observed an increase in both the viscous and elastic moduli (more rigid films) and more stable emulsions as the salt content increased in a crude oil and NaCl-brine system The contradictory results suggest a different combination of surface active components in the oil from each study, but no clear conclusion is possible without knowing more about the chemistry of the oils.

Nonetheless, Figure 4.10a shows that salt addition decreased the crumpling ratio of all the asphaltenes considered in this study, although the effect is small for the CSS asphaltene films for model systems. This trend was observed at all asphaltene contents and aging times

considered (Appendix A.2 and A.3). It is possible that the salts are attracting different components from within the asphaltenes to the interface. Kiran *et al.* (2011) showed more compressible films were formed when naphthenic acids were present at the interface compared with the films formed with pure asphaltenes. Similarly, if salt addition causes smaller asphaltene components to be attracted to the interface, the films may become more compressible. Figure 4.10b also shows that the same trends were observed for OS, CSS and SAGD asphaltenes films and for bitumen films. Again, it appears that the interfacially adsorbed material is derived from the asphaltenes.

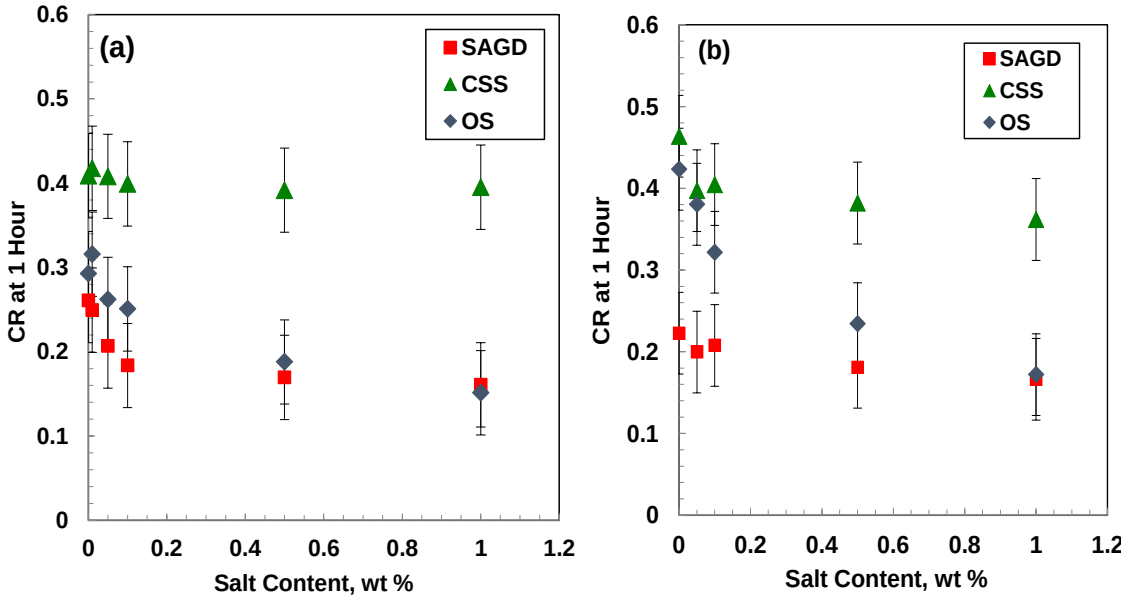

Figure 4.10 Effect of salt content on crumpling ratios (CR) of asphaltene films after 60 minutes aging at 21°C in 25/75 heptol: a) 10 g/L asphaltene; b) 10 wt% bitumen; aqueous phase: NaCl brine at 21°C.

4.3 Effect of Salt on Surface Coverage

4.3.1 *Molar Surface Coverage*

IFT can be related to the asphaltene concentration as follows (Yarranton and Masliyah, 1996; Kumar, 2012):

$$\gamma = \gamma^o - RT\Gamma_{m,S} \ln(1 + K_S^{org} x_S^{org}) \quad (4.1)$$

where γ° is the IFT between pure solvent and brine, R is the universal gas constant, T is the absolute temperature, x^{org} is the asphaltene mole fraction, K_s^{org} is the adsorption constant and $\Gamma_{m,s}$ is the molar surface coverage. Since the product, $x^{org}K_s^{org}$, is much greater than unity (even at small salts concentrations), the derivative of Equation 4.1 can be simplified to:

$$\Gamma_{m,s} = -\frac{1}{RT}\left(\frac{d\gamma}{d\ln x^{org}}\right) \tag{4.2}$$

The molar surface coverage on the interface was calculated at each salt concentration for each asphaltene sample. The average area of a molecule at the interface is the reciprocal of the surface coverage and is given by:

$$A = -\frac{1}{N_A}\frac{RT}{\left(d\gamma/d\ln x^{org}\right)} \tag{4.3}$$

where A is the average area occupied per molecule of asphaltene and N_A is Avogadro's number. The molecular weights of the asphaltenes in solution were required to calculate the asphaltene mole fraction in these experiments. Here, the molecular weight depends upon the concentration because solubilized asphaltenes self-associate (Agrawala and Yarranton, 2001; Sztukowski *et al.*, 2003). The mole fraction at each concentration was determined using the known mass fraction and the molecular weight data presented in Figure 4.11.

The increase in molecular weight of the OS and CSS asphaltenes with concentration shown in Figure 4.11 is typical for self-associating asphaltenes (Agrawala and Yarranton, 2001; Barrera *et al.*, 2013; Sztukowski, 2005). Interestingly, the SAGD asphaltenes show little evidence of self-association, this behaviour is likely due to prolonged exposure to the steam at high temperatures. Note that the molecular weight of the asphaltenes on the interface does not necessarily have the same values or follow the same trend with concentration as

the molecular weight of the bulk asphaltenes. Hence, the bulk phase molecular weights were only used to calculate the mole fraction of asphalenes in the bulk phase. The molecular weight of the interfacial asphaltenes is discussed later.

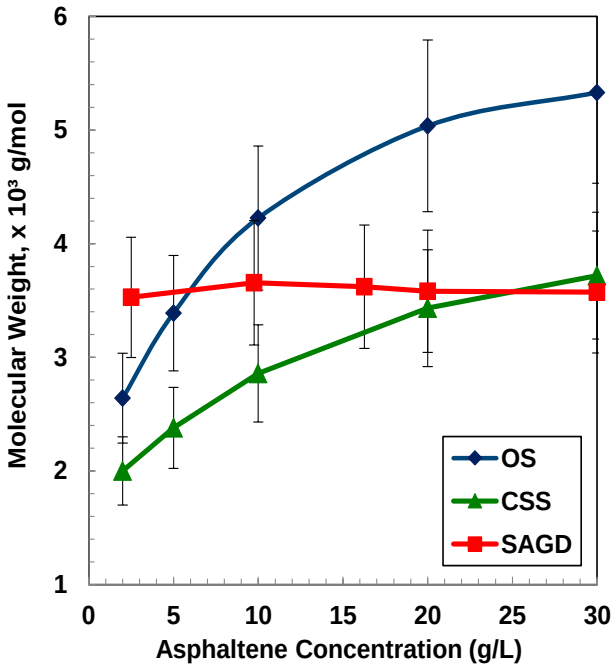

Figure 4.11 Molecular weight of asphaltenes extracted from SAGD, CSS and OS bitumen samples in toluene; 50°C.

Interfacial tension measurements are plotted against the logarithm of asphaltene concentration to calculate the slope required to determine the molar surface coverage and the average area of a molecule adsorbed at the water-oil interface. Figure 4.12 shows the plot of IFT versus mole fraction for the OS, CSS and SAGD asphaltenes when no salts are present. Figure 4.13 shows that the interfacial tension of OS asphaltenes in 25/75 heptol at different NaCl concentration. In all cases, the IFT is linearly related to the natural log of the asphaltene concentration indicating that the asphaltenes adsorb on the interface with a constant area over a wide concentration range.

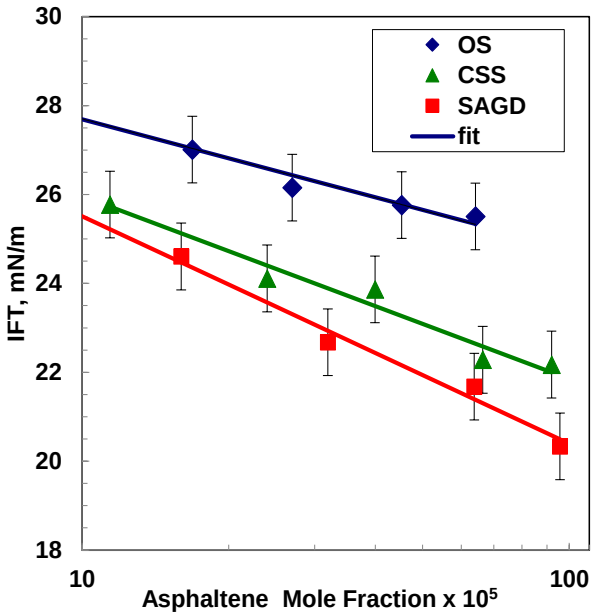

Figure 4.12 Interfacial tension of 10 g/L OS, CSS and SAGD asphaltenes in 25/75 heptol versus brine at 0 wt% NaCl at 21°C.

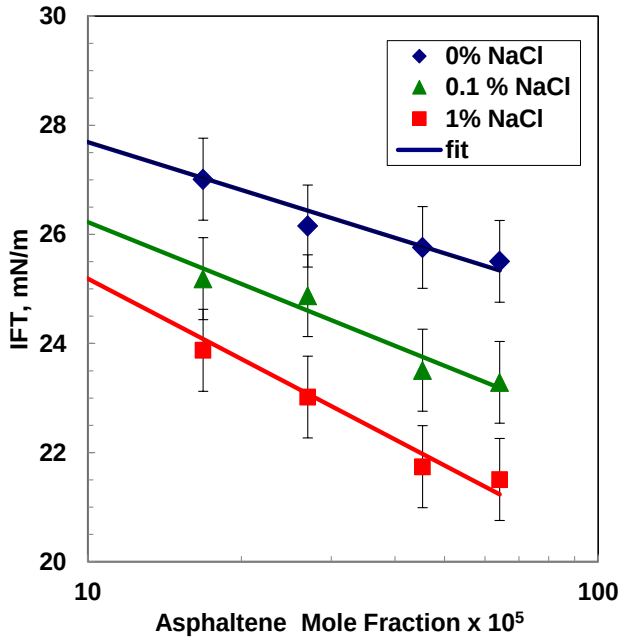

Figure 4.13 Interfacial tension of 10 g/L OS asphaltenes in 25/75 heptol versus brine at 0, 0.1 and 1 wt%; aqueous phase: NaCl brine at 21°C.

The molar surface coverage and the asphaltene molecular area at 0, 0.1 and 1 wt% NaCl for each asphaltene sample were calculated and are summarized in Figure 4.14. When no salt was present, the area of the asphaltene molecule varied from 1.8 to 3.2 nm² depending of the asphaltene source. These areas are consistent with the literature. For example, Rogel *et al.* (2000) observed an average interfacial area of asphaltenes in numerous solvent/water systems ranging from 1 to 4 nm². Sztukowski, (2005) observed asphaltenes interfacial areas varying from 1.26 to 1.55 nm^2 for asphaltenes diluted in 25/75 heptol. Figure 4.14a also shows that, as the salt content increased from 0 to 1 wt%, the molar surface coverage increased approximately 40% for all three of the asphaltene samples. Similarly, the area per molecule decreased by approximately 40%.

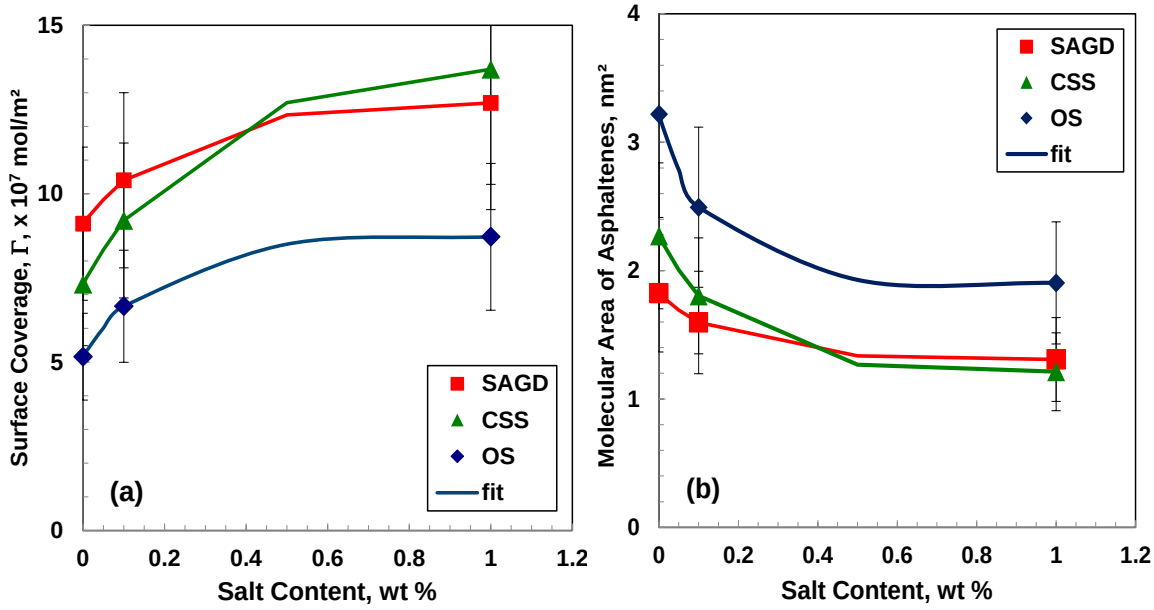

Figure 4.14 Effect of salt content on (a) surface molar coverage and (b) asphaltene molecular area (b) for 10 g/L asphaltenes in 25/75 heptol versus brine at 21°C.

4.3.2 *Mass Surface Coverage*

Figure 4.15a shows the mass of asphaltenes on the interface versus the salt content for the model emulsions prepared with different asphaltenes. For the OS and CSS asphaltenes, the adsorption increased from approximately 4 mg/m² at 0 wt% NaCl to almost 10 mg/m² at 1 wt% NaCl, an approximately 150% increase in the mass surface coverage. However, for the SAGD asphaltenes, the mass adsorbed at the interface was invariant at 3 mg/m², within

the error of the measurements. Figure 4.15b shows that similar results were observed for emulsions prepared with OS asphaltenes and $CaCl_2$ brines, consistent with lack of sensitivity of emulsion stability to the type of salt.

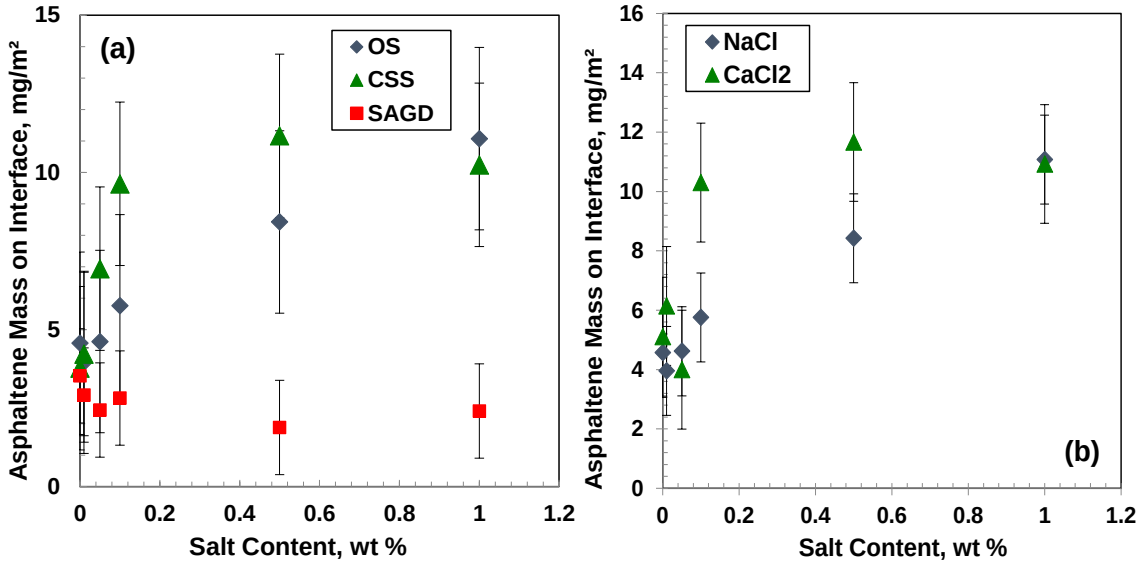

Figure 4.15 Effect of salt content on mass of asphaltenes on the interface of model emulsions at 21°C: a) OS, CSS, and SAGD asphaltenes and NaCl brine; b) OS asphaltenes and NaCl and $CaCl_2$ brines. Organic phase: 10 g/L asphaltenes in 25/75 heptol; 40 vol% aqueous phase.

The increase in surface coverage of the CSS and OS asphaltenes with increased salt content is not surprising for a substance that contains polar components that will interact with the salt ions in the aqueous phase. The added electrolytes can screen the electrostatic repulsive forces between these surfactants in the monolayer and allow for closer packing together on the interface (Gu *et al.*, 2003). Another possibility is selective adsorption of larger species or nanoaggregates at higher salt contents. The SAGD sample may be deficient in the more polar material or large nanoaggregates.

Note, that the mass surface coverage for the water-in-diluted bitumen emulsions was not measured because the equilibrium asphaltene concentration could not be determined with sufficient accuracy when a large proportion of maltenes is present. Also, the CSS and

SAGD water-in-diluted bitumen emulsions evolved free water even at initial conditions, invalidating the assumptions for the calculation.

It is surprising that the increase in the mass adsorbed at the interface observed for the OS and CSS asphaltenes with an increased salt content corresponds to more compressible interfacial films. This observation and the relatively small changes in molar surface coverage suggest that the molecules are not packing more closely together, but instead are forming a thicker layer.

4.3.3 *Apparent Molecular Weight of Interfacial Material*

Since the molar and mass surface coverage are known at the same conditions, the apparent molecular weight of the interfacial material can be determined from the ratio of the mass surface coverage to the molar surface coverage. Figure 4.16 shows the molecular weight of asphaltene on the interface versus salt content for the model emulsions. For the OS and CSS asphaltenes, the apparent molecular weight of asphaltenes on the interface increases sharply with the salt content and reaches a plateau by approximately 0.2 wt% NaCl. The salt appears to attract larger asphaltene nanoaggregates or to promote self-association at the interface. However, for the SAGD sample, the apparent molecular weight decreased slightly with increased salt content. The failure to build up higher molecular weight material on the interface is consistent with the lack of self-association observed for the SAGD asphaltenes, Figure 4.11.

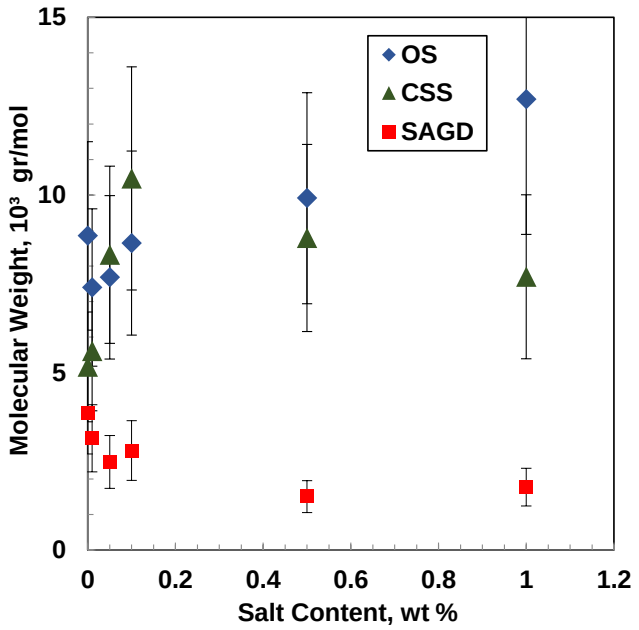

Figure 4.16 Effect of salt content on molecular weight on the interface of model emulsions at 21°C. Organic phase: 10 g/L of asphaltenes in 25/75 heptol; aqueous phase: RO and NaCl; 40 vol% aqueous phase.

4.4 The Effect of Salt on Droplet Size

Gafonova *et al.*, (2001) demonstrated that, for asphaltene stabilized emulsions, the micrometer-scale droplets generated by the homogenizer will coalesce until sufficient asphaltenes are trapped at the interface to prevent further coalescence. As discussed in Section 3.3.4, drop size distributions were gathered after a model emulsion had been settled for 1.5 hours, well after this initial period of rapid coalescence had occurred.

Figure 4.17a shows that, for the model emulsions in this study, the "stabilized" Sauter mean diameter (prior to emulsion treatment) decreased by 40%, on average, as the salt content increased from 0 to 1 wt% and was invariant at higher salt contents within the error of the measurements. Figure 4.17b shows that similar results with $CaCl_2$. Aman *et al.* (2015) observed a similar reduction in droplet size (by up to 50%) after 24 hours of settling when the salt content increased from 0 to 4 wt% NaCl in model water-in-crude oil emulsions. The micrographs in Figure 4.18 and the histograms in Figure 4.19a show that the distributions become narrower as the average drop size decreases. The narrower

distributions with the increased salt contend was also observed for the CSS and SAGD sample as shown in Appendix B. Note, the shape of the distributions was similar for all three asphaltenes at any given salt content, Figure 4.19b. The shape of the distribution is likely set by the homogenizer and only altered slightly by the limited coalescence that occurs in these emulsions before treatment.

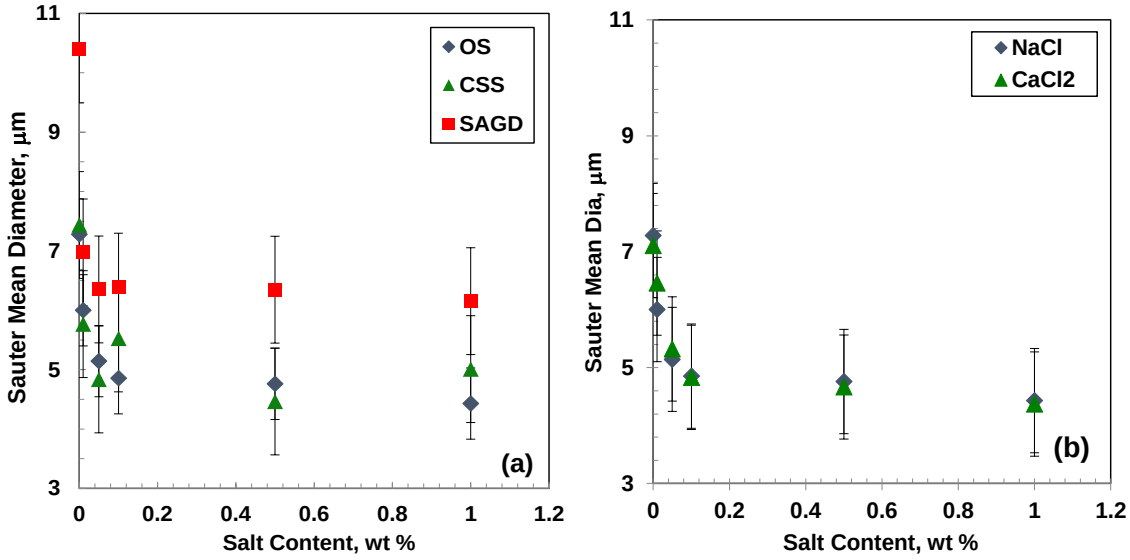

Figure 4.17 Effect of salt content on the Sauter mean diameter of emulsified water droplets from model emulsions at 21°C a) OS, CSS, and SAGD asphaltenes and NaCl brine; b) OS asphaltenes and NaCl and $CaCl_2$ brines. Organic phase: 10 g/L of asphaltenes in 25/75 heptol; 40 vol% aqueous phase.

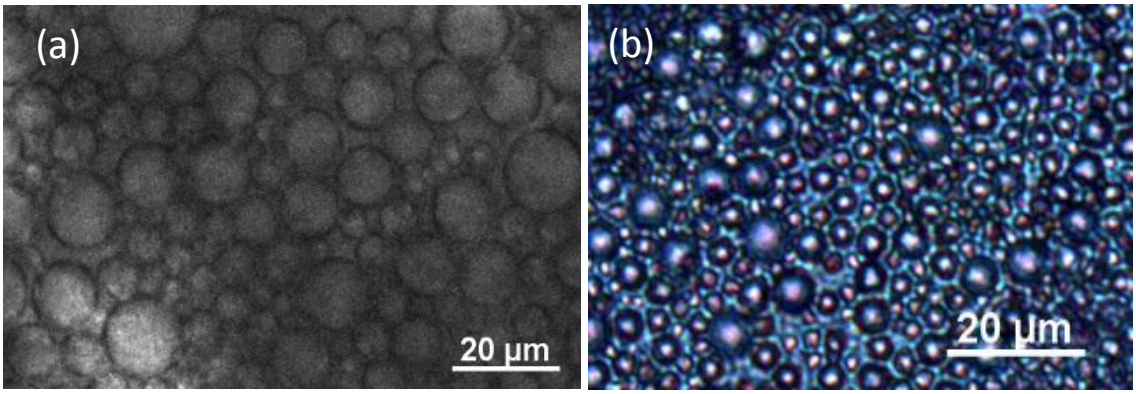

Figure 4.18 Micrographs of settled emulsions stabilized with OS asphaltenes. For a) 0 wt% NaCl b) 0.1 wt% NaCl. . Organic phase: 10 g/L asphaltenes in 25/75 heptol; aqueous phase: RO water and NaCl; 40 vol% aqueous phase.

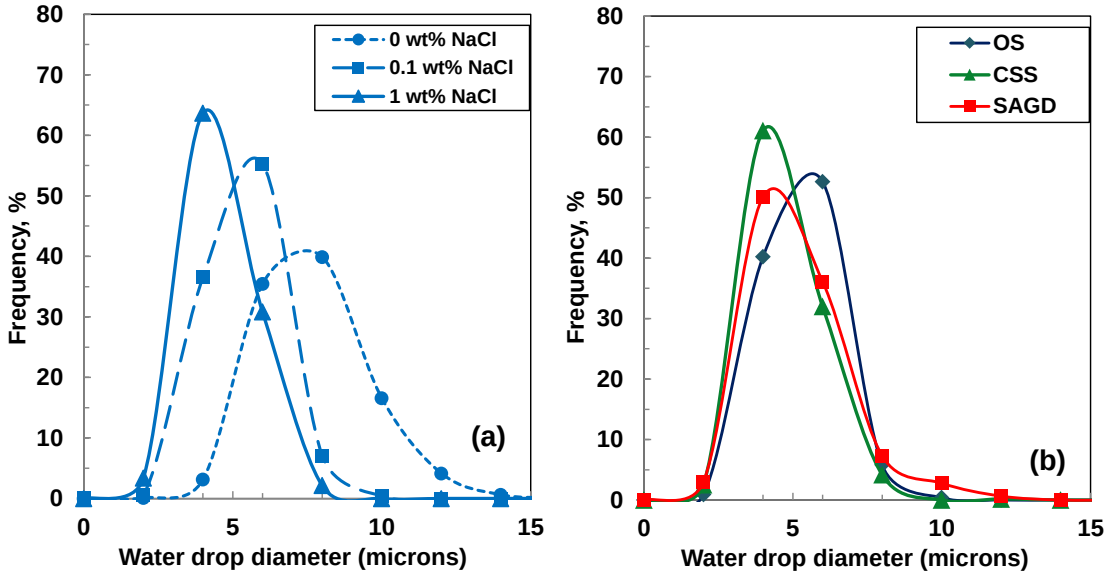

Figure 4.19 Drop size distributions of model emulsions prepared from: a) OS asphaltenes at different NaCl contents; b) different asphaltenes at 0.5 wt% NaCl content. Organic phase: 10 g/L asphaltenes in 25/75 heptol; aqueous phase: RO water and NaCl; 40 vol% aqueous phase. All distributions taken before emulsion stability testing.

4.5 The Effect of Salt on Emulsion Packing

Figure 4.20a shows the effect of salt content on the water volume fraction in the settled emulsion. The water volume fraction is a measure of the packing of the emulsion droplets: the higher the water volume fraction, the more closely packed the emulsion. The volume fraction of water in the settled emulsion decreased from approximately 55 vol% at 0 wt% NaCl to 40 vol% at 1 wt% NaCl. In other words, as the salt content increased, the droplets were further apart on average, leaving space for more continuous phase in the emulsion. Figure 4.20b shows that similar water volume fractions were observed for the OS model asphaltene-stabilized emulsions and the bitumen stabilized emulsions. Again, it appears that the asphaltenes are responsible for the interfacial and emulsion properties. Note, the comparison could not be made for the SAGD and CSS samples because some free water separated when settling in the bitumen emulsions and, therefore, the emulsified volume of water could not be accurately measured. No free water was observed during the settling time for the other emulsions. Similar results were observed for emulsions prepared with OS asphaltenes and $CaCl_2$ brines as shown in Appendix B.

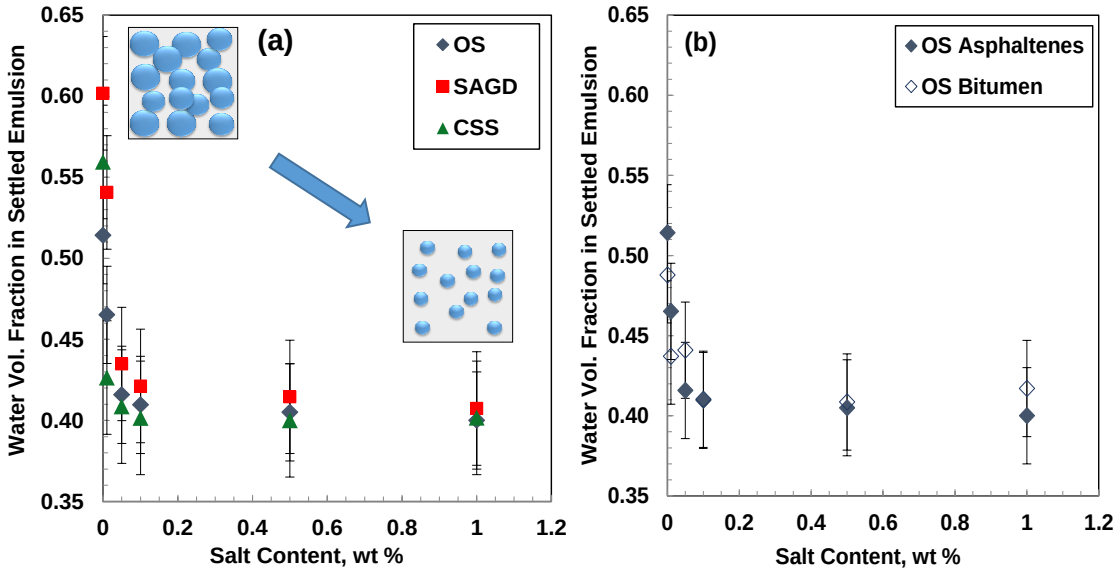

Figure 4.20 Effect of salt content on the water volume fraction of the settled emulsion (a) 10 g/L of asphaltenes in 25/75 heptol (b) 10wt% of bitumen in 25/75 heptol; aqueous phase: reverse osmosis water and NaCl; 40 vol% aqueous phase.

A number of explanations are possible for the change in packing. One possibility is that increased electrostatic repulsion increased the distance between the droplets. However, electrostatic forces are negligible in a low dielectric constant medium such as a hydrocarbon. Also, the addition of salt tends to neutralize the charge at the interface and decrease the repulsion, contrary to the observed trend. Another possibility is that the drop size distribution became less uniform at higher salt contents allowing more efficient packing. However, as noted previously, the opposite trend is observed (Figure 4.19). A third possibility is that the increased thickness of the interfacial film increased the space between the droplets, but the change in thickness is orders of magnitude too small to account for the large change in water volume fraction. Yet another possible explanation is that the salt alters the surface interactions (*e.g.*, van der Waals interactions) between the droplets and the surrounding medium. If the dielectric constants or refractive indexes of the interacting materials and the surrounding medium are matched, the attractive forces (by van der Waal interactions) can be reduced to a minimum (Israelachvili, 1992). Márquez *et al.* (2010) noted that an increased electrolyte concentration decreased the dielectric

constant of the aqueous phase, reduced the difference between the aqueous and organic phase constants and lowered the Hamaker constant of van der Waals interactions. Hence, the attractive forces between droplets are reduced and the distance between droplets can be larger. However, even after salt addition, the dielectric constant of the aqueous phase is significantly higher than that of the organic phase.

The most plausible explanation is that the addition of salt changed the aggregation state of the asphaltenes at the water/oil interface (as indicated with the apparent molecular weight changes), thereby affecting the interaction force between the water droplets and the emulsion packing. Generally, stronger attraction or adhesion between water droplets leads to closer packing; that is, a relatively higher apparent water volume fraction (Natarajan *et al.,* 2011). To test this hypothesis, the interaction force between two asphaltene coated droplets (measured using a Droplet Probe AFM) was compared at two different salt concentrations, 0.0059 wt% (1 mM) NaCl and 0.59 wt% (100 mM) NaCl. These measurements were performed by Dr. Zeng's group at the University of Alberta, Department of Chemical and Materials Engineering.

Figure 4.21a shows a typical force curve measured between two water droplets with the interaction force normalized by the droplet radius. When the two water droplets were pushed together (black curve), the repulsive force was strong and the water droplets were stable against coalescence. This observation agrees well with previous reports that asphaltenes can stabilize water droplets through steric repulsion (Wang *et al.,* 2010; Natarajan *et al.,* 2011) When the two water droplets were pulled apart (red curve), there was a step change in the force indicating interfacial adhesion between the water droplets. The adhesion is attributed mainly to interpenetration/bridging between asphaltenes at the water/oil interface through van der Waals interactions and aromatic interaction (*e.g.*, $\pi-\pi$ interaction).

Figure 4.21b shows the evolution of the measured adhesion with aging time. The adhesive force decreased with aging time for both the 0.0059 wt% and the 0.59 wt% NaCl contents

but, interestingly, the evolution of adhesion with aging time was different in each case. While the initial adhesion (at an aging time of ~5 min) was similar, the adhesion between water drops with higher salt content decreased more significantly with time than that for water drops with lower salt content. In other words, the "equilibrium" adhesive force is less for water drops with high salinity, consistent with the observed looser packing. As discussed in the Section 4.3, the addition of salt appears to promote the self-association of interfacial asphaltenes which reduces the probability of interpenetration/bridging and lowers the adhesion between the asphaltene films. Finally, note that the surface force measurements were conducted at asphaltene concentrations 1000 times lower than the emulsion stability tests. The changes in aggregation behavior and steric interaction of the asphaltenes at the interface observed at low asphaltene concentrations are expected to be even more significant at higher concentrations due to the greater aggregation of the asphaltenes.

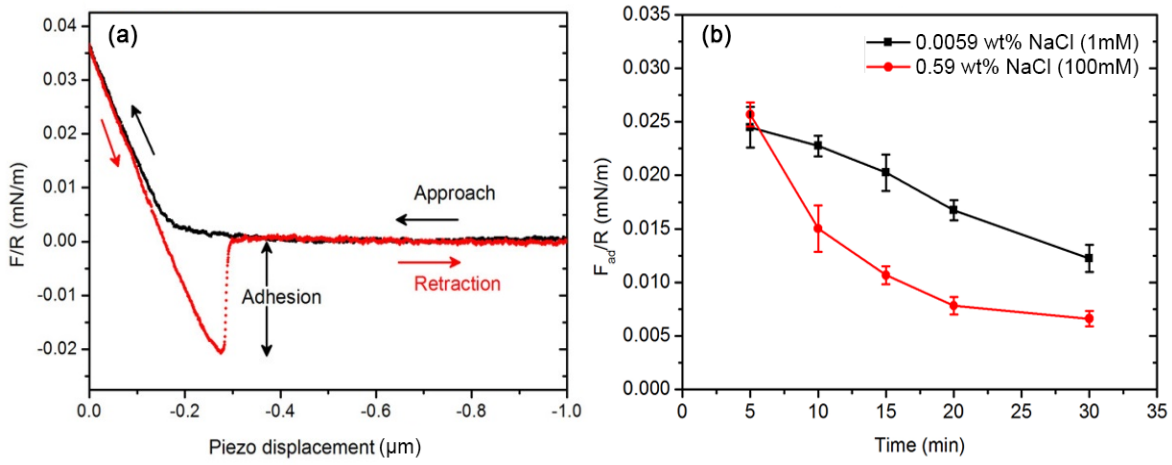

Figure 4.21 (a) Typical force curve measured between two water droplets in asphaltene-heptol solution. The arrows represent the movement of the droplet. The jump-out shown in the retraction curve indicates the adhesion measured between the two water droplets. (b) Adhesion between two water drops with 0.0059 wt% (1 mM) and 0.59 wt% (100 mM) NaCl as a function of aging time (Rocha *et al.*, 2016).

4.6 Factors Controlling Emulsion Stability

To understand what factors determine the stability of the emulsions in this study, it is necessary to consider both the effect of salt addition and the differences between the three asphaltenes. The effects of salt addition on factors that contribute to emulsion stability are each discussed below.

Interfacial Tension: Salt addition decreased the interfacial tension. A reduction in IFT can enhance emulsion stability by reducing the driving force for coalescence (Kumar, 2012; Serrano *et al.*, 2004).

Film Compressibility: Salt addition increased the film compressibility and reduced the crumpling ratio. For irreversible films, the higher the crumpling ratio and the steeper the rise in the surface pressure isotherm, the more resistant to coalescence and the more stable the emulsion (all else being equal). If crumpling was the determining factor for emulsion stability, salt addition would be expected to decrease emulsion stability, contrary to what was observed. Hence, the additional stability provided by the salt is not related to film rigidity. Although the literature suggests that more rigid films (lower compressibility and higher crumpling ratios) lead to more stable emulsions (Alves *et al.*, 2014; Yarranton *et al.*, 2007b; Ortiz *et al.*, 2010), this work shows this correlation does not always hold. Rigid films may be only one of several factors determining emulsion stability.

Surface Coverage and Molecular Weight: Salt addition increased the molar surface coverage and significantly increased the mass surface coverage and apparent molecular weight of the interfacial material. An increase in surface coverage could enhance emulsion stability by increasing (1) the rigidity of the interfacial film, (2) the thickness of the film. The surface pressure isotherms demonstrated that the rigidity of the film decreased at higher salt content. An increase in the apparent molecular weight indicates that either larger molecules and/or nanoaggregates are adsorbing at the interface or multilayers are building up. In either case, because the area per molecule at the interface decreased by only 40% while the apparent molecular weight increased by 150%, the film thickness must increase

by a factor of 3-4. Thicker films increase the potential for steric stabilization (Gafonova and Yarranton, 2001).

Drop Size: Salt addition decreased the average drop size and narrowed the shape of the drop size distribution. A decrease in drop size reduces the collision diameter of the droplets and the probability of coalescence and therefore is associated with an increase in emulsion stability.

Emulsion Packing: Salt addition significantly increased the average distance between the droplets in the settled emulsion. The greater distance between the droplets may correlate with increased emulsion stability if it correlates with an increase in the smallest distance between the droplet, *i.e.*, the point of closest contact where coalesce would be initiated. The larger this distance, the lower the probability of coalescence and the more stable the emulsion.

Adhesion: Salt addition decreased the adhesive force between the droplets. A decrease in adhesion means that more energy is required to keep the droplets in relatively close contact and the droplets can be separated more easily. Hence, the chance of coalescence is lowered and might contribute to emulsion stability.

All of the above factors, except the increase in film compressibility, could explain the enhanced emulsion stability when salt is added. Hence, the key factors determining the stability of these emulsions cannot be determined from the salt effects alone. Now consider the differences between the three asphaltene samples. The emulsion prepared with OS and CSS were relatively stable while those prepared with SAGD asphaltenes were much less stable. The relative magnitude of the factors affecting emulsion stability is as follows:

- Interfacial tension: OS > CSS > SAGD
- Crumpling ratio: CSS>OS>SAGD
- Molar surface coverage: SAGD = CSS > OS
- Mass surface coverage: OS = CSS > SAGD

- Molecular weight: OS = CSS > SAGD
- Drop size: OS = CSS = SAGD
- Separation distance: OS = CSS = SAGD

Of these, only the trends in mass surface coverage, apparent molecular weight of the interfacial material, and possibly drop size follow the expected relationship with emulsion stability. Figure 4.22 shows the water resolved versus asphaltene mass surface coverage (a) and the molecular weight (b) for the three different asphaltenes at different salt contents. There appears to be a minimum threshold for emulsion stability at a mass surface coverage of 5 mg/m² and an apparent molecular weight of 7000 g/mol. This threshold may be equivalent to an interfacial thickness, but the exact value is not known because the density of the asphaltenes at the interface is not known. The results suggest that the emulsions become sterically stabilized when irreversibly adsorbed films are compressed during preliminary coalescence to the point the film thickness prevents further coalescence between droplets.

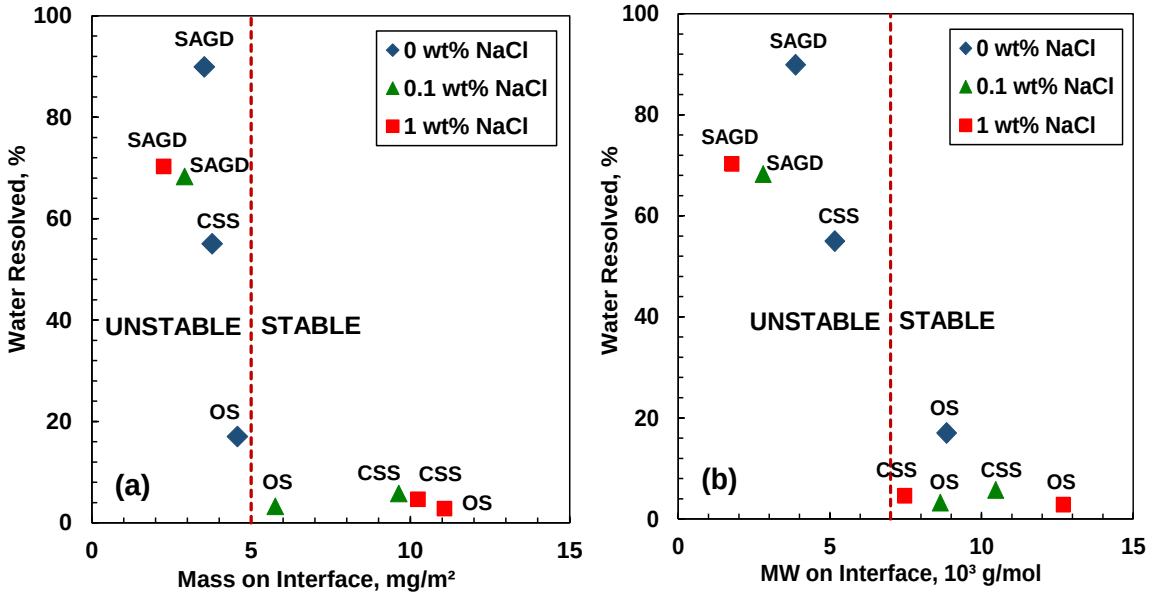

Figure 4.22 The correlation of emulsion stability (less water resolved) to: a) mass surface coverage; b) apparent molecular weight of the interfacial material. Organic phase: 10 g/L of asphaltenes in 25/75 heptol; aqueous phase: RO water and NaCl. Emulsions prepared with 40 vol% aqueous phase.

Figure 4.23 shows the water resolved versus Sauter mean diameter for the three asphaltene samples at different salt contents. There is a decrease in emulsion stability as the average drop size increases. However, the magnitude of the drop size change is small and the SAGD emulsions with salt are off trend. It is more likely that the change in diameter is a consequence of the reduced emulsion stability at low mass surface coverage. Lower mass surface coverage means that more rapid initial coalescence occurs before the droplets are stabilized.

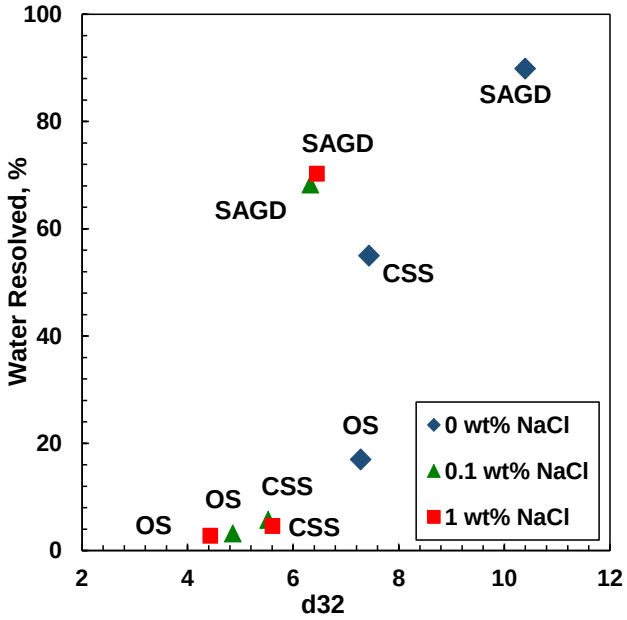

Figure 4.23 Effect of salt content on the Sauter mean diameter of emulsified water droplets from model emulsions at 21°C. Organic phase: 10 g/l of asphaltenes in 25/75 heptol; aqueous phase: RO water and NaCl; 40 vol% aqueous phase.

A possible explanation for the high emulsion stability of the OS asphaltenes is that they contain a large number of asphaltene aggregates with higher molecular weight that adsorb on the water-oil interface. These species form an interfacial layer thick enough to stabilize the emulsion even when no salt is present. Salt enhances the emulsion stability at least partly by increasing the thickness of the interfacial layer. In some cases, such as the CSS asphaltenes, the emulsion is below the threshold in the absence of salt, but salt addition increases the thickness past the threshold and the emulsion becomes stable. The SAGD

film thickness is so low that even when salt is added, the threshold is not reached and the emulsions remain unstable.

The reason the SAGD asphaltenes are different than the other asphaltenes is not known. One possibility is that the prolonged exposure to steam temperatures in the SAGD process partly reacted the asphaltenes causing the asphaltene nanoaggregates to partially dissociate, reducing the amount of self-associated material and the interfacial film thickness. Another possibility is that the OS and CSS processes liberate natural surfactants that were originally adsorbed on the rock surfaces. The OS process is designed to do so. The short-term exposure to high shear and temperature in the CSS process may have a similar outcome. And, of course, the three oils may simply consist of asphaltenes with different surface properties.

CHAPTER FIVE:

CONCLUSIONS AND RECOMMENDATIONS

Very small salt contents were found to substantially increase the stability of water-in-heavy oil emulsions. Salt addition decreased the interfacial tension, increased the molar and mass surface coverage, increased the apparent molecular weight of interfacial material, decreased the droplet size, decreased the adhesion between water droplets and increased the distance between the settled emulsion droplets. All of these factors can enhance emulsion stability. However, the main factor in determining the stability of these emulsion was found to be the mass surface coverage of the asphaltenes (or the apparent molecular weight of the adsorbed interfacial asphaltenes). The difference in stability of OS, CSS, and SAGD emulsions could be explained by differences in the mass surface coverage. The specific conclusions from this work and recommendations for future research in the area are presented below.

5.1 Conclusions

Specific conclusions from this work are:

1) Salt addition was found to dramatically increase the stability of asphaltene-stabilized water-in-oil emulsions at less than 0.1 wt % salt addition. The type of salt was shown to have no significant effect on emulsion stability, surface coverage, drop size distribution and emulsion packing. Apparently, an ionic strength as high as 0.03 M is sufficient to stabilize these emulsions regardless of the type of salt present in the aqueous phase.

2) The pH in the aqueous phase affected the stability of the emulsions with more stable emulsions formed at high pH and asphaltene source dependent effects at low pH. However, when salts at a concentration as low as 0.1 wt% were present in the aqueous phase, the emulsion stability increased dramatically at all pH, although the changes were most pronounced at low pH (<4) and high pH (>12).

3) The stability and properties of model emulsions prepared with asphaltenes and prepared with bitumen were similar. It appears that water-in-bitumen emulsions are stabilized by asphaltenes or components within the asphaltenes. However, the CSS bitumen solutions, an unexpected decrease in stability was observed with the increased salt content (0.5% NaCl). A possible explanation for this is that some low molecular weight surface-active material present in the maltenes, such as organic acids, compete with the asphaltene at the interface and altered the interfacial properties.

4) Salt addition increased the compressibility of the interfacial films even while increasing the surface coverage. This behavior is likely driven by salts attracting selective components from the asphaltenes to the interface, but no clear conclusion is possible without knowing more about the chemistry of the oils.

5) Asphaltenes from an OS extraction process, a CSS process and a SAGD process were compared. The emulsions prepared from the SAGD asphaltenes were much less stable than the emulsions prepared from OS and CSS asphaltenes. Similar results were obtained for water-in-diluted bitumen emulsions. The differences in stability correlate to the mass surface coverage and apparent molecular weight of the interfacial material.

6) Emulsion stability appears to require a threshold asphaltene surface coverage of 5 mg/m^2 or a molecular weight of 7,000 g/mol. The addition of salt increased the mass surface coverage and molecular weight, and so an emulsion may cross the threshold from unstable in water to stable in brine. The SAGD asphaltenes contain so little high molecular weight surface-active material that salt addition did not stabilize these emulsions. This observation raises the possibility that prolonged exposure to steam temperatures may reduce asphaltene self-association or that the

SAGD process is less intense (in combined shear rate and temperature) than the other processes and does not liberate natural surfactants.

5.2 Recommendations

Some recommendations for future work are:

1) All the emulsion stability, drop size distribution and emulsion packing tests in this thesis were measured at ambient pressure and temperature. Some of these experiments could be repeated at the higher pressures and temperatures such as those encountered at production facilities in order to determine if there are any changes in stability behavior.

2) Expose the OS bitumen to elevated pressure and an operating temperature of approximately 200°C over extended periods of time and then repeat the stability and property tests. Exposure to high temperature could alter the OS asphaltene self-association to more closely emulate the SAGD asphaltenes. In such a scenario, the thermally exposed asphaltenes would show a lower apparent molecular weight. This could lead to a better understanding about the conditions that make SAGD asphaltenes less prone to self-association and less likely to create stable emulsions.

References

Agrawala, M., Yarranton, H. W. **(2001)**. An Asphaltene Association Model Analogous to Linear Polymerization. *Industrial & Engineering Chemistry Research*, *40*(21), 4664–4672.

Aguilera, B. M., Delgado, J. G., Cárdenas, A. L. **(2010)**. Water-in-Oil Emulsions Stabilized by Asphaltenes Obtained from Venezuelan Crude Oils. *Journal of Dispersion Science and Technology*, *31*(3), 359–363.

Akbarzadeh, K., Dhillon, A., Svrcek, W. Y., Yarranton, H. W. **(2004)**. Methodology for the Characterization and Modeling of Asphaltene Precipitation from Heavy Oils Diluted with n-Alkanes. *Energy & Fuels*, *18*(5), 1434–1441.

Alvarez, G., Poteau, S., Argillier, J. F., Langevin, D., Salager, J.-L. **(2009)**. Heavy Oil−Water Interfacial Properties and Emulsion Stability: Influence of Dilution. *Energy & Fuels*, *23*(15), 294–299.

Alves, D. R., Carneiro, J. S. A., Oliveira, I. F., Façanha, F., Santos, A. F., Dariva, C., Fortuny, M. **(2014)**. Influence of the Salinity on the Interfacial Properties of a Brazilian Crude Oil-Brine Systems. *Fuel*, *118*, 21–26.

Aman, Z. M., Haber, A., Ling, N. A., Thornton, A., Johns, M. L., May, E. F. **(2015)**. Effect of Brine Salinity on the Stability of Hydrate-in-Oil Dispersions and Water-in-Oil Emulsions. *Energy & Fuels*, *29*, 7948–7955.

Arla, D., Flesisnki, L., Bouriat, P., Dicharry, C. **(2011)**. Influence of Alkaline pH on the Rheology of Water / Acidic Crude Oil Interface. *Energy*, *25*(3), 1118–1126.

Arla, D., Sinquin, A., Palermo, T., Hurtevent, C., Graciaa, A., Dicharry, C. **(2007)**. Influence of pH and Water Content on the Type and Stability of Acidic Crude Oil Emulsions. *Energy & Fuels*, *21*(3), 1337–1342.

Asekomhe, S. O., Chiang, R., Masliyah, J. H., Elliott, J. A. W. **(2005)**. Some Observations on the Contraction Behavior of a Water-in-Oil Drop with Attached Solids. *Industrial & Engineering Chemistry Research*, *44*(5), 1241–1249.

Barnes G, I. G. **(2005)**. An Introduction to Interfacial Science (Vol 1). New York: OXFORD *University Press*.

Barrera, D. M., Ortiz, D. P., Yarranton, H. W. **(2013)**. Molecular Weight and Density Distributions of Asphaltenes from Crude Oils. *Energy & Fuels*, *27*(5), 2474–2487.

Binks, B. **(1998)**. Emulsions-Recent Advances in Understanding. *In Modern Aspects of Emulsion Science* (The Royal).

Buckley, J. S., Fan, T. **(2007)**. Crude Oil /Brine Interfacial Tensions. *Petrophysics*, *43*, 1–12.

Collins, A.G., **(1992)** Properties of Produced Waters, *Petroleum Engineering Handbook*, Ch. 24.

Czarnecki, J. **(2009)**. Stabilization of Water in Crude Oil Emulsions. Part 2 Stabilization of Water in Crude Oil Emulsions. Part 2. *Water*, *77*(7), 2–7.

Czarnecki, J., Moran, K. **(2005)**. On the Stabilization Mechanism of Water-in-Oil Emulsions in Petroleum Systems. *Energy & Fuels*, *19*(5), 2074–2079.

Dandekar, A.Y., **(2006)** Petroleum Reservoir Rocks and Fluids Properties, *Taylor and Francis.*

Dickie, J.P., Yen, T.F., **(1967)**. Macrostructures of the Asphaltic Fractions by Various Instrumental Methods," *Anal. Chem., 39,* 1847-1852.

Elsharkawy, A. M., Yarranton, H. W., Al-sahhaf, T. A., Fahim, M. A. **(2008)**. Water in Crude Oil Emulsions in the Burgan Oilfield: Effects of Oil Aromaticity, Resins to Asphaltenes Content (R/(R+A)), and Water pH. *Journal of Dispersion Science and Technology*, *29,* 224–229.

Eyssautier, J., Frot, D., Barré, L. **(2012)**. Structure and Dynamic Properties of Colloidal Asphaltene Aggregates. *Langmuir*, *28*(33), 11997–2004.

Gafonova, O. V., Yarranton, H. W. **(2001)**. The Stabilization of Water-in-Hydrocarbon Emulsions by Asphaltenes and Resins. *Journal of Colloid and Interface Science*, *241*(2), 469–478.

Gao, S., Moran, K., Xu, Z., Masliyah, J. **(2009)**. Role of Bitumen Components in Stabilizing Water-in-Diluted Oil Emulsions. *Energy & Fuels*, *23*(5), 2606–2612.

Gray, M. **(1994)**. Upgrading Petroleum Residues and Heavy Oils, *Marcel Dekker*, New York.

Hiemenz P., Rajagopalan R. **(1996)** Principles of Colloids and Surface Chemistry. *Marcel Dekker*, New York.

Ghannam, M. T., **(2007)**. Water-in-Crude Oil Emulsion Stability Investigation. *Petroleum Science and Technology*, 37–41.

Groenzin, H., Mullins, O. C. **(2000)**. Molecular Size and Structure of Asphaltenes from Various Sources. *Energy, (12),* 677–684.

Gu, G., Zhou, Z., Xu, Z., Masliyah, J. H. **(2003)**. Role of Fine Kaolinite Clay in Toluene-Diluted Bitumen/Water Emulsion. Colloids and Surfaces A: *Physicochemical and Engineering Aspects, 215*(1-3), 141–153.

Hannisdal, A., Orr, R., Sjöblom, J. **(2007)**. Viscoelastic Properties of Crude Oil Components at Oil-Water Interfaces. 2: Comparison of 30 Oils. *Journal of Dispersion Science and Technology, 28*(3), 361–369.

Hellman, B. O., Ulfendahl, H. R. **(1967)**. Microphotometry Utilizing a Shrinking, 434–443.

Horváth-Szabó, G., Czarnecki, J., Masliyah, J. H. **(2002)**. Sandwich Structures at Oil-Water Interfaces under Alkaline Conditions. *Journal of colloid and interface science, 253*(2), 427–434.

Israelachvili, J. **(1992)**. Intermolecular and Surface Forces, Second Ed. In *Academic Press*. London.

Jarvis, J. M., Robbins, W. K., Corilo, Y. E., Rodgers, R. P. **(2015)**. Novel Method to Isolate Interfacial Material. *Energy & Fuels, 29*(11), 7058–7064.

Jestin, J., Simon, S., Zupancic, L., Barré, L. **(2007)**. A Small Angle Neutron Scattering Study of the Adsorbed Asphaltene Layer in Water-in-Hydrocarbon Emulsions: Structural Description Related to Stability. *Langmuir, 23*(21), 10471–10478.

Jiang, T., Hirasaki, G. J., Miller, C.A, Ng, S. **(2011)**. Effects of Clay Wettability and Process Variables on Separation of Diluted Bitumen Emulsion. *Energy & Fuels*, *25*(2), 545–554.

Keleşoğlu, S., Meakin, P., Sjöblom, J. **(2011)**. Effect of Aqueous Phase pH on the Dynamic Interfacial Tension of Acidic Crude Oils and Myristic Acid in Dodecane. *Journal of Dispersion Science and Technology, 32*(11), 1682–1691.

Kent, P., Saunders, B. R. **(2001)**. The Role of Added Electrolyte in the Stabilization of Inverse Emulsions. *Journal of Colloid and Interface Science, 242*(2), 437–442.

Kiran, S. K., Ng, S., Acosta, E. J. **(2011)**. Impact of Asphaltenes and Naphthenic Amphiphiles on the Phase Behavior of Solvent-Bitumen-Water Systems. *Energy & Fuels, 25*(5), 2223–2231.

Kokal, S. **(2002)**. Crude Oil Emulsions: A State-of-the-Art Review. Proceedings of *SPE Annual Technical Conference and Exhibition*, 11.

Kumar, B. **(2012)**. Effect of Salinity on the Interfacial Tension of Model and Crude Oil Systems. M.Sc. Thesis. *University of Calgary*.

Kumar, D., Zhu, .J, Shin. **(2012)**. Material Selection for Designing SAGD Plants. *NACE International-Corrosion Expo.*

Langevin, D., Poteau, S., Hénaut, I., Argillier, J. F. **(2004)**. Crude Oil Emulsion Properties and their Application to Heavy Oil Transportation. *Gas Science Technology 59*(5), 511–521.

Lashkarbolooki, M., Ayatollahi, S., Riazi, M. **(2014)**. Effect of Salinity, Resin, and Asphaltene on the Surface Properties of Acidic Crude Oil / Smart Water / Rock System. *Energy & Fuels, 28*, 6820–6829.

Levine, M., Ramsey, P., Smidt, R. **(2001)**. Applied Statistics for Engineers and Scientist. First ed. *Prentice-Hall, Inc*. New Jersey

Li, B., Fu, J. **(1992)**. Interfacial Tensions of Two-Liquid-Phase Ternary Systems. *Journal of Chemical & Engineering Data*, *37*(2), 172–174.

Li, M., Guo, J., Lin, M., Wu, Z. **(2006)**. Studies on Properties of Interfacial Active Fractions from Crude and their Effect on Stability of Crude Emulsions. *Journal of Dispersion Science and Technology*, *27*(5), 677–687.

Liu, J., Zhang, L., Xu, Z., Masliyah, J. **(2006)**. Colloidal Interactions between Asphaltene Surfaces in Aqueous Solutions. *Langmuir*, *22*(4), 1485–1492.

Márquez, A. L., Medrano, A., Panizzolo, L.A, Wagner, J. R. **(2010)**. Effect of Calcium Salts and Surfactant Concentration on the Stability of Water-In-Oil (W/O) Emulsions Prepared with Polyglycerol Polyricinoleate. *Journal of Colloid and Interface Science*, *341*(1), 101–108.

Masliyah, J., Zhou, Z. J., Xu, Z., Czarnecki, J., Hamza, H. **(2004)**. Understanding Water-Based Bitumen Extraction from Athabasca Oil Sands. *The Canadian Journal of Chemical Engineering*, *82*(4), 628–654.

McLean, J., Kilpatrick, P. **(1997)**. Effects of Asphaltene Aggregation in Model Heptane-Toluene Mixtures on Stability of Water-in-Oil Emulsions. *Journal of Colloid and Interface Science*, *196*(1), 23–34.

Moradi, M., Alvarado, V., Huzurbazar, S. **(2011)**. Effect of Salinity on Water-in-Crude Oil Emulsion: Evaluation through Drop-Size Distribution Proxy. *Energy & Fuels*, *25*(17), 260–268.

Moradi, M., Topchiy, E., Lehmann, T. E., Alvarado, V. **(2013)**. Impact of Ionic Strength on Partitioning of Naphthenic Acids in Water-Crude Oil Systems - Determination Through High-Field NMR Spectroscopy. *Fuel*, *112*, 236–248.

Moran, K. **(2007)**. Roles of Interfacial Properties on the Stability of Emulsified Bitumen Droplets. *Langmuir*, *23*(5), 4167–4177.

Moran, K., & Czarnecki, J. **(2007)**. Competitive Adsorption of Sodium Naphthenates and Naturally Occurring Species at Water-In-Crude Oil Emulsion Droplet Surfaces. Colloids and Surfaces A: *Physicochemical and Engineering Aspects*, *292*(2-3), 87–98.

Moran, K., Yeung, a., Czarnecki, J., Masliyah, J. **(2000)**. Micron-Scale Tensiometry for Studying Density-Matched and Highly Viscous Fluids - With Application to Bitumen-in-Water Emulsions. Colloids and Surfaces A: *Physicochemical and Engineering Aspects*, *174*(1-2), 147–157.

Mullins, O. C. (Schlumberger-D. R., Sheu, E. Y., Hammami, A., Marshall, A. G. **(2007)**. Asphaltenes, Heavy Oils, and Petroleomics.

Natarajan, A., Xie, J., Wang, S., Masliyah, J., Zeng, H., Xu, Z. **(2011)**. Understanding Molecular Interactions of Asphaltenes in Organic Solvents Using a Surface Force Apparatus. *Journal of Physical Chemistry C*, *115*(32), 16043–16051.

Ortiz, D. P., Baydak, E. N., Yarranton, H. W. **(2010)**. Effect of Surfactants on Interfacial Films and Stability of Water-In-Oil Emulsions Stabilized by Asphaltenes. *Journal of Colloid and Interface Science*, *351*(2), 542–555.

Overbeek, J. Th. G. **(1952a)**. Electrokinetics: in Colloid Science, Vol. 1, H. R. Kruyt, ed., Elsevier, Amsterdam, 194- 244.

Peramanu, S., Pruden, B. B., Rahimi, P. **(1999)**. Molecular Weight and Specific Gravity Distributions for Athabasca and Cold Lake Bitumens and their Saturate, Aromatic, Resin, and Asphaltene Fractions. *Industrial & Engineering Chemistry Research, 38*(8), 3121–3130.

Poteau, S., Argillier, J. F., Langevin, D., Pincet, F., Perez, E. **(2005)**. Influence of pH on Stability and Dynamic Properties of Asphaltenes and other Amphiphilic Molecules at the Oil-Water Interface. *Energy & Fuels, 19*(4), 1337–1341.

Rogel, E., León, O., Torres, G., Espidel, J., **(2000)**. Aggregation of Asphaltenes in Organic Solvents Using Surface Tension Measurements," *Fuel, 79*, 1389-1394.

Rocha, J. A., Baydak, E. N., Yarranton, H. W., Sztukowski, D. M., Ali-Marcano, V., Gong, L., Zeng, H. **(2016)**. Role of Aqueous Phase Chemistry, Interfacial Film Properties, and Surface Coverage in Stabilizing Water-in-Bitumen Emulsions. *Energy & Fuels*, acs.energyfuels.6b00114.

Sarac, S., Civan, F. **(2007)**. Experimental Investigation and Modeling of Naphthenate Soap Precipitation Kinetics in Petroleum Reservoirs. *International Symposium on Oilfield Chemistry*, 1–9.

Serrano-Saldaña, E., Domínguez-Ortiz, A., Pérez-Aguilar, H., Kornhauser-Strauss, I., Rojas-González, F. **(2004)**. Wettability of Solid/Brine/n-Dodecane Systems: Experimental Study of the Effects of Ionic Strength and Surfactant Concentration. Colloids and Surfaces A: *Physicochemical and Engineering Aspects, 241*, 343–349.

Sjoblom, J., Aske, N., Harald, I., Brandal, Ø. Erik, T., Sæther, Ø. **(2003)**. Our Current Understanding of Water-in-Crude Oil Recent Characterization Techniques and High Pressure Performance. *Advances in Colloid and Interface Science 100*(102), 399–473.

Solovyev, A., Zhang, L. Y., Xu, Z., Masliyah, J. H. **(2006)**. Langmuir Films of Bitumen at Oil/Water Interfaces. *Energy & Fuels, 20*(13), 1572–1578.

Strausz, O., Mojelsky, T., Lown E. M. **(1992)**.The Molecular Structure of Asphaltene: An Unfolding Story. *Fuel, 71*(12): 1355-1363.

Sztukowski, D. M. **(2005)**. Asphaltene and Solid-Atabilized Water-in-Oil Emulsions. *Ph.D. Thesis*. University of Calgary.

Sztukowski, D. M., Jafari, M., Alboudwarej, H., Yarranton, H. W. **(2003)**. Asphaltene Self-Association and Water-in-Hydrocarbon Emulsions. *Journal of Colloid and Interface Science, 265*(1), 179–186.

Sztukowski, D. M., Yarranton, H. W. **(2005)**. Oilfield Solids and Water-in-Oil Emulsion Stability. *Journal of Colloid and Interface Science, 285*(2), 821–33.

Taylor, P. (1995). Ostwald Ripening in Emulsions. Colloids and Surfaces A: *Physicochemical and Engineering Aspects, 99*(2-3), 175–185.

Taylor, S. D., Czarnecki, J., Masliyah, J. **(2002)**. Disjoining Pressure Isotherms of Water-in-Bitumen Emulsion Films. *Journal of Colloid and Interface Science, 252*(1), 149–160.

Thimm, H. F. **(2005)**. Low pressure SAGD Operations. *Journal of Canadian Petroleum Technology, 44*(9), 58–64.

Urrutia, P. I. **(2006)**. Predicting Water-in-oil- Emulsion Coalescence from Surface Pressure Isotherms. *M.Sc. Thesis.* University of Calgary.

Van Hunsel, J. **(1988).** Dynamic Interfacial Tension at Oil-Water Interfaces. *Ph.D. Thesis*. University of Antwerp.

Vander Kloet, J., Schramm, L. L., Shelfantook, B. **(2001)**. The Influence of Bituminous Froth Components on Water-in-Oil Emulsion Stability as Determined by the Micropipette Technique. Colloids and Surfaces A: *Physicochemical and Engineering Aspects, 192*(1-3), 15–24.

Varadaraj, R., Brons, C. **(2007)**. Molecular Origins of Heavy Crude Oil Interfacial Activity Part 2: Fundamental Interfacial Properties of Model Naphthenic Acids and Naphthenic Acids Separated from Heavy Crude Oils. *Energy &Fuels, 21*(1), 199–204.

Verruto, V. J., Kilpatrick, P. K. **(2008)**. Water-in-Model Oil Emulsions Studied by Small-Angle Neutron Scattering: Interfacial Film Thickness and Composition. *Langmuir, 24*(22), 12807–12822.

Verwey, E. J. W., Overbeek, J. **(1948)**. Theory of the Stability of Lyophobic Colloids." Elsevier, Amsterdam, 205 pp.

Wang, S., Liu, J., Zhang, L., Masliyah, J., Xu, Z. **(2010)**. Interaction Forces between Asphaltene Surfaces in Organic Solvents. *Langmuir, 26*(1), 183–190.

Whittaker, J., Liu, Q., Brown, D. J., Marsden, R. **(2014)**. Corrosion Management and Mechanism Study on SAGD Brackish Water System. *Corrosion 2014*, (3809), 1–14.

Wu, X. A., Czarnecki, J. **(2005)**. Modeling Diluted Bitumen-Water Interfacial Compositions Using a Thermodynamic Approach. *Energy & Fuels, 19*(4), 1353–1359.

Xu, Y., Dabros, T., Hamza, H., Shefantook, W. **(1999)**. Destabilization of Water in Bitumen Emulsion by Washing with Water. *Petroleum Science and Technology, 17*(9-10), 1051–1070.

Yan, N., Gray, M.R., Masliyah, J.H., **(2001)**. On Water-in-Oil Emulsions Stabilized by Fine Solids, Colloids Surfaces A: *Physicochem. Eng. Aspects, 193*, 97-107.

Yang, F., Liu, S., Xu, J., Lan, Q., Wei, F., Sun, D. **(2006)**. Pickering Emulsions Stabilized Solely By Layered Double Hydroxides Particles: The Effect of Salt on Emulsion Formation and Stability. *Journal of Colloid and Interface Science, 302*(1), 159–169.

Yang, F., Tchoukov, P., Dettman, H., Teklebrhan, R. B., Liu, L., Dabros, T., Xu, Z. **(2015)**. Asphaltene Subfractions Responsible for Stabilizing Water-in-Crude Oil Emulsions. Part 2: Molecular Representations and Molecular Dynamics Simulations. *Energy & Fuels, 29*(8), 4783–4794.

Yang, F., Tchoukov, P., Pensini, E., Dabros, T., Czarnecki, J., Masliyah, J., Xu, Z. **(2014)**. Asphaltene Subfractions Responsible for Stabilizing Water-in-Crude Oil Emulsions. Part 1 : Interfacial Behaviors. *Energy & Fuels 28,* 6897-6904.

Yarranton, H. W., Alboudwarej, H., Jakher, R. **(2000)**. Investigation of Asphaltene Association with Vapor Pressure Osmometry and Interfacial Tension Measurements. *Industrial & Engineering Chemistry Research, 39*(8), 2916–2924.

Yarranton, H. W., Masliyah, J. H. **(1996)**. Gibbs - Langmuir Model for Interfacial Tension of Non-ideal Organic Mixtures over Water. *J. Phys. Chem., 100*, 1786–1792.

Yarranton, H. W., Ortiz, D. P., Barrera, D. M., Baydak, E. N., Barré, L., Frot, D., Oake, J. **(2013)**. On the Size Distribution of Self-Associated Asphaltenes. *Energy & Fuels*, *27*(9), 5083–5106.

Yarranton, H. W., Sztukowski, D. M., Urrutia, P. **(2007a)**. Effect of Interfacial Rheology on Model Emulsion Coalescence (Part I). *Journal of Colloid and Interface Science*, *310*(1), 246–252.

Yarranton, H. W., Sztukowski, D. M., Urrutia, P. **(2007b)**. Effect of Interfacial Rheology on Model Emulsion Coalescence (Part II). *Journal of Colloid and Interface Science*, *1*(310), 253–259.

Yeung, A., Moran, K., Masliyah, J., Czarnecki, J. **(2003)**. Shear-Induced Coalescence of Emulsified Oil Drops. *Journal of Colloid and Interface Science*, *265*(2), 439–443.

Zahabi, A., Gray, M. R., Czarnecki, J., Dabros, T. **(2010)**. Flocculation of Silica Particles from a Model Oil Solution: Effect of Adsorbed Asphaltenes. *Energy & Fuels*, *24*(6), 3616–3623.

Zhang, L. Y., Lawrence, S., Xu, Z., Masliyah, J. H. **(2003)**. Studies of Athabasca Asphaltene Langmuir Films at Air-Water Interface. *Journal of Colloid and Interface Science*, *264*(1), 128–140.

Zhang, L. Y., Xu, Z. H., Masliyah, J. H. **(2005)**. Characterization of Adsorbed Athabasca Asphaltene Films at Solvent-Water Interfaces Using a Langmuir Interfacial Trough. *Industrial & Engineering Chemistry Research*, *44*(5), 1160–1174.

APPENDIX A

Emulsion Stability

Table A.1 and A.2 show the bitumen solutions used for the emulsion stability tests with their density and asphaltene content for the CSS and SAGD bitumen samples, respectively. Results for OS were described in Section 4.1.2.

Table A.1 Bitumen wt% and their equivalent in asphaltene (g/L) for CSS sample.

Bitumen wt %	Density of Solution kg/m³	Asphaltene Concentration g/L
10	0.8359	13.5
20	0.8569	27.7
30	0.8730	42.4

Table A.2 Bitumen wt% and their equivalent in asphaltene (g/L) for SAGD sample

Bitumen wt %	Density of Solution kg/m³	Asphaltene Concentration g/L
10	0.8351	15.2
20	0.8530	31.2
30	0.8719	47.8

Surface Pressure Isotherms

Figures A.1-A.4 show the comparison of surface pressure isotherms for asphaltene and bitumen solutions at different salt contents. The same trends were observed for OS, CSS and SAGD asphaltenes films and for bitumen films confirming that the interfacially adsorbed material is derived primarily from the asphaltenes.

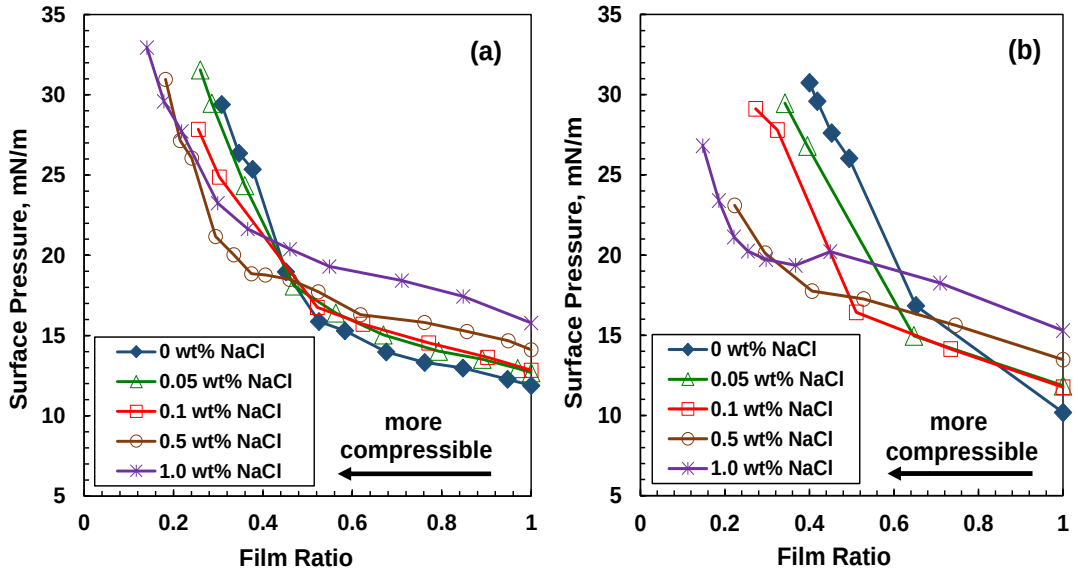

Figure A.1 Surface pressure isotherms for a) 10 g/L of OS asphaltene; b) 10 wt% OS bitumen in 25/75 heptol, after 60 minutes; aqueous phase: NaCl brine at 21°C.

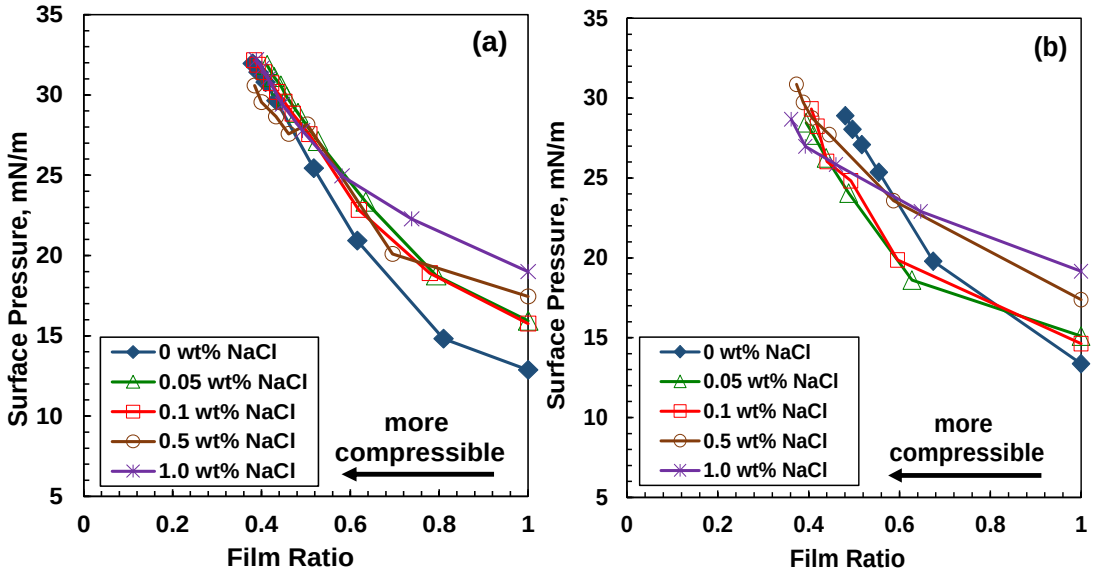

Figure A.2 Surface pressure isotherms for a) 10 g/L of CSS asphaltene; b) 10 wt% CSS bitumen in 25/75 heptol, after 60 minutes; aqueous phase: NaCl brine at 21°C.

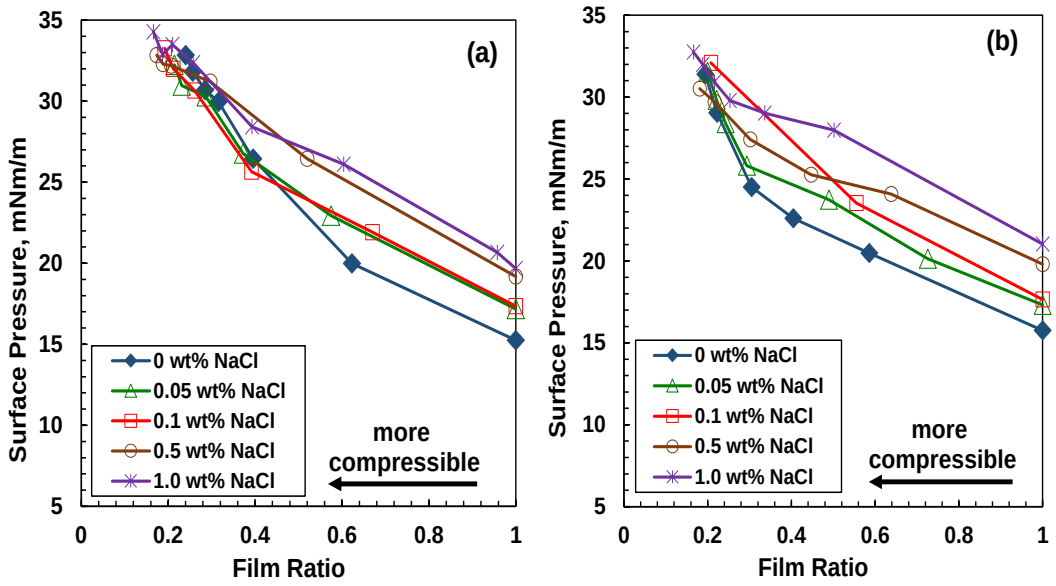

Figure A.3 Surface pressure isotherms for a) 10 g/L of SAGD asphaltene; b) 10 wt% SAGD bitumen in 25/75 heptol, after 60 minutes; aqueous phase: NaCl brine at 21°C.

The effect of asphaltene concentration on surface pressure isotherms and crumpling ratios was evaluated for model systems at 2, 10 and 30 g/L asphaltenes in 25/75 heptol and at different salt contents for the OS, CSS and SAGD samples, as shown in Figures A.4-A.6. The similarity of the surface pressure isotherms and crumpling ratios with the increased asphaltene content for all the bitumen samples suggests that the interfaces are nearly saturated with asphaltenes molecules even at asphaltene concentrations as low as 2 g/L.

These results are consistent with the findings made by Yarranton *et al.* (2007b) where it was shown that asphaltene concentration had little effect on surface pressure isotherms. Urrutia (2006), showed that at asphaltene concentrations above 1 g/l in 25/75 heptol the water-oil interface was already saturated with asphaltene molecules and therefore no changes on surface pressure isotherms were observed. Figures A.4-A.6 shows that the changes in interfacial film properties are dominated by the salt content rather than the asphaltene concentration.

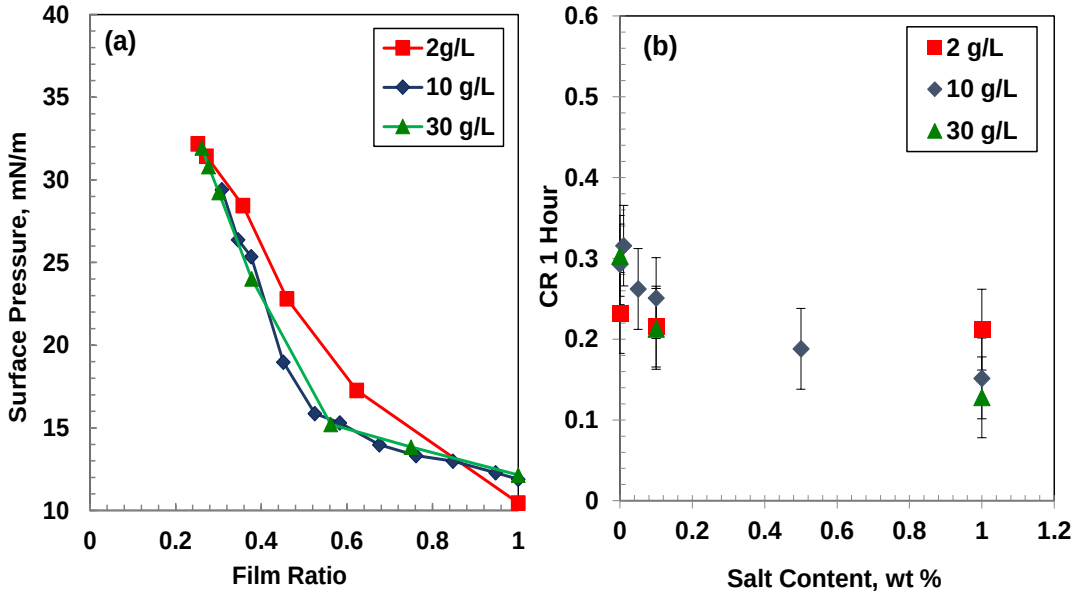

Figure A.4 Effect of OS asphaltene concentration in 25/75 heptol on (a) surface pressure isotherms, no salts; (b) crumpling ratios, aqueous phase: NaCl brine at 21°C.

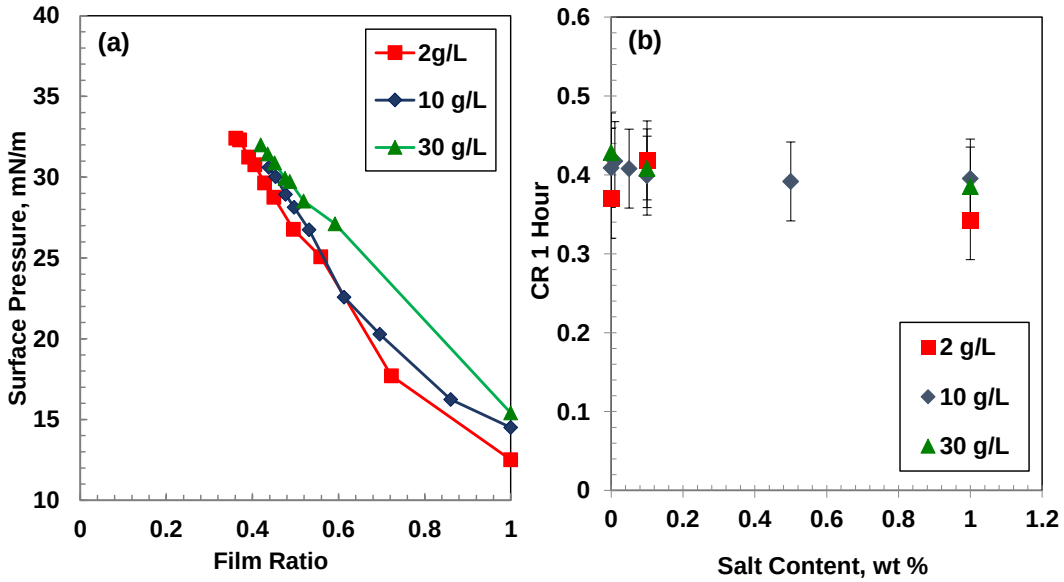

Figure A.5 Effect of CSS asphaltene concentration in 25/75 heptol on (a) surface pressure isotherms no salts; (b) crumpling ratios (CR), aqueous phase: NaCl brine at 21°C.

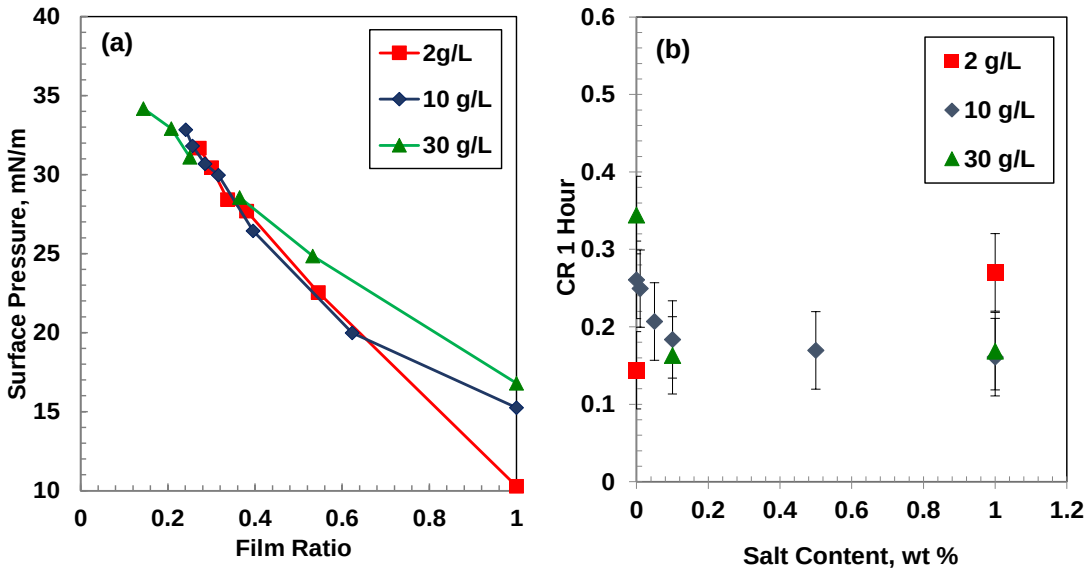

Figure A.6 Effect of SAGD asphaltene concentration in 25/75 heptol on (a) surface pressure isotherms, no salts; (b) crumpling ratios (CR), aqueous phase: NaCl brine at 21°C.

Figure A.7 shows the surface pressure isotherms at 10, 30, 60, and 240 min of aging time when salt were no present at 21°C. Results show more compressible films as the aging time increases (steeper curves and higher CR), demonstrating the capacity of asphaltene to lower IFT and gradually reorganize along the interface to form a rigid irreversibly adsorbed network over long periods of time. The increase in "phase change" and film ratios with the aging was previously observed (Yarranton *et al.*, 2007a; Ortiz *et al.*, 2010; Sztukowski *et al.*, 2003;Urrutia, 2006). As the time increases, the asphaltene molecules become more tightly packed on the interface, the films become more incompressible upon further compression and the asphaltene crumples at higher film ratios.

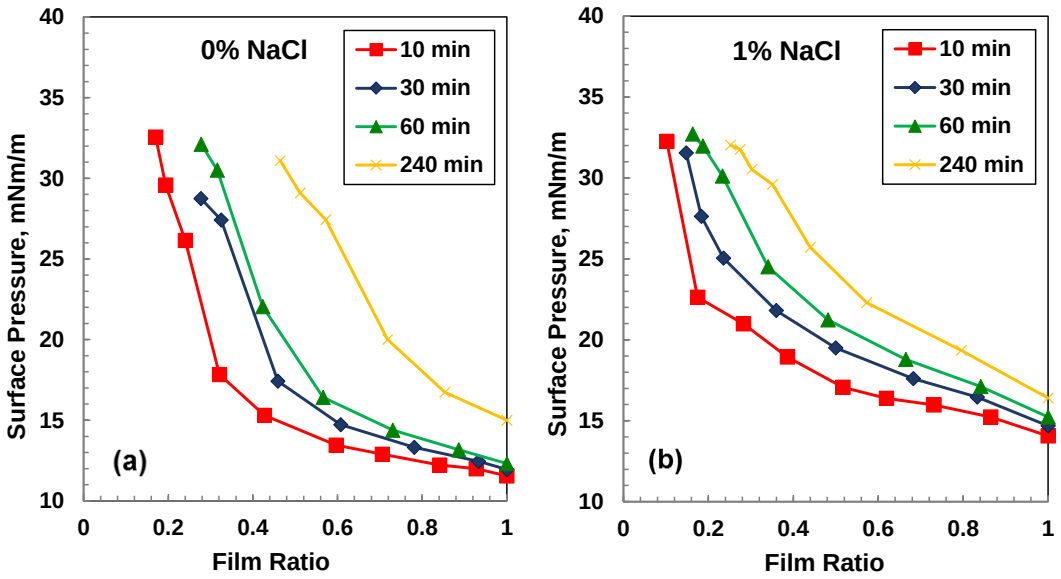

Figure A.7 Effect of aging time of OS asphaltenes in 25/75 heptol on surface pressure isotherms (a) RO water (b) 1 wt% NaCl brine; 21°C

APPENDIX B

Drop Size Distributions

Figure B.1 shows the drop size distribution for the CSS and SAGD model emulsions. Result show that the distributions become narrower and the average drop size decreases with the increased salt content.

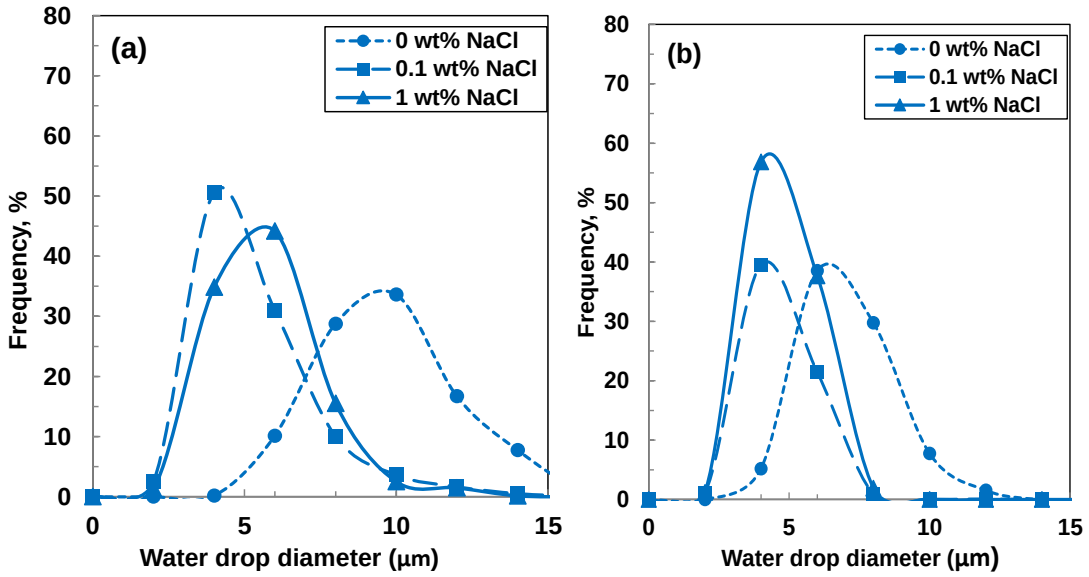

Figure B.1 Drop size distributions of model emulsions prepared from: a) CSS asphaltenes; b) SAGD asphaltenes at different salt contents. Organic phase: 10 g/L of asphaltenes in 25/75 heptol; aqueous phase: reverse osmosis water and NaCl; 40 vol% aqueous phase.

Emulsion Packing

Figure B.2 shows similar results for NaCl and $CaCl_2$ brines on emulsion packing. As previously describes in Chapter 4, these results are consistent with lack of sensitivity of emulsion stability, drop distribution, and mass surface coverage to the type of salt.

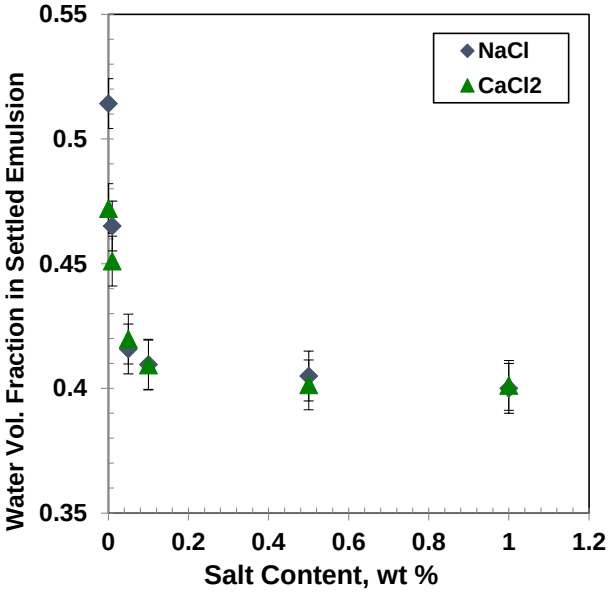

Figure B.2 Effect of salt content on the water volume fraction of the settled emulsion; Organic phase: 10 g/L of asphaltenes in 25/75; aqueous phase: reverse osmosis water and NaCl and $CaCl_2$; 40 vol% aqueous phase.

APPENDIX C: ERROR ANALYSIS

This appendix shows the sample error analysis for asphaltene and solids yield, emulsion stability, drop size distribution, asphaltene mass and molar surface coverage, interfacial tension and crumpling ratios. Every experiment was repeated at least twice at each experimental conditions. For repeat measurements made at one experimental condition, the error was calculated based on the standard deviations of sets of repeated measurements at 90% confidence interval using the *t*-distribution. Otherwise, the confidence interval was stablished based on the cumulative frequency of the standard deviation.

The sample mean $\bar{y}$ of a sample of *n* observations is defined as:

$$\bar{y} = \frac{\sum_{i=1}^{n} y_i}{n} \tag{C.1}$$

where y_i is the measured value and n is the number of repeated measurements at each experimental condition. The variability of scatter in the data is described by the sample standard deviation, *s*, defined by:

$$s = \sqrt{\frac{\sum_{i=1}^{n}(y_i - \bar{y})^2}{n-1}} \tag{C.2}$$

In this work, the population mean, μ, and the population standard deviation are unknown, hence the statistical *t*-distribution is employed to determine the confidence interval as follow:

$$\bar{y} - t_{\left(\frac{\alpha}{2},\nu\right)}\frac{s}{\sqrt{n}} \leq \mu \leq \bar{y} + t_{\left(\frac{\alpha}{2},\nu\right)}\frac{s}{\sqrt{n}} \tag{C.3}$$

where $\nu = n - 1$ is the degrees of freedom and $\alpha = (1 - \%\ confidence\ interval/100)$. In this study the confidence interval is chosen to be 90%. Therefore, α =0.10.

C.1 Error in Measurements Made at a Single Experimental Condition

C.1.1 Asphaltene Yield and Toluene Insoluble Solids

The error analyses for the yield of asphaltenes-solids precipitated with C7 from OS, CSS, and SAGD bitumen are summarized in Table C.1. On average, the yield of asphaltene varies by ±0.5% for a confidence interval of 90%. For example, the yield of OS asphaltenes is 17.2% ±0.46%.

Table C.1 Error analyses of asphaltene yields

Sample	$\bar{y}$(%)	n	s(%)	t	$t_{\left(\frac{\alpha}{2},\nu\right)}\frac{s}{\sqrt{n}}$ (%)
OS	14.7	10	0.74	1.26	0.46
CSS	16.2	9	1.29	1.37	0.75
SAGD	18.3	4	0.29	1.43	0.35

The error analyses for the fraction of toluene insoluble solids (TI) are summarized in Table C.2. On average, the fraction of solids for all bitumen samples varies by ±0.2% for a confidence interval of 90%. For example, the fraction of solids for CSS asphaltenes is 0.41% ±0.2%.

Table C.2 Error analyses for (TI) solids

Sample	$\bar{y}$(%)	n	s(%)	t	$t_{\left(\frac{\alpha}{2},\nu\right)}\frac{s}{\sqrt{n}}$ (%)
OS	4.65	6	0.50	2.015	0.41
CSS	1.70	4	0.16	2.353	0.19
SAGD	0.41	4	0.03	2.353	0.04

C.2 Error in Measurements Made at Different Experimental Conditions

Since the number of repeats can vary at different experimental conditions (*e.g.*, different aqueous phase chemistries) a total standard deviation can be calculated for each bitumen sample as follows (Levin *et al.*, 2001):

$$s = \sqrt{\frac{\sum_{i=1}^{n}(n-1)s^2}{\sum_{i=1}^{n}(n-1)}} \quad \text{(C.4)}$$

In this section we compare the error calculated using the *t, Z* and cumulative frequency distribution.

C.2.1 Emulsion Stability

The free water resolved was used to measure the relative emulsion stability. The data shown in this section is for water resolved after ten hours of treatment. Table C.3 and C.4 show the statistical parameters relevant to calculate the standard deviation at different experimental conditions, Equation C4. The error in water resolved for OS, CSS and SAGD are summarized in Table C.5. The variation on free water resolution of emulsions stabilized by OS asphaltenes was ±2.4% and ±6.4% for CSS and SAGD asphaltenes for a confidence interval of 90% using the cumulative frequency distribution.

Table C.3 Statistic Parameters for emulsion stability for OS asphaltenes

Model OS

NaCl, %	mean, vol%	*S*	S^2	n	n-1	$(n-1)S^2$
0	17.00	4.15	17.19	2	1	17.19
0.01	4.11	0.50	0.25	2	1	0.25
0.05	3.37	1.51	2.28	2	1	2.28
0.1	3.22	1.33	1.77	2	1	1.77
0.5	3.03	1.07	1.15	2	1	1.15
1	2.81	1.84	3.38	2	1	3.38
$CaCl_2$%						
0	12.62	2.05	4.21	2	1	4.21
0.01	9.38	1.31	1.72	2	1	1.72
0.05	5.26	1.23	1.50	2	1	1.50
0.1	5.85	2.98	8.91	2	1	8.91
0.5	3.99	2.42	5.84	2	1	5.84
1	2.63	1.09	1.20	2	1	1.20
$Na_2C\ O_3$%						
0	13.25	0.35	0.13	2	1	0.13
0.01	7.11	0.37	0.14	2	1	0.14
0.05	5.09	2.84	8.06	2	1	8.06
0.1	3.74	2.03	4.13	2	1	4.13
0.5	2.66	0.54	0.30	2	1	0.30
1	2.88	2.47	6.09	2	1	6.09

$Na_2S\ O_4$%						
0	11.31	2.99	8.94	2	1	8.94
0.01	4.09	0.90	0.81	2	1	0.81
0.05	2.72	0.09	0.01	2	1	0.01
0.1	3.02	1.07	1.15	2	1	1.15
0.5	2.31	0.00	0.00	2	1	0.00
1	2.87	0.79	0.63	2	1	0.63
KCl,%						
0	12.83	1.80	3.23	2	1	3.23
0.01	4.64	1.36	1.84	2	1	1.84
0.05	4.22	2.86	8.18	2	1	8.18
0.1	3.02	2.69	7.22	2	1	7.22
0.5	2.25	1.61	2.61	2	1	2.61
1	1.86	1.03	1.05	2	1	1.05
pH						
2	9.88	2.35	5.54	2	1	5.54
4	9.51	1.30	1.70	2	1	1.70
6	9.67	1.18	1.40	2	1	1.40
8	10.72	0.44	0.19	2	1	0.19
10	7.90	3.68	13.53	2	1	13.53
12	3.84	2.21	4.90	2	1	4.90
				Sum	36	131.15

Table C.4 Statistic Parameters for emulsion stability for CSS and SAGD asphaltenes

Model CSS

NaCl, %	mean, %	*S*	S^2	n	n-1	$(n-1)s^2$
0	54.66	2.93	8.57	2	1	8.57
0.01	59.47	3.71	13.74	2	1	13.74
0.05	6.93	1.91	3.64	2	1	3.64
0.1	5.75	1.31	1.72	2	1	1.72
0.5	4.51	0.41	0.17	2	1	0.17
1	4.60	0.94	0.88	2	1	0.88
$CaCl_2$,%						
0	28.33	7.38	54.45	2	1	54.45
0.01	18.68	6.64	44.10	2	1	44.10
0.05	9.96	1.77	3.15	2	1	3.15
0.1	5.87	0.70	0.49	2	1	0.49
0.5	4.05	0.78	0.61	2	1	0.61
1	4.72	0.75	0.57	2	1	0.57
pH						
2	69.05	4.28	18.31	2	1	18.31
4	26.44	4.47	19.97	2	1	19.97
6	20.70	6.28	150.91	2	1	150.91
8	23.30	7.26	232.87	2	1	232.87
10	26.91	2.38	5.67	2	1	5.67
12	7.10	1.46	2.12	2	1	2.12

Model SAGD						
NaCl, %						
0	89.94	1.71	2.93	2	1	2.93
0.01	84.17	1.87	3.49	2	1	3.49
0.05	68.08	1.01	1.02	2	1	1.02
0.1	68.30	6.09	37.03	2	1	37.03
0.5	70.37	5.23	27.39	2	1	27.39
1	70.27	6.60	43.62	2	1	43.62
				Sum	12	677.42

Table C.5 Error Analysis for emulsion tests

Sample	S^2	S	$t\frac{s}{\sqrt{n}}\%$	$Z\frac{s}{\sqrt{n}}\%$	**Cum Frequency %**
OS	3.64	1.9	8.52	2.22	**2.42**
CSS,SAGD	28.20	5.31	23.71	6.64	**6.71**

Figure C.1 illustrates a graphic representation of the cumulative frequency of standard deviations for the OS sample, data shown in Table C.3. This method, also known as cumulative polygon (Levin *et al.*, 2001) shows that 90% of all the standard deviations for water resolved fall below 2.4 vol%. The cumulative frequency method best captures the distribution of the standard deviation of the multiples measurements. Note, the values obtained were very similar to those obtained with the *Z* distribution, which applies when the population variance is known.

The error on water resolved of emulsions stabilized with 10, 20 and 30 wt% bitumen diluted in 25/75 heptol was found to be ±11% for a confidence interval of 90% for all the bitumen samples. The statistical analyses was similar for the model solutions and are therefore not shown here. Note, the error was relative smaller for OS, compare with CSS and SAGD bitumen, this is primarily due to the higher emulsion stability and larger number of repeats at each experimental condition. Therefore, an overall error for emulsion stability, drop size and water volume fraction was calculated for CSS and SAGD asphaltenes.

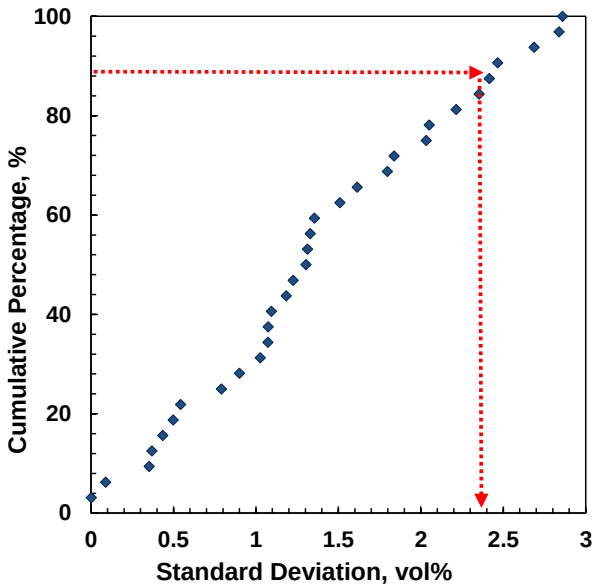

Figure C.1 Cumulative frequency of the standard deviations for the volume of water resolved.

C.2.2 Sauter Mean Diameter and Water Volume Fraction in the Settled Emulsion

Table C.6 shows the error analysis of sauter mean diameter for model emulsions. The variation was ±0.6 μm for OS and ±0.9 μm for CSS and SAGD emulsions for a 90% confidence interval. Table C.7 shows the variation of the water volume fraction in settle emulsions was ±0.03 for OS and ±0.015 for CSS and SAGD asphaltenes, for a 90% confidence interval. Note that the cumulative frequency was used in both cases to calculate the variation, however, comparable values were obtained when using the *t* and *Z* distributions.

Table C.6 Error analysis of Sauter Mean Diameter

Sample	S^2	S	$t\frac{s}{\sqrt{n}}$ μm	$Z\frac{s}{\sqrt{n}}$ μm	**Cum Frequency μm**
OS	0.16	0.40	0.47	0.32	**0.61**
CSS,SAGD	0.39	0.62	1.03	0.72	**0.94**

Table C.7 Error analysis of water fraction in settle emulsions

Sample	S^2	S	$t\frac{s}{\sqrt{n}}$	$Z\frac{s}{\sqrt{n}}$	**Cum Frequency**
OS	0.0003	0.016	0.020	0.014	**0.03**
CSS,SAGD	0.0004	0.02	0.023	0.016	**0.02**

C.2.3 Mass Surface Coverage

The error analyses of mass surface coverage for model systems are summarized in the Table C.8. The variation was ±2.9 mg/m² for OS and CSS asphaltenes and ±1.5 mg/m² for the SAGD asphaltenes based on 90% confidence interval. The mass surface coverage for SAGD asphaltenes was almost invariant at any salt content and therefore the error of the repeats was relatively low. An overall error was calculated for the OS and CSS samples.

Table C.8 Summary of errors for mass adsorbed on interface

Sample	S^2	S	$t\frac{s}{\sqrt{n}}\frac{\text{mg}}{\text{m}^2}$	$Z\frac{s}{\sqrt{n}}\frac{\text{mg}}{\text{m}^2}$	**Cum Frequency**
OS, CSS	3.07	1.75	7.82	2.03	**2.93**
SAGD	0.43	0.65	2.94	0.76	**1.5**

C.2.4 Interfacial Tension

The error analyses for the interfacial tension of solutions of OS, CSS and SAGD asphaltenes are summarized in the Table C.9 In these experiments, the measurements were made directly with the (DSA), in sets of two repeats for each asphaltene sample. An overall error of IFT was calculated for all the asphaltene samples. The interfacial tension varies on average by ±0.75 mN/m for a 90% confidence interval using the cumulative frequency. For diluted bitumen solutions the IFT the variability was found to be ±0.95 mN/m based on a 90% confidence interval, for 2 sets of repeats of 10 wt% bitumen diluted in 25/75 heptol.

Table C.9 Summary of errors of interfacial tension for model emulsions

Sample	S^2	S	$t\frac{s}{\sqrt{n}}\frac{\text{Nm}}{m}$	$Z\frac{s}{\sqrt{n}}\frac{\text{Nm}}{m}$	**Cum Frequency**
OS, CSS, SAGD	0.18	0.43	0.71	0.49	**0.75**

C.2.5 Crumpling Ratios

The error analyses for crumpling rations was calculated at 2, 10, 30 g/L asphaltene concentrations and 10 wt% bitumen in 25/75 heptol over NaCl brine. The variation of crumpling rations was ±0.05 for both asphaltene and bitumen solutions, based on a 90% confidence interval.

Table C.10 Error analysis for crumpling ratios for model emulsions

Sample	S^2	S	$t\frac{s}{\sqrt{n}}$	$Z\frac{s}{\sqrt{n}}$	**Cum Frequency**
OS, CSS, SAGD	0.0006	0.025	0.040	0.03	**0.05**